

A Large Ion Collider Experiment



Electromagnetic probes in small to large collision systems with ALICE

32nd Lepton-Photon Symposium | Madison, USA
25–29 August 2024



Jerome Jung
for the ALICE collaboration

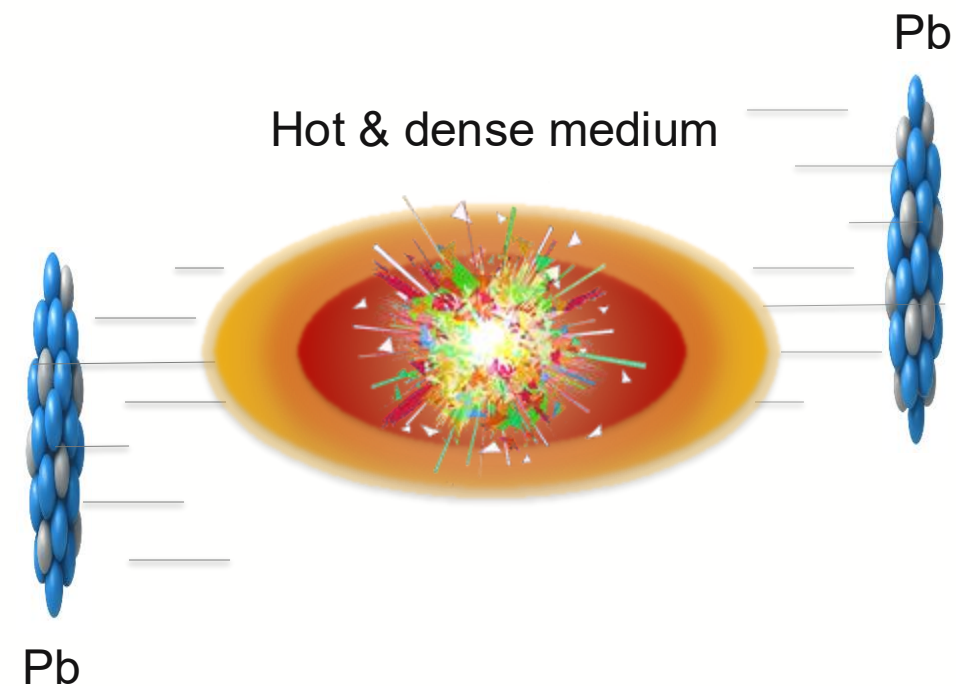


Motivation

Physics objectives

Energy density in heavy-ion collisions sufficient to create a quark-gluon plasma (QGP)

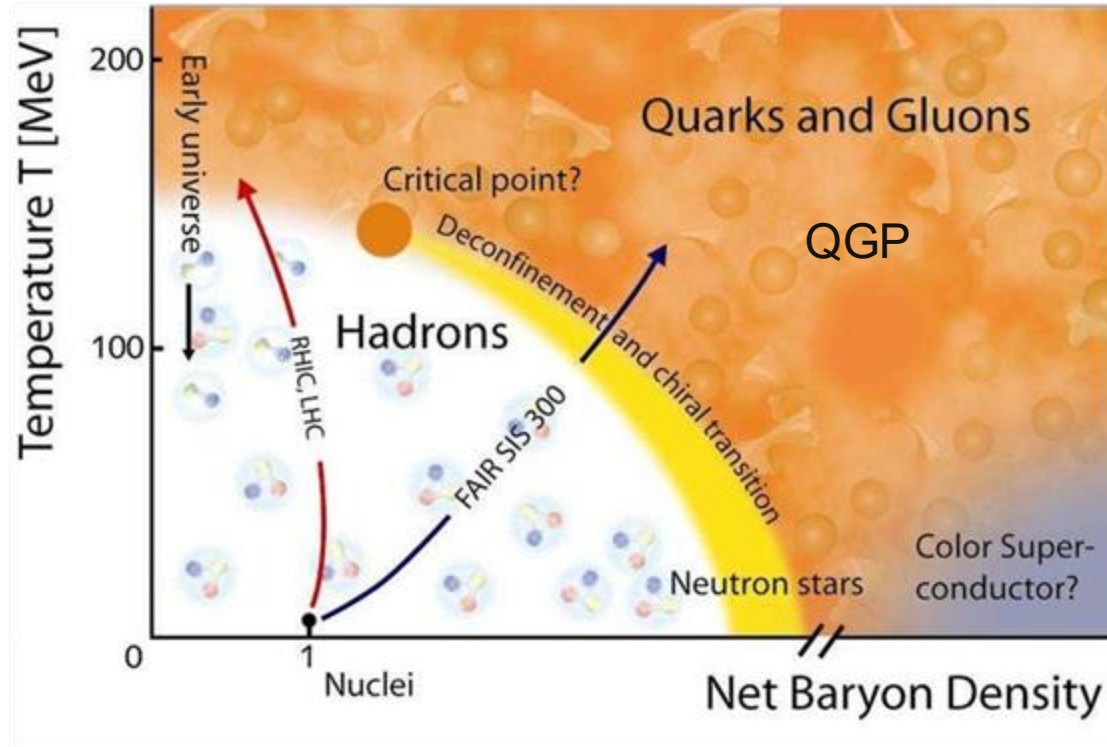
Sketch of the collision



Motivation

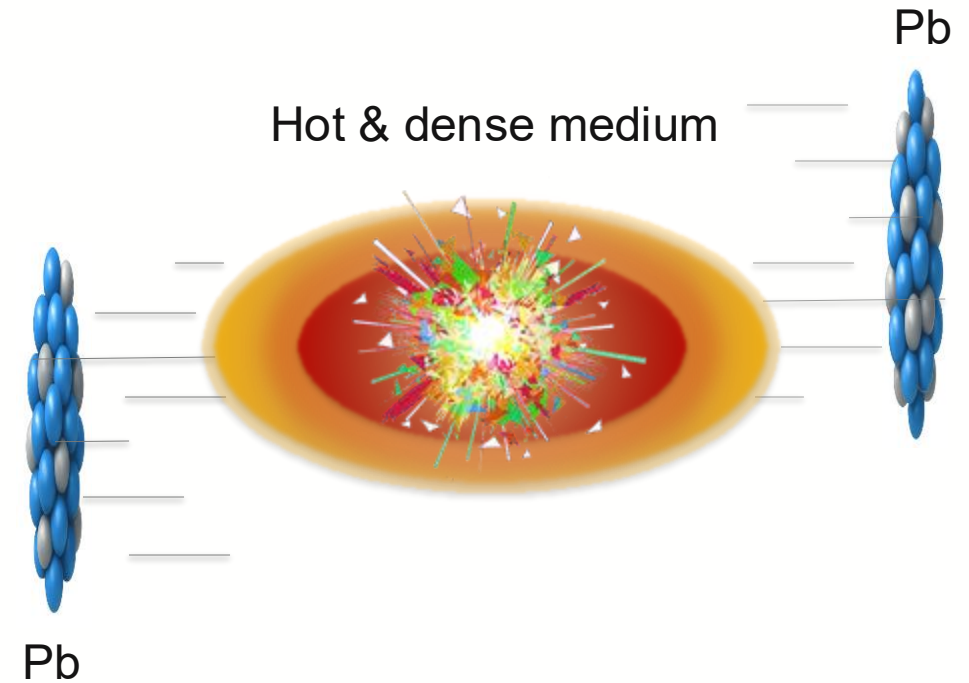
Physics objectives

Energy density in heavy-ion collisions sufficient to create a quark-gluon plasma (QGP)



Aarts, Gert & Attanasio, Felipe & Jäger, Benjamin & Seiler, Erhard & Sexty, Dénes & Starnatescu, Ion-Olimpiu. (2014)

Sketch of the collision



Motivation

Physics objectives

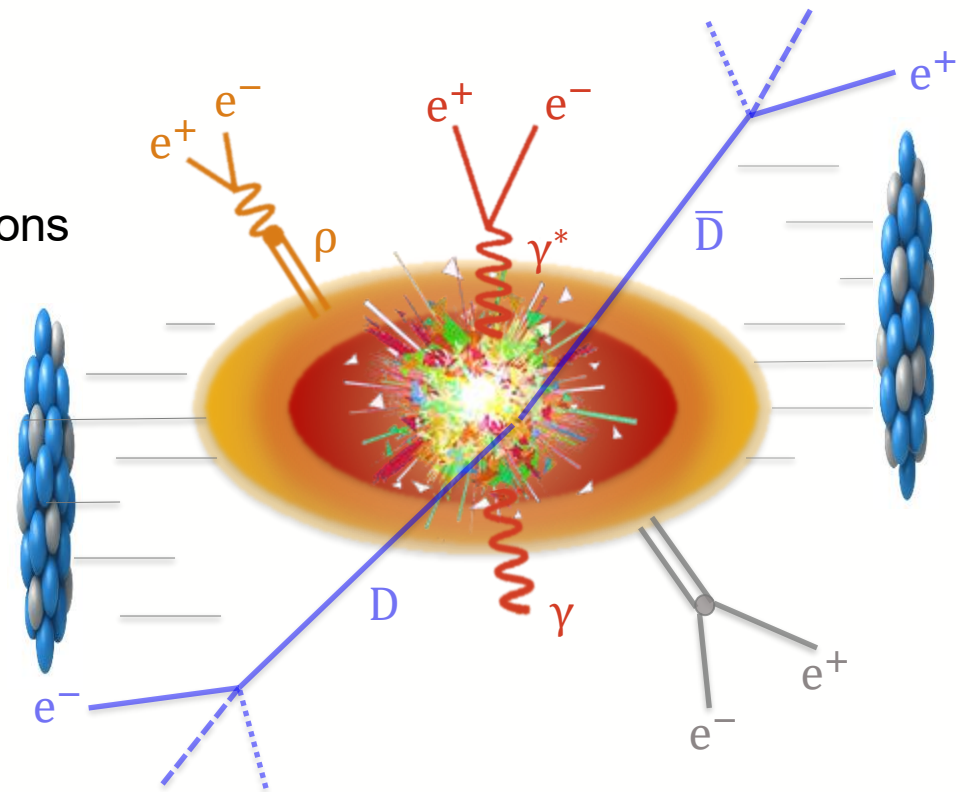
Energy density in heavy-ion collisions sufficient to create a quark-gluon plasma (QGP)

Photons & dielectrons are a unique probe:

Produced at all collision stages with negligible final-state interactions

→ Keep the information about their production mechanism

Sketch of the collision



Motivation

Physics objectives

Energy density in heavy-ion collisions sufficient to create a quark-gluon plasma (QGP)

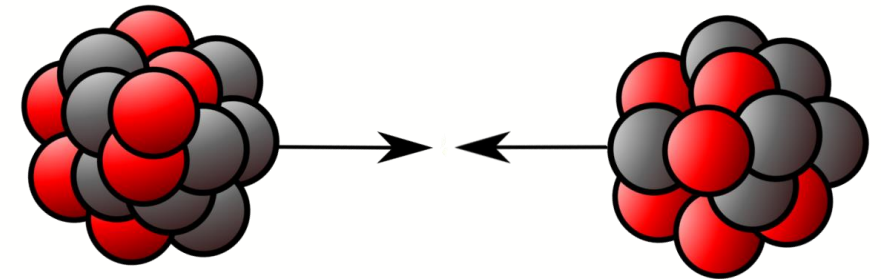
Photons & dielectrons are an unique probe:

Produced at all collision stages with negligible final-state interactions

→ Keep the information about their production mechanism

Pb–Pb collisions:

- Chiral-symmetry restoration: modification of vector mesons
- Thermal radiation throughout the medium evolution
- Decorrelation of heavy-flavor pairs in the medium
- Constrain the space-time evolution of the collision



Motivation

Physics objectives

Energy density in heavy-ion collisions sufficient to create a quark-gluon plasma (QGP)

Photons & dielectrons are an unique probe:

Produced at all collision stages with negligible final-state interactions

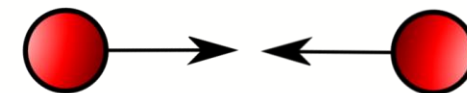
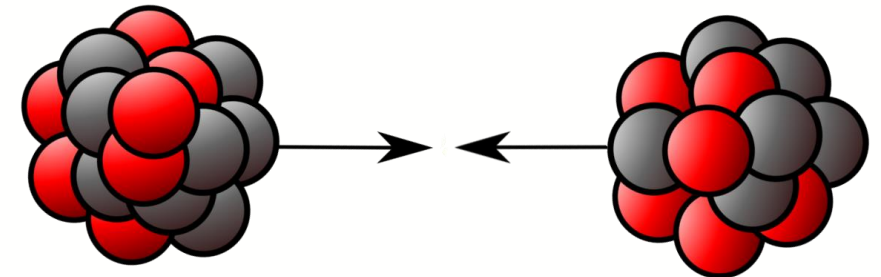
→ Keep the information about their production mechanism

Pb–Pb collisions:

- Chiral-symmetry restoration: modification of vector mesons
- Thermal radiation throughout the medium evolution
- Decorrelation of heavy-flavor pairs in the medium
- Constrain the space-time evolution of the collision

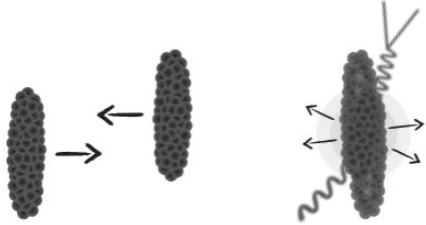
pp collisions:

- Vacuum baseline for Pb–Pb studies (heavy-flavor, direct photons, Drell–Yan)
- Establish new analysis techniques (high stat., better S/B)
- Search for new physics (Onset of thermal rad., dark photons)



Motivation

EM probes in Pb–Pb collisions

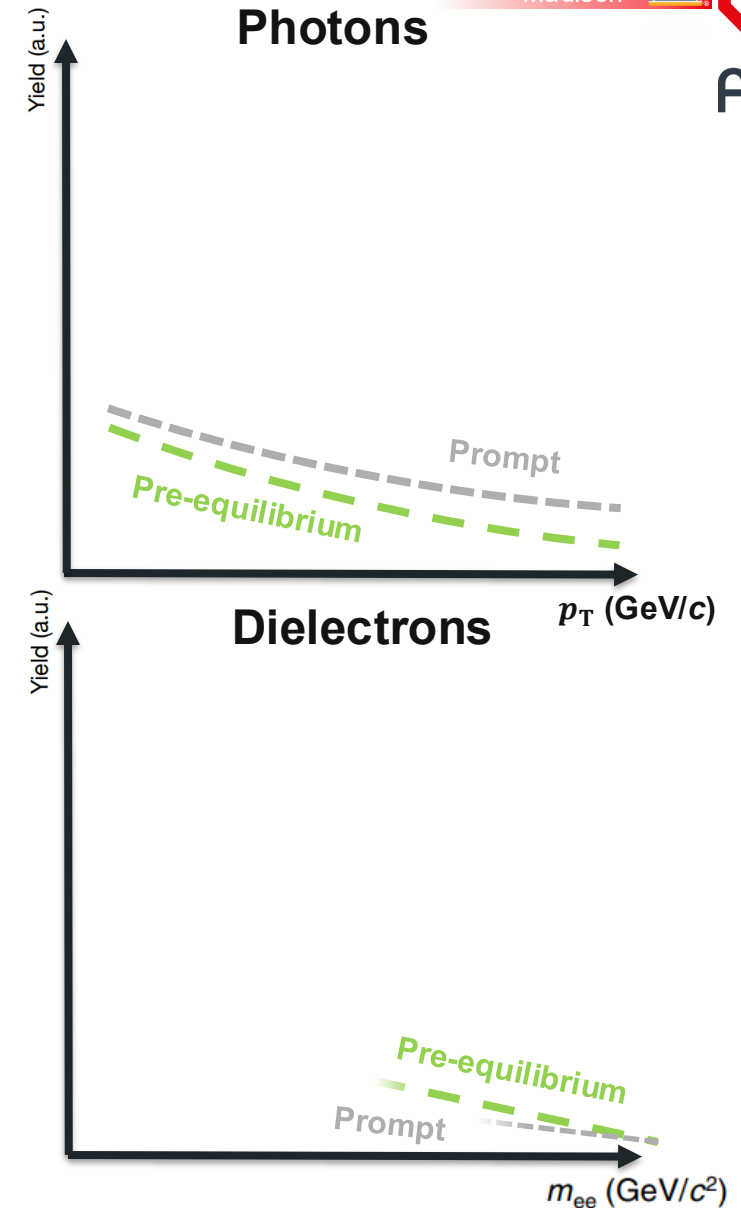


Initial stage

Contribution to the EM spectrum:

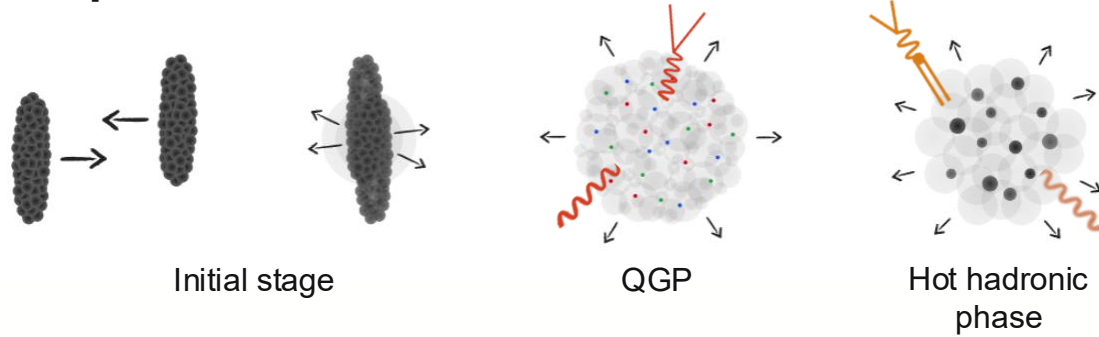
Initial stage of the collision

- **Prompt:** Drell–Yan & hard scatterings
- **Pre-equilibrium** contributions



Motivation

EM probes in Pb–Pb collisions



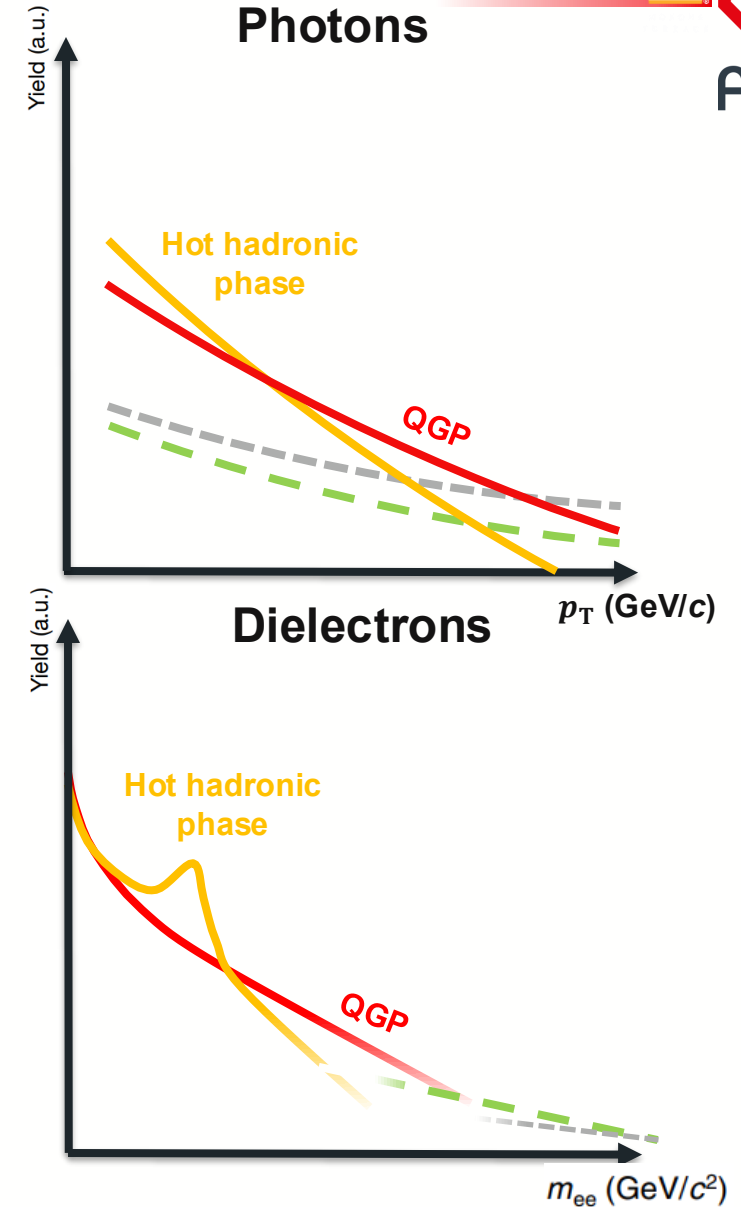
Contribution to the EM spectrum:

Initial stage of the collision

- **Prompt:** Drell–Yan & hard scatterings
- **Pre-equilibrium** contributions

Thermal radiation from the medium

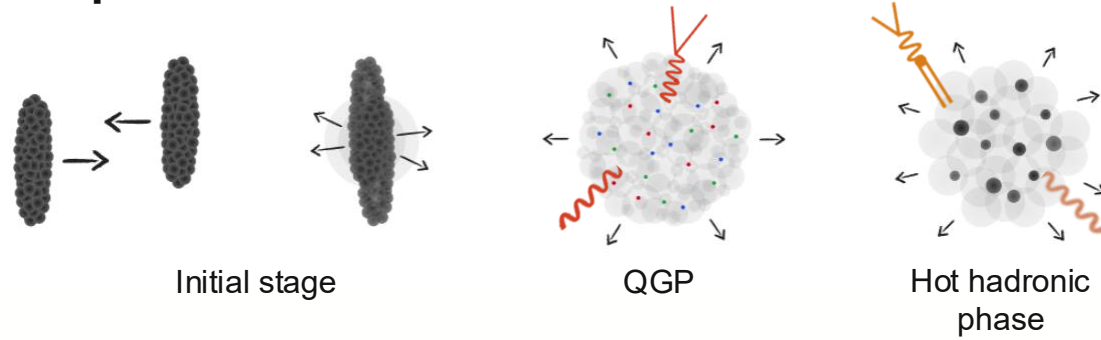
- Quark-Gluon Plasma (**QGP**)
- Hot **hadronic phase**





Motivation

EM probes in Pb–Pb collisions



Contribution to the EM spectrum:

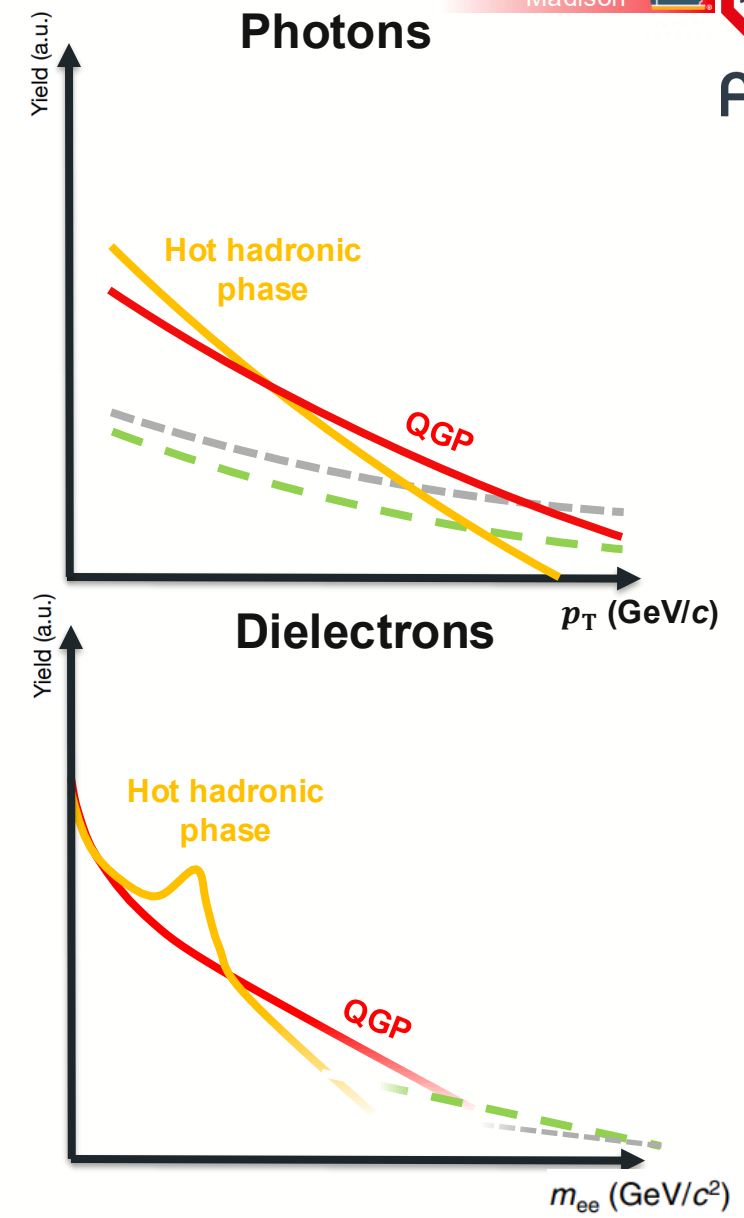
Initial stage of the collision

- **Prompt:** Drell–Yan & hard scatterings
- **Pre-equilibrium** contributions

Thermal radiation from the medium

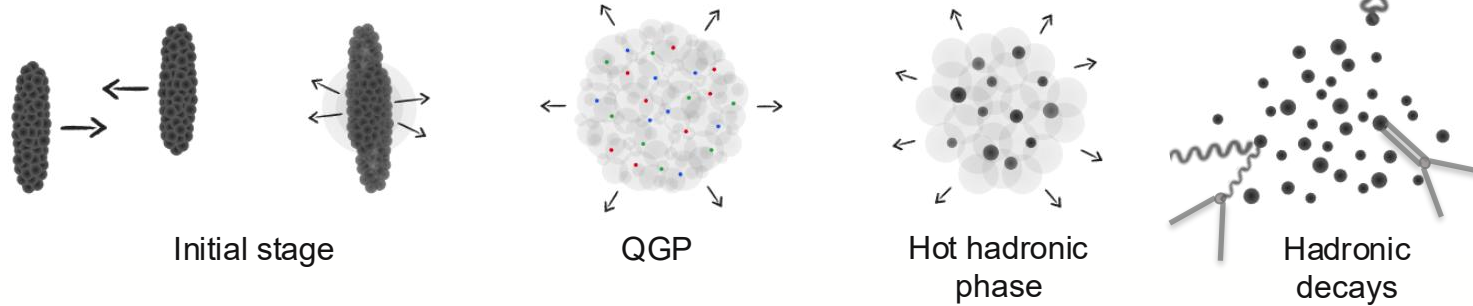
- Quark-Gluon Plasma (**QGP**)
- Hot **hadronic phase**

Direct-photon contributions



Motivation

EM probes in Pb–Pb collisions



Contribution to the EM spectrum:

Initial stage of the collision

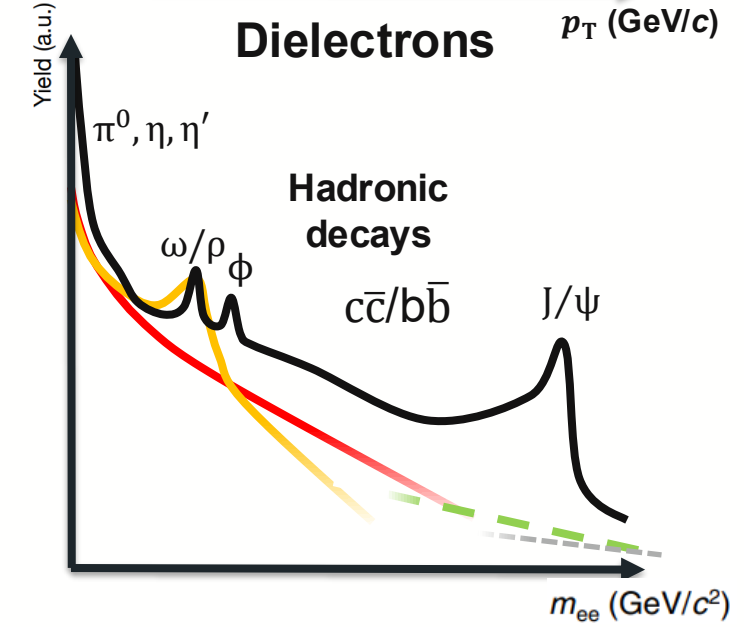
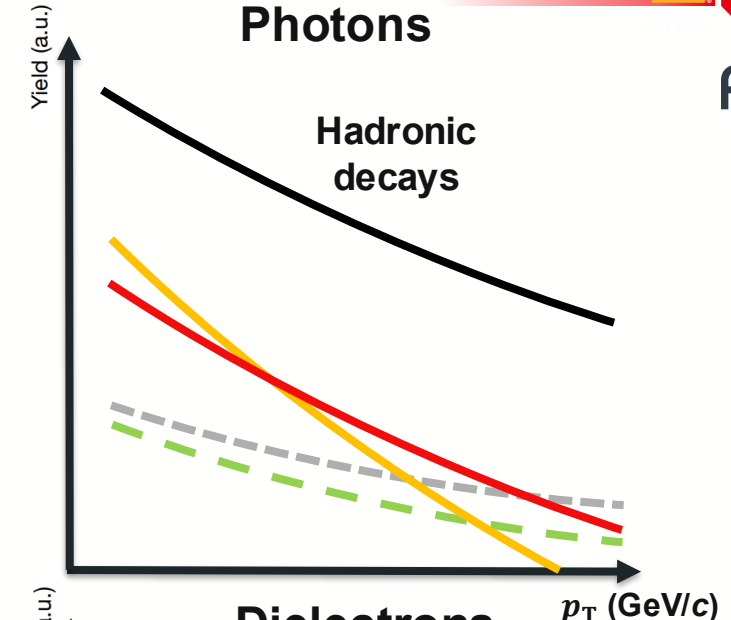
- **Prompt:** Drell–Yan & hard scatterings
- **Pre-equilibrium** contributions

Thermal radiation from the medium

- Quark-Gluon Plasma (**QGP**)
- Hot **hadronic phase**

Hadronic decays

- Large combinatorial & physical backgrounds
→ Additional separation with invariant mass of dielectrons





ALICE apparatus

Run 2 (2015–18)

Dielectrons:

Inner Tracking System
• Tracking & vertex

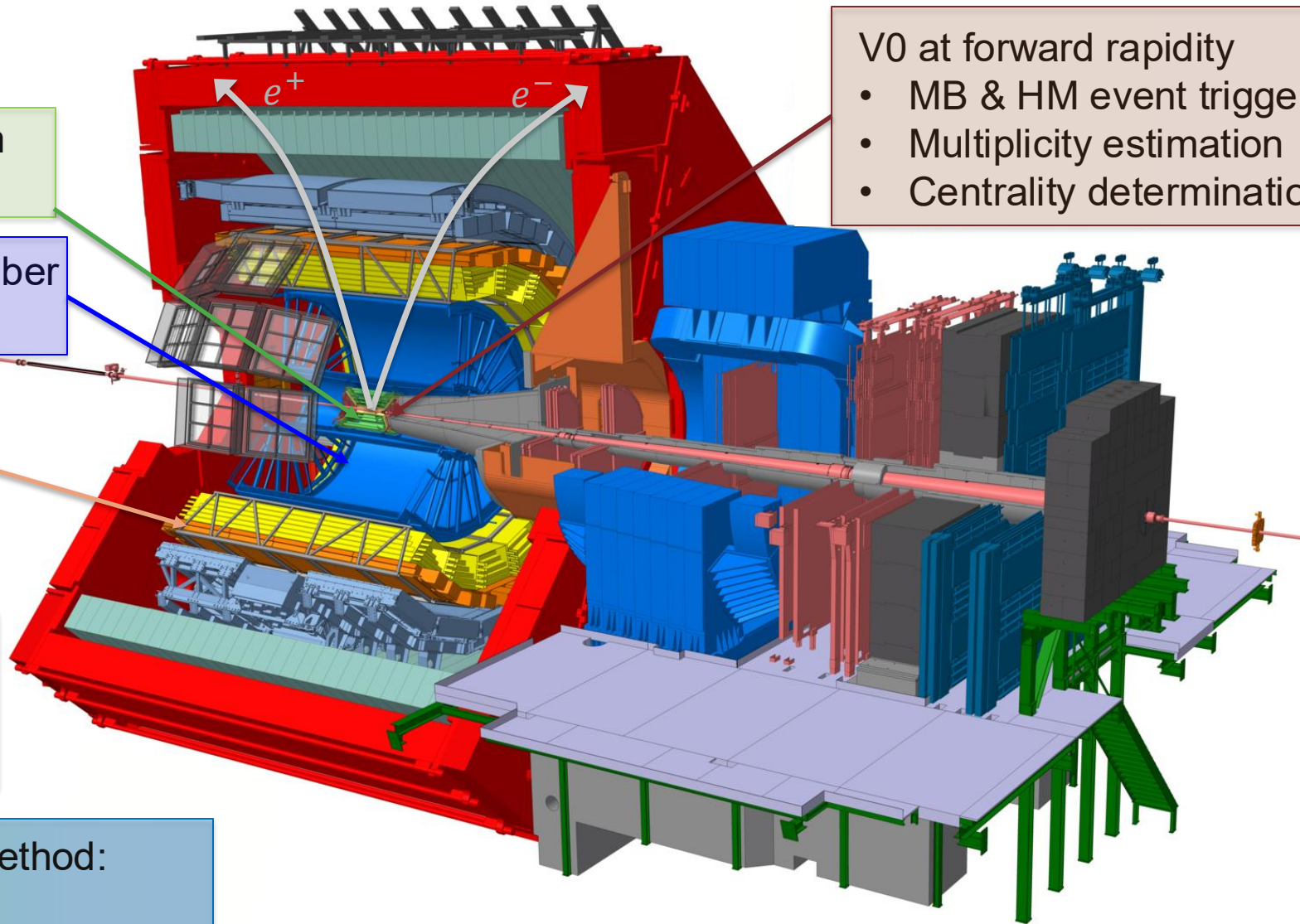
Time Projection Chamber
• Tracking & PID

Time of Flight
• PID

Photons:

Calorimeter-based:
• PHOS
• EMCal

Photon Conversion Method:
• Detector material



V0 at forward rapidity
• MB & HM event triggering
• Multiplicity estimation
• Centrality determination



ALICE apparatus

Run 2 (2015–18)

Dielectrons:

Inner Tracking System

- Tracking & vertex

Time Projection Chamber

- Tracking & PID

Time of Flight

- PID

Photons:

Calorimeter-based:

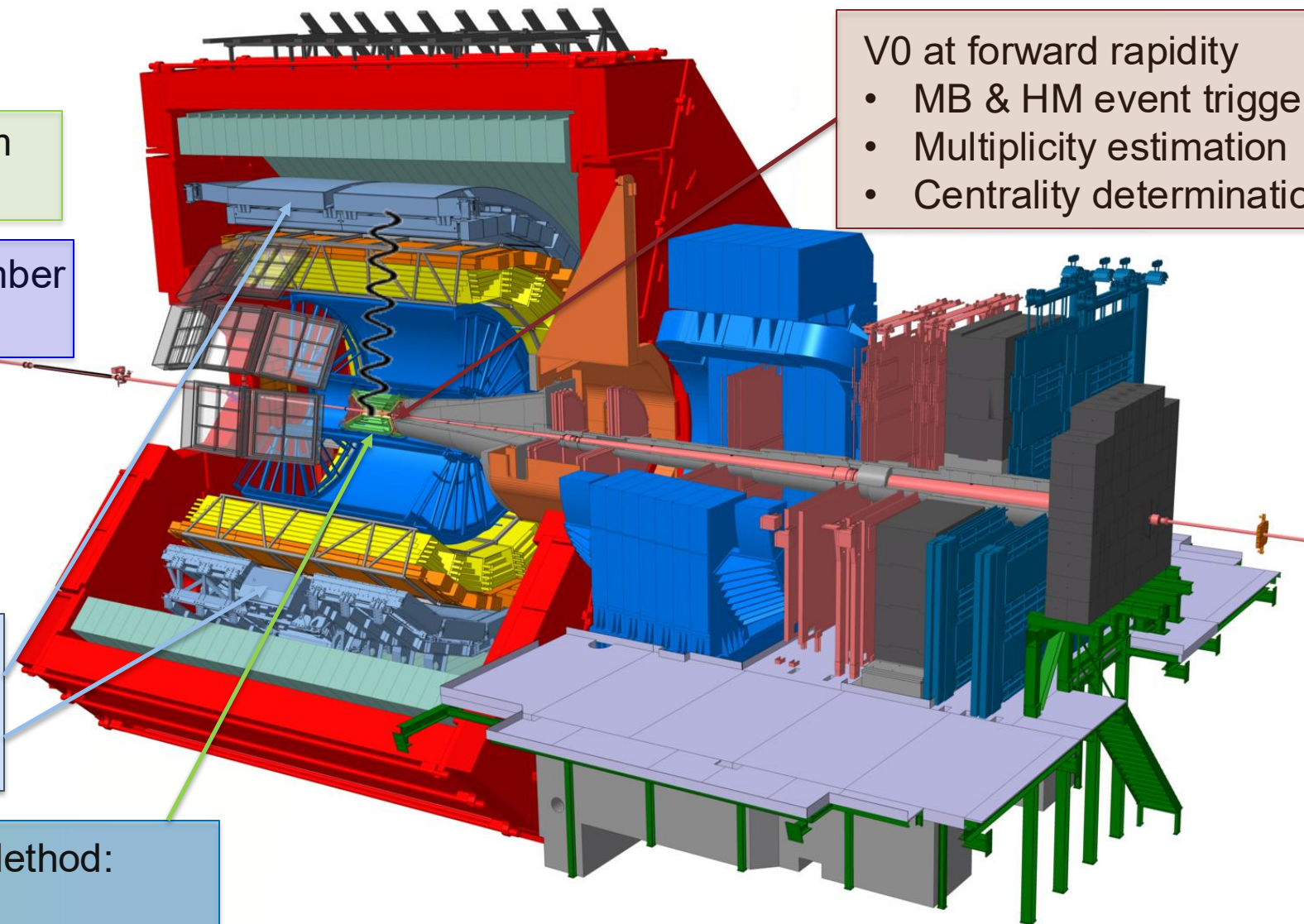
- PHOS
- EMCal

Photon Conversion Method:

- Detector material

V0 at forward rapidity

- MB & HM event triggering
- Multiplicity estimation
- Centrality determination



Real direct photons γ_{dir} pp & Pb–Pb collisions

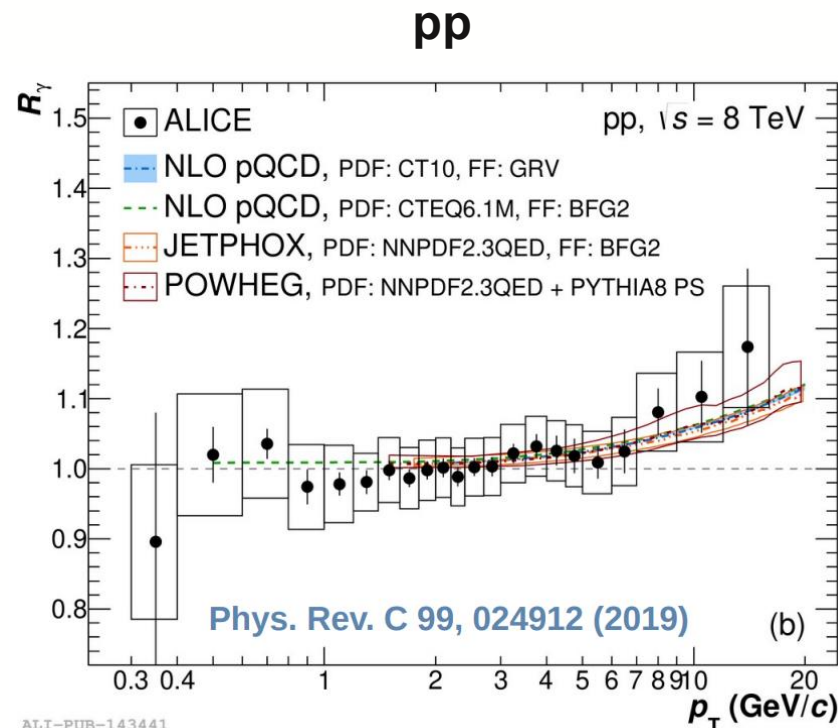
Signal extraction via
statistical subtraction of
decay photons γ_{dec}

$$R_\gamma = \frac{Y_{\gamma,\text{incl}}}{Y_{\gamma,\text{dec}}} = \left(\frac{Y_{\gamma,\text{incl}}}{Y_{\pi^0}} \right)_{\text{meas}} / \left(\frac{Y_{\gamma,\text{dec}}}{Y_{\pi^0}} \right)_{\text{sim}}$$

In pp collisions:

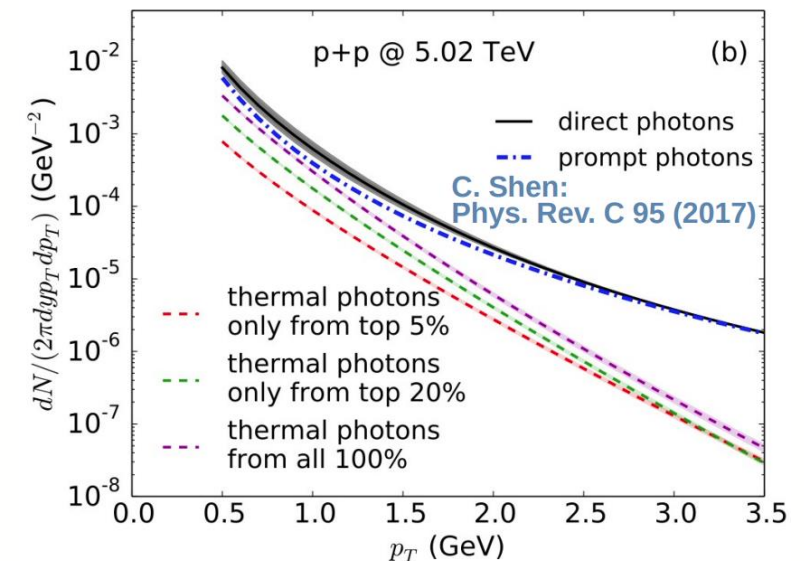
Increase of R_γ for $p_T > 7 \text{ GeV}/c$
→ consistent with pQCD

No excess for $p_T < 3 \text{ GeV}/c$
→ Region sensitive to
thermal radiation
→ Issue: Large background
from decay photons



ALI-PUB-143441

Theory prediction



Real direct photons γ_{dir} pp & Pb–Pb collisions

Signal extraction via
statistical subtraction of
decay photons γ_{dec}

$$R_\gamma = \frac{Y_{\gamma,\text{incl}}}{Y_{\gamma,\text{dec}}} = \left(\frac{Y_{\gamma,\text{incl}}}{Y_{\pi^0}} \right)_{\text{meas}} / \left(\frac{Y_{\gamma,\text{dec}}}{Y_{\pi^0}} \right)_{\text{sim}}$$

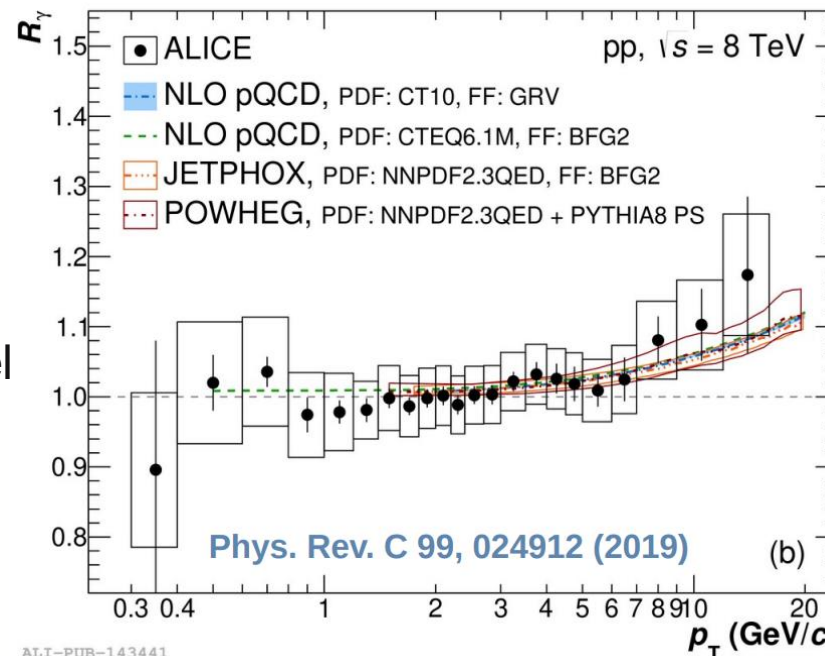
In Pb–Pb collisions:

Rise of R_γ with p_T similar
to pp collisions

Increase of R_γ in more central
collisions

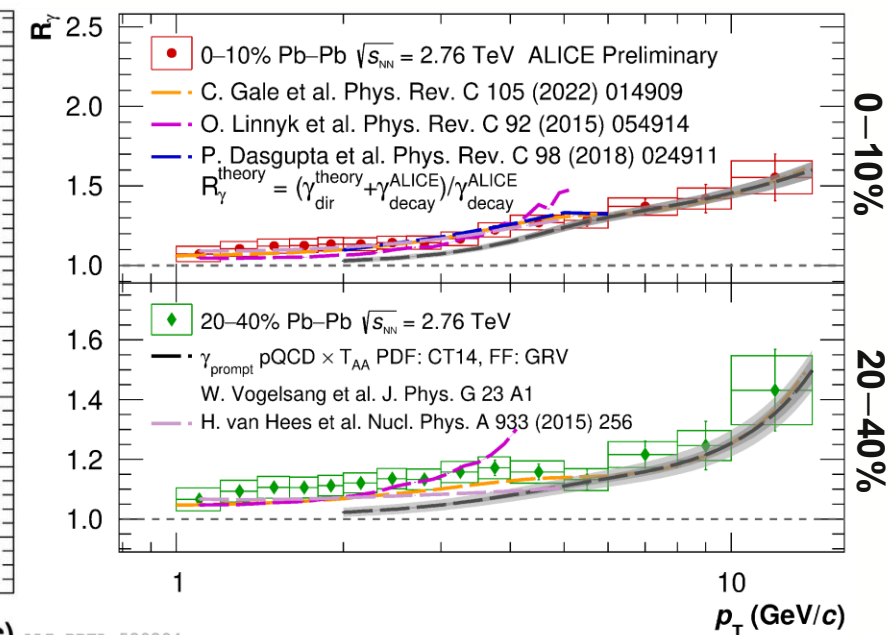
→ Consistent with different model
predictions that include QGP

pp



ALI-PUB-143441

Pb–Pb





Real direct photons γ_{dir} pp & Pb–Pb collisions

Signal extraction via
statistical subtraction of
decay photons γ_{dec}

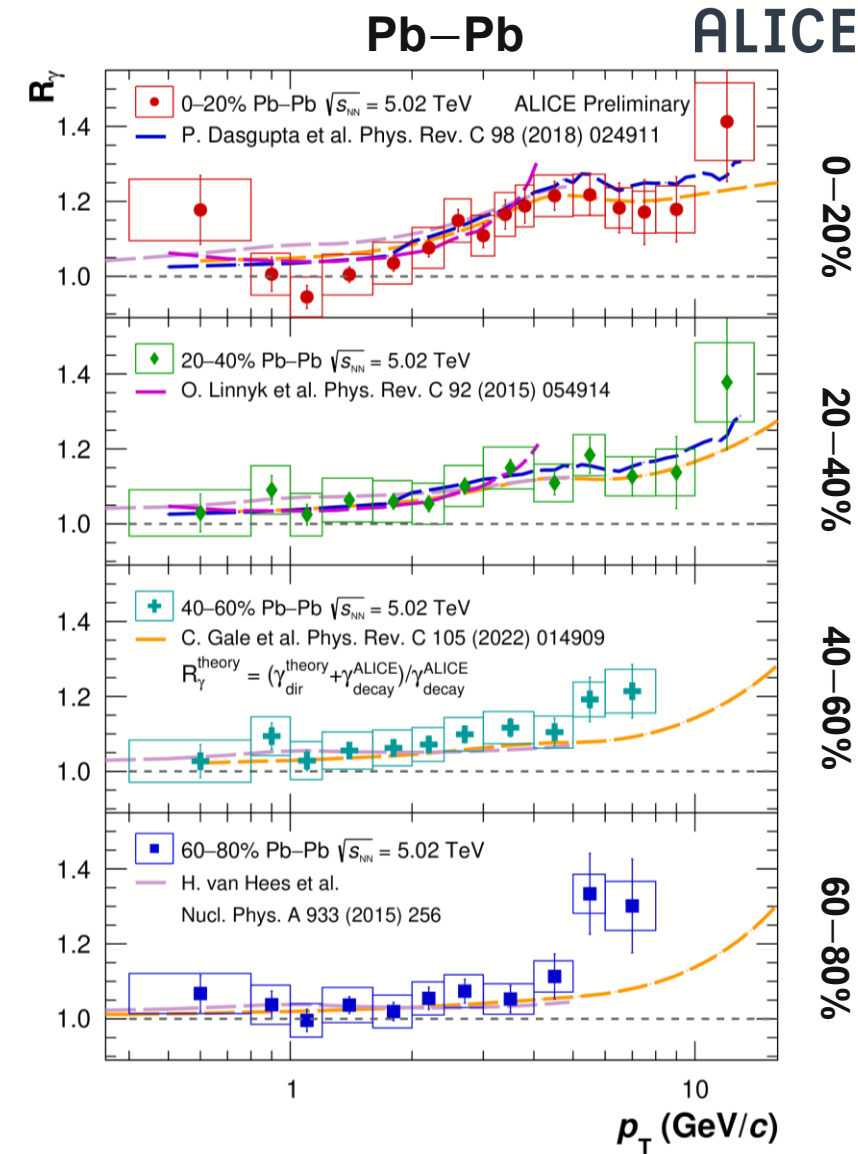
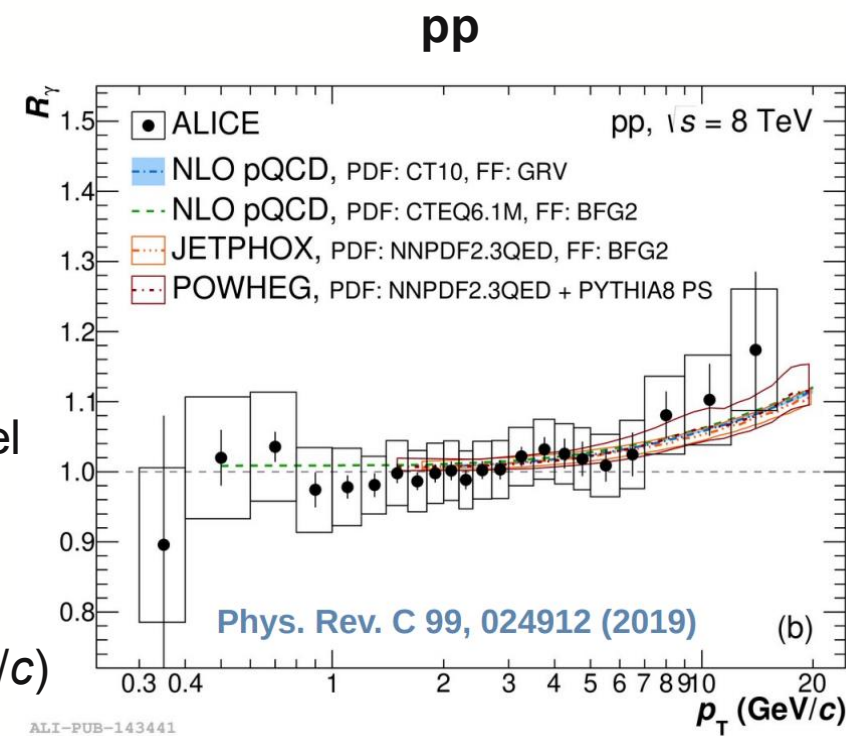
$$R_\gamma = \frac{Y_{\gamma,incl}}{Y_{\gamma,dec}} = \left(\frac{Y_{\gamma,incl}}{Y_{\pi^0}} \right)_{meas} / \left(\frac{Y_{\gamma,dec}}{Y_{\pi^0}} \right)_{sim}$$

In Pb–Pb collisions:

Rise of R_γ with p_T similar
to pp collisions

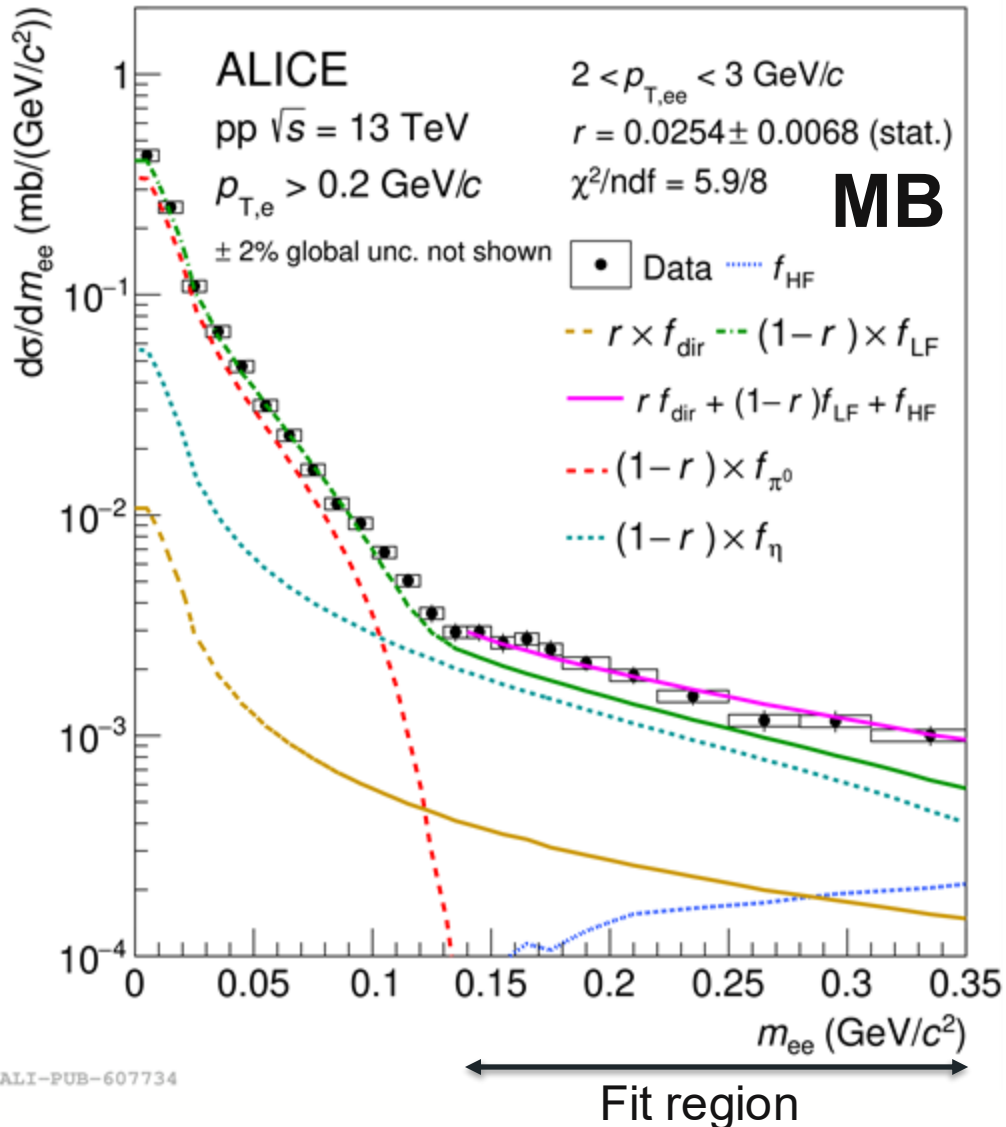
Increase of R_γ in more central
collisions
→ Consistent with different model
predictions that include QGP

However: No significant signal
of thermal radiation ($p_T < 3 \text{ GeV}/c$)



Virtual direct-photon fraction

pp at $\sqrt{s} = 13$ TeV



Analysis of the full Run 2 data set

→ Increase of statistics compared to previous publication:

[ALICE, Phys. Lett. B 788 \(2019\) 505](#)

MB: a factor of 3.8 & HM: a factor of 4.4

[ALICE, Phys. Lett. B 868 \(2025\) 139645](#)

Direct-photon fraction $r = 1 - 1/R_\gamma$:

$$r = \gamma_{\text{dir}}^* / \gamma_{\text{incl}}^* \stackrel{m_{ee} \rightarrow 0}{=} \gamma_{\text{dir}} / \gamma_{\text{incl}} \quad \text{Link to real-photon yield}$$

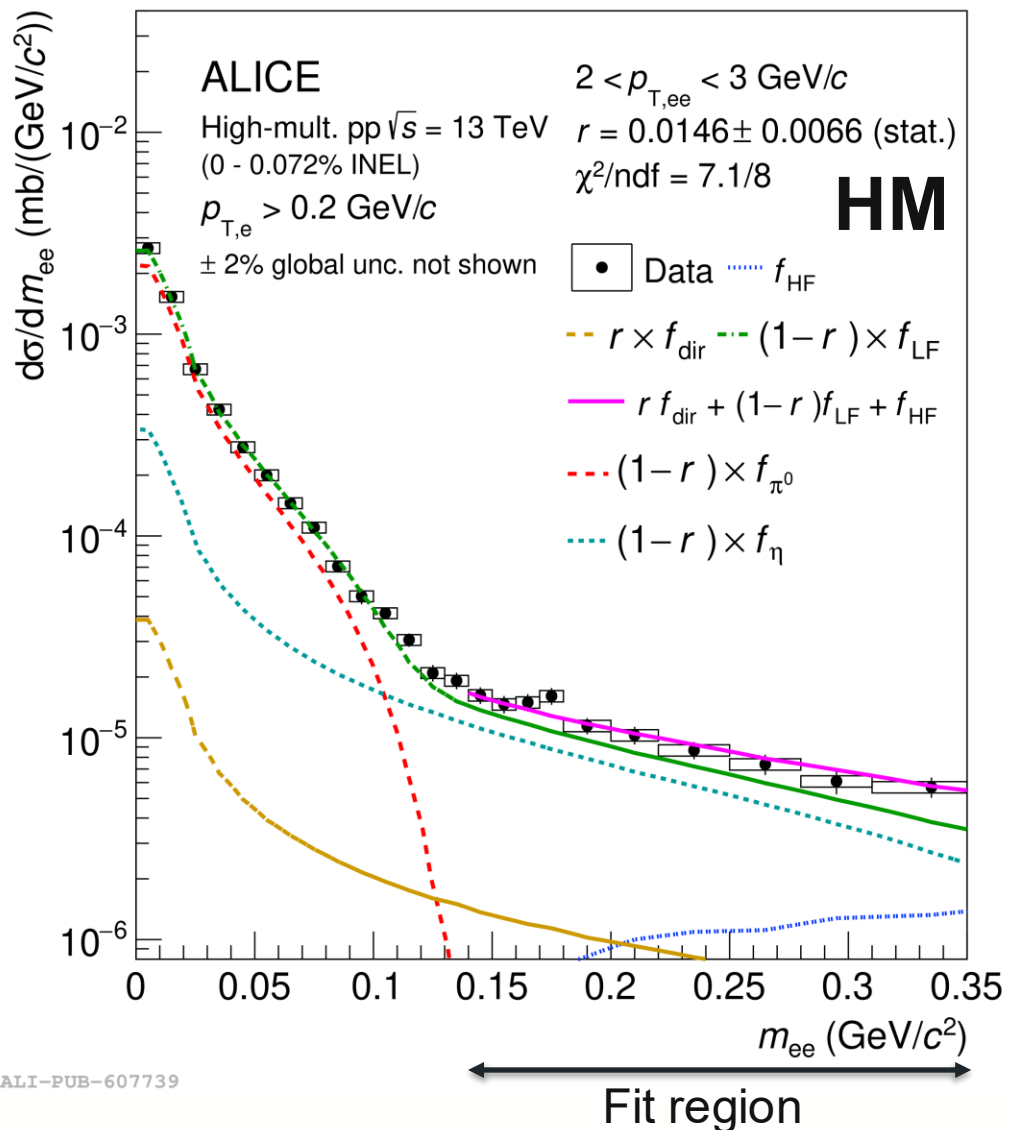
Kroll-Wada formula f_{dir} used for extraction:

$$f_{\text{fit}} = r \times f_{\text{dir}} + (1 - r) \times f_{\text{LF}} + f_{\text{HF}}$$

- Direct-photon fraction r : only free parameter
- Spectrum fitted above pion mass
 - Large reduction of systematic uncertainties compared to real-photon measurement
- Access the real direct-photon yield: $\gamma^{\text{dir}} = r \cdot \gamma^{\text{incl}}$

Virtual direct-photon fraction

pp at $\sqrt{s} = 13$ TeV



Analysis of the full Run 2 data set

→ Increase of statistics compared to previous publication:

[ALICE, Phys. Lett. B 788 \(2019\) 505](#)

MB: a factor of 3.8 & HM: a factor of 4.4

[ALICE, Phys. Lett. B 868 \(2025\) 139645](#)

Direct-photon fraction $r = 1 - 1/R_\gamma$:

$$r = \gamma_{\text{dir}}^* / \gamma_{\text{incl}}^* \stackrel{m_{ee} \rightarrow 0}{=} \gamma_{\text{dir}} / \gamma_{\text{incl}} \quad \text{Link to real-photon yield}$$

Kroll-Wada formula f_{dir} used for extraction:

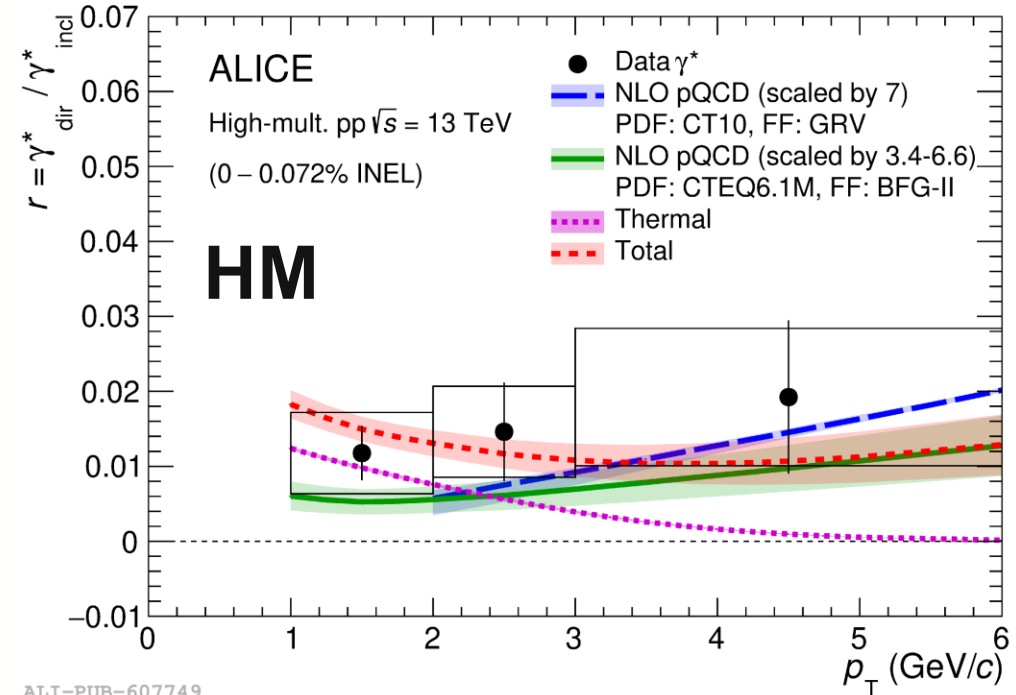
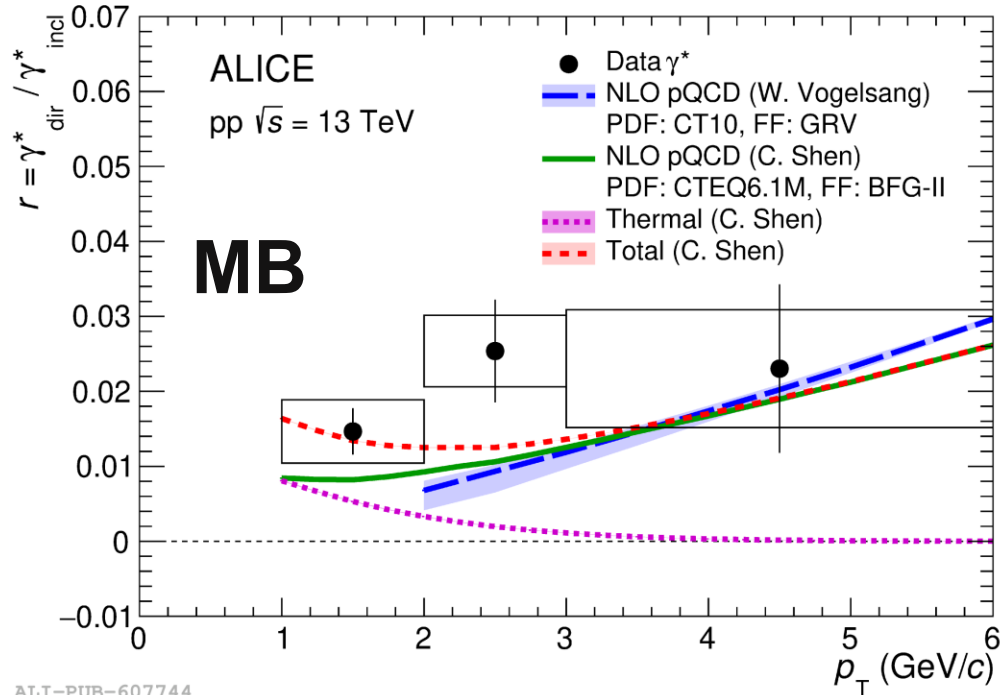
$$f_{\text{fit}} = r \times f_{\text{dir}} + (1 - r) \times f_{\text{LF}} + f_{\text{HF}}$$

- Direct-photon fraction r : only free parameter
- Spectrum fitted above pion mass
→ Large reduction of systematic uncertainties compared to real-photon measurement
- Access the real direct-photon yield: $\gamma^{\text{dir}} = r \cdot \gamma^{\text{incl}}$



Virtual direct-photon fraction

Search for thermal radiation in small systems



First significant measurement of direct photons in small systems at low p_T at the LHC
 → Signal observed in both event classes (MB: 3.2σ HM: 1.9σ)

Comparison to theoretical calculations

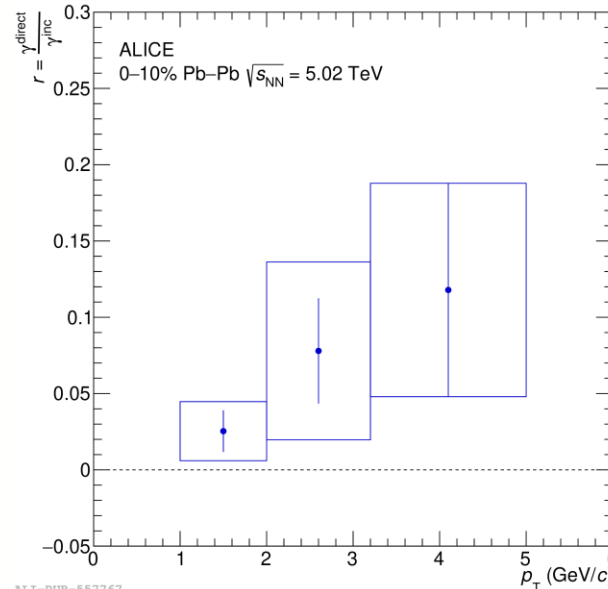
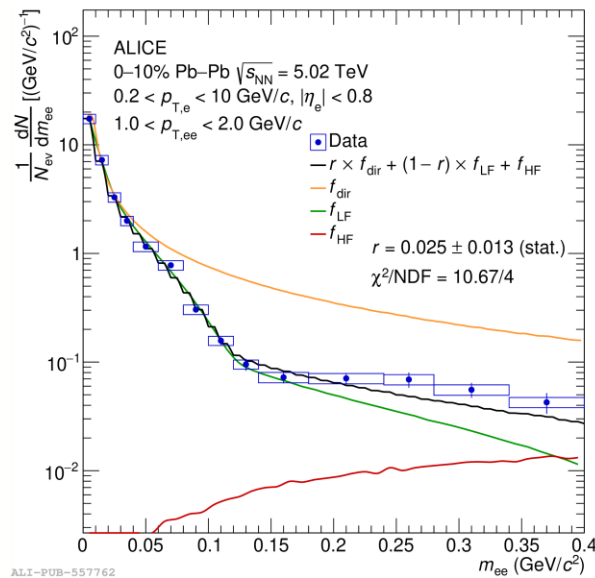
→ Additional scaling of the pQCD calculation for HM events

→ Data reproduced by **prompt only**, better description with **prompt + thermal radiation**

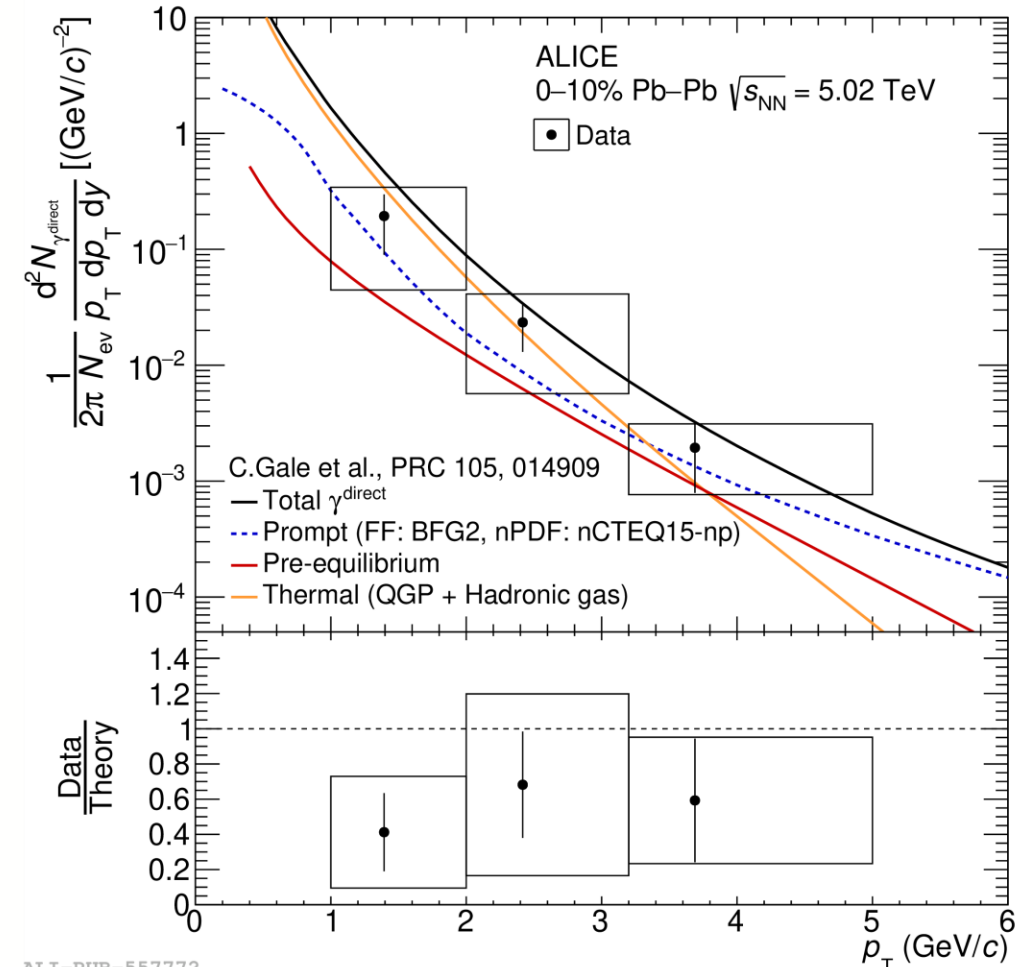


Virtual direct-photon fraction

Central Pb–Pb at $\sqrt{s_{NN}} = 5.02$ TeV



ALICE, arXiv:2308.16704, accepted by PRC



First direct-photon p_T -differential spectrum at $\sqrt{s_{NN}} = 5.02$ TeV

Hybrid model: Contributions from all stages of the collision

→ $N_{\gamma_{dir}}$ consistent with **only prompt** photons

However: All central values above pQCD baseline

→ Measurement also described by **full model** prediction

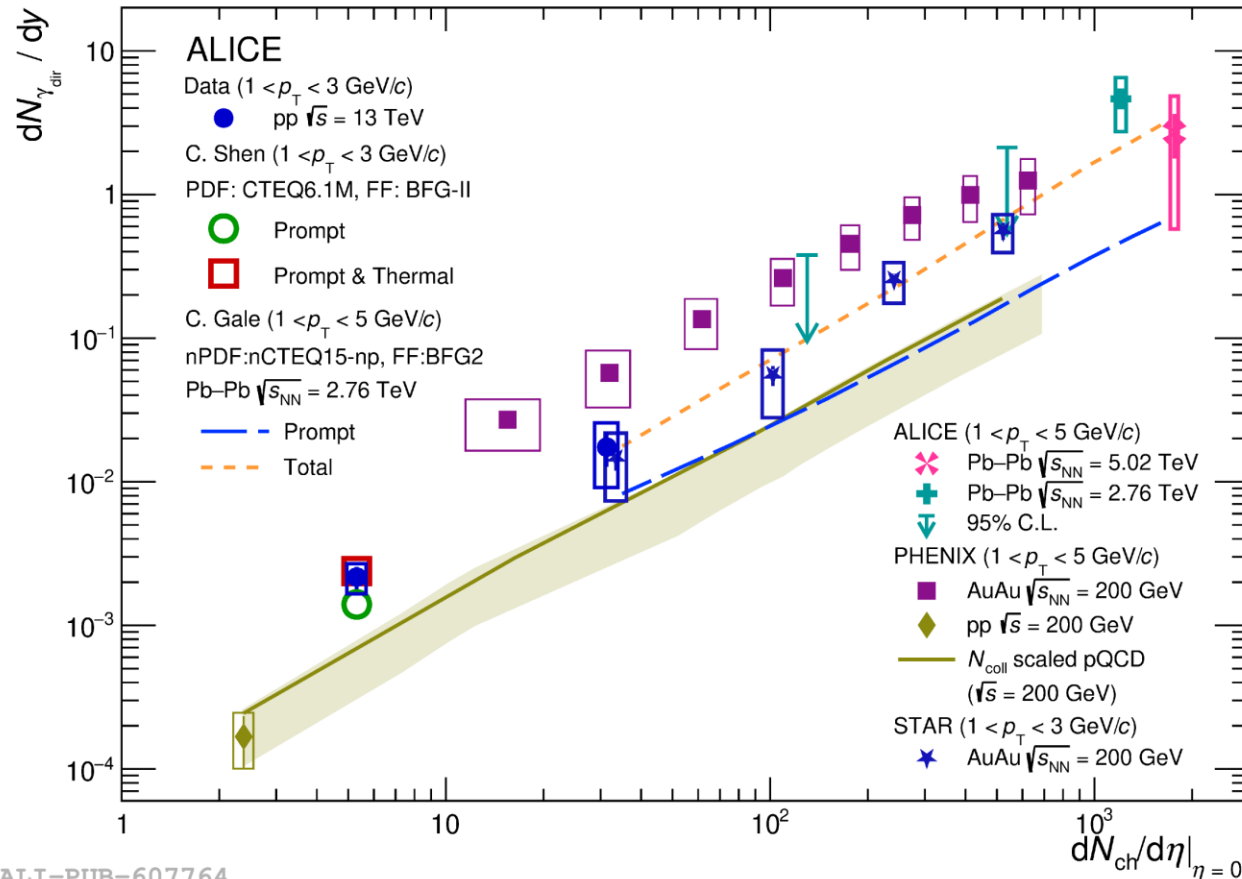
But: Data overestimated by $\sim 1\sigma$

ALI-PUB-557772



Direct-photon signal

p_T -integrated direct photon yields



Power-law dependence of direct-photon yield on charged-particle multiplicity proposed by PHENIX
→ Suggests scaling independent of energy or centrality

Real photons in 0-20% Pb-Pb at $\sqrt{s_{NN}} = 2.76$ TeV

ALICE, Phys. Lett. B 754 (2016) 235-248

Virtual photons in 0-10% Pb-Pb at $\sqrt{s_{NN}} = 5.02$ TeV

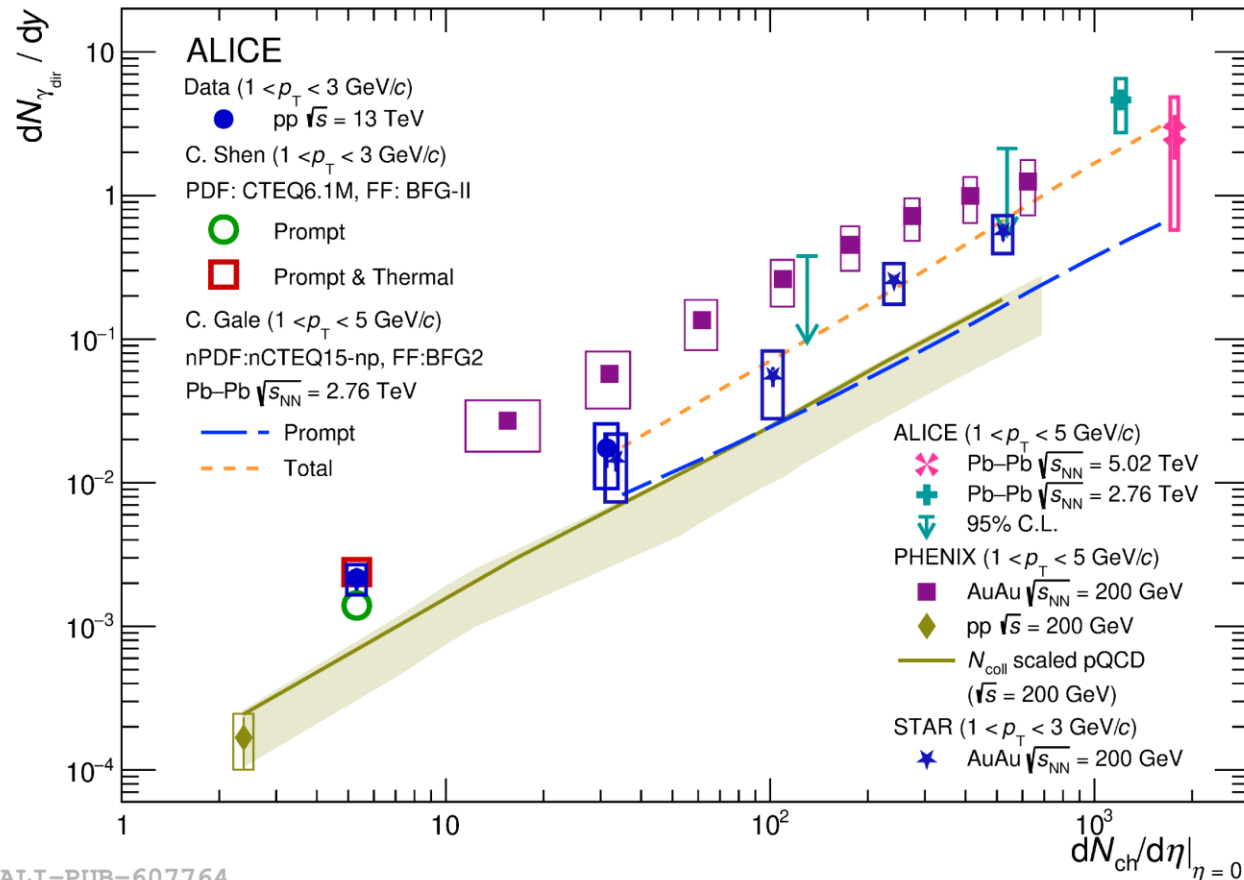
ALICE, arXiv:2308.16704, accepted by PRC

→ Both measurements consistent with model predictions



Direct-photon signal

p_T -integrated direct photon yields



Power-law dependence of direct-photon yield on charged-particle multiplicity proposed by PHENIX
→ Suggests scaling independent of energy or centrality

Real photons in 0-20% Pb-Pb at $\sqrt{s_{NN}} = 2.76$ TeV

ALICE, Phys. Lett. B 754 (2016) 235-248

Virtual photons in 0-10% Pb-Pb at $\sqrt{s_{NN}} = 5.02$ TeV

ALICE, arXiv:2308.16704, accepted by PRC

→ Both measurements consistent with model predictions

Virtual photons in pp at $\sqrt{s} = 13$ TeV

ALICE, Phys. Lett. B 868 (2025) 139645

→ Crucial inputs to constrain theoretical developments

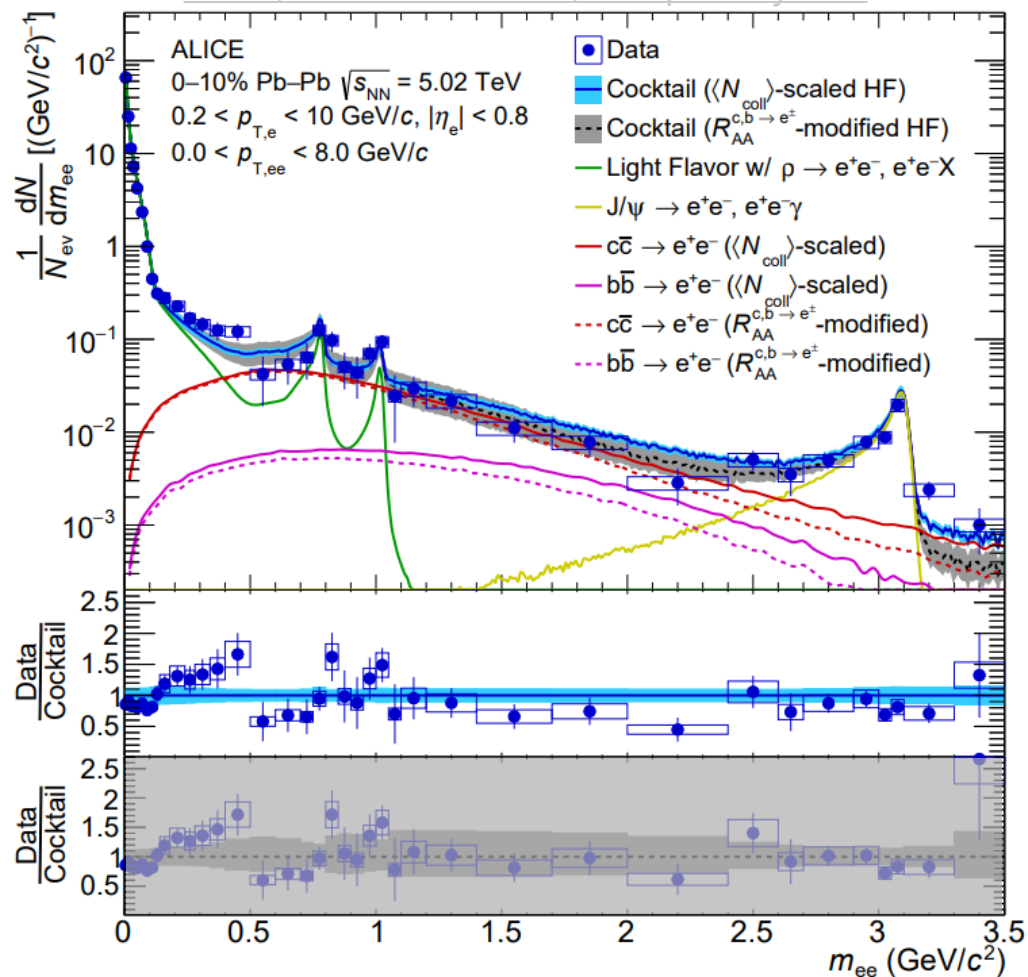
Results at LHC not sensitive enough yet to confirm:

- Universal scaling behavior
- Onset of thermal radiation

Dielectron production in central Pb–Pb at $\sqrt{s_{NN}} = 5.02$ TeV

Invariant-mass spectrum

ALICE, arXiv:2308.16704, accepted by PRC



Intermediate-mass region

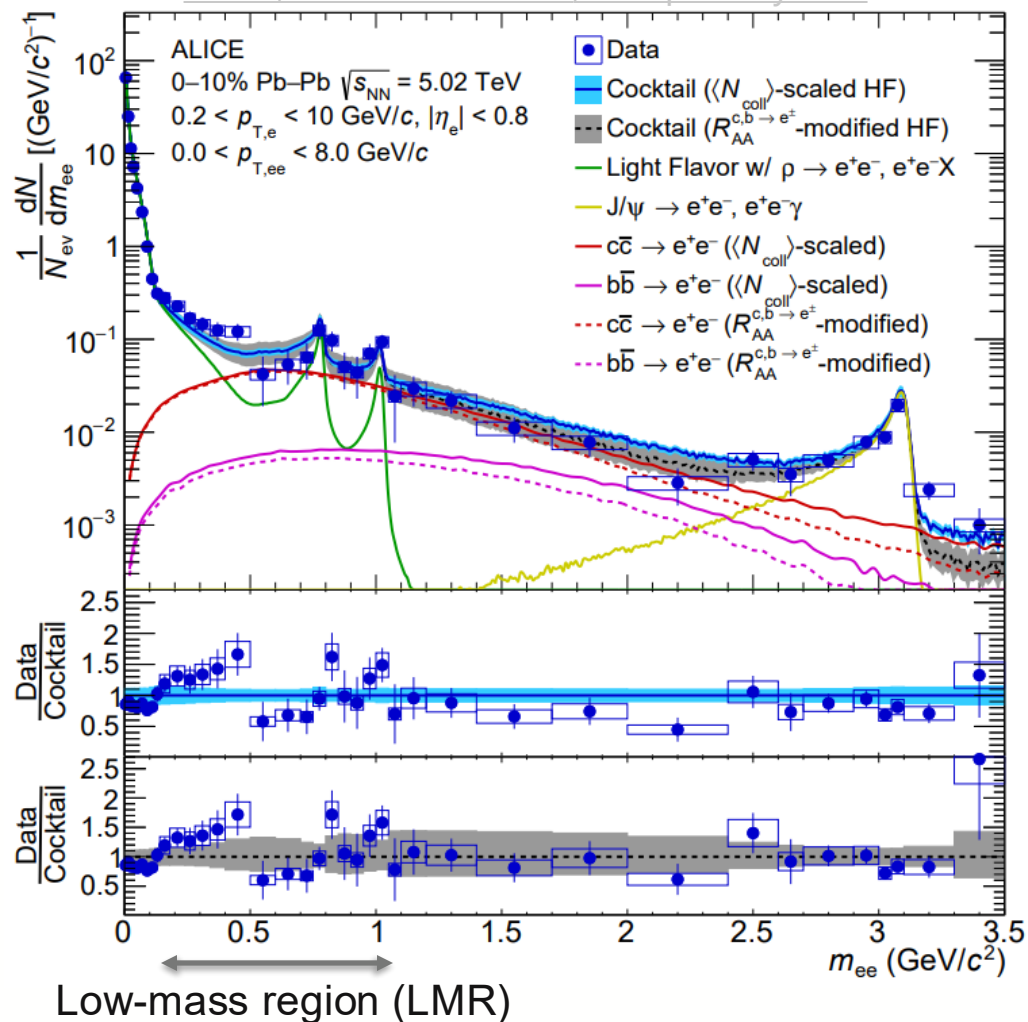
Comparison to hadronic cocktail, including:

- N_{coll} -scaled HF measured in pp at $\sqrt{s} = 5.02$ TeV
→ Vacuum baseline
- Good description of π^0 -Dalitz and J/ψ decays
- Indication of HF suppression compared to pp
- Expected due to cold-nuclear matter (CNM) and hot-nuclear matter (HNM) effects

Dielectron production in central Pb–Pb at $\sqrt{s_{NN}} = 5.02$ TeV

Invariant-mass spectrum

ALICE, arXiv:2308.16704, accepted by PRC

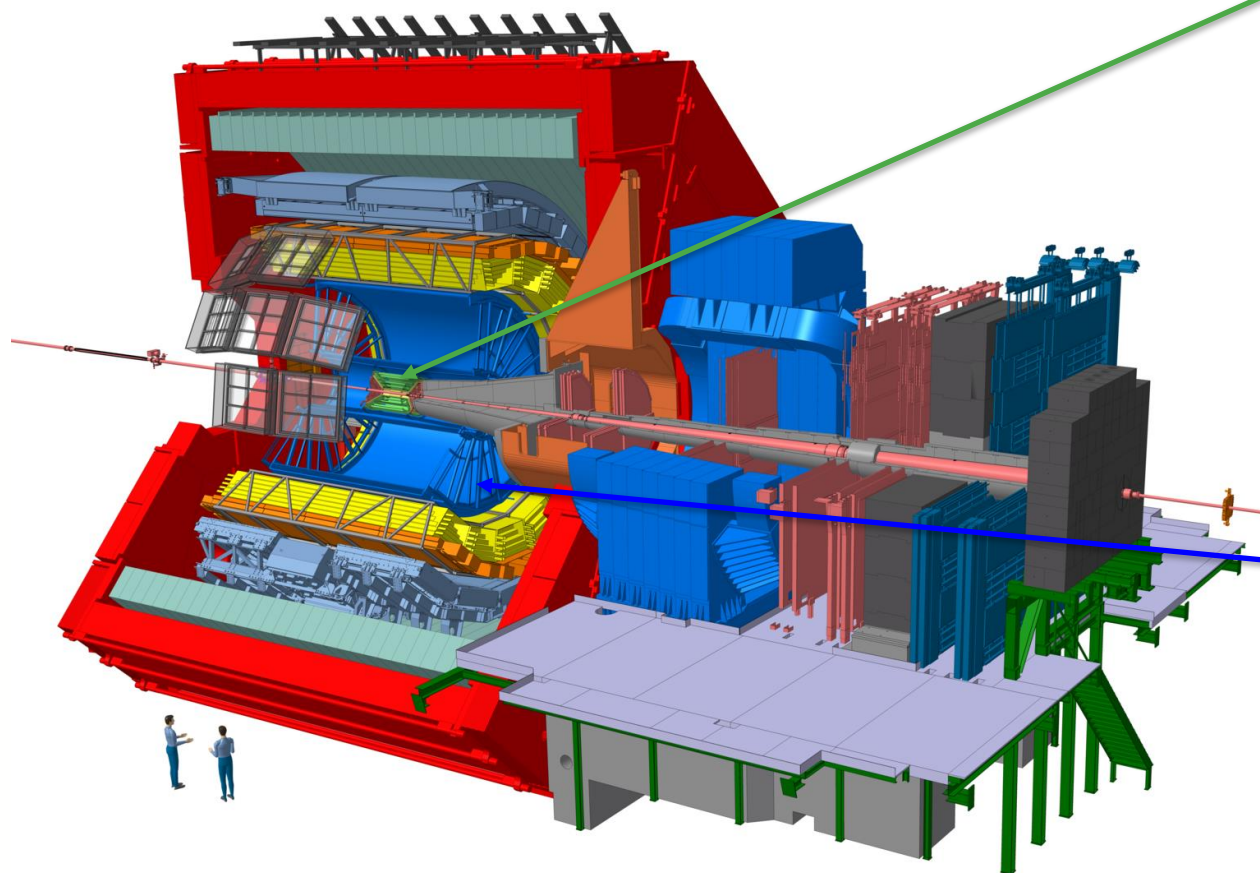


Comparison to hadronic cocktail, including:

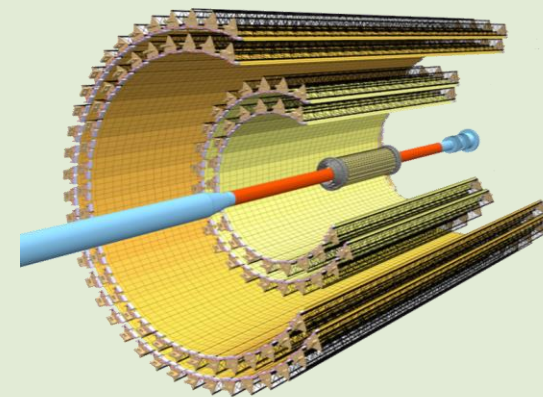
- N_{coll} -scaled HF measured in pp at $\sqrt{s} = 5.02$ TeV
→ Vacuum baseline
 - Include measured R_{AA} of $c/b \rightarrow e^{\pm}$
→ Modified-HF cocktail
- Overall improved description of the data including the HF suppression
- A hint for an excess at low m_{ee} (1.3σ)

ALICE apparatus

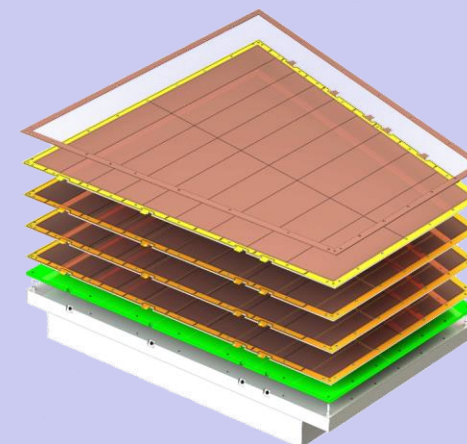
Run 3 upgrades



Inner Tracking System
→ CMOS MAPS technology

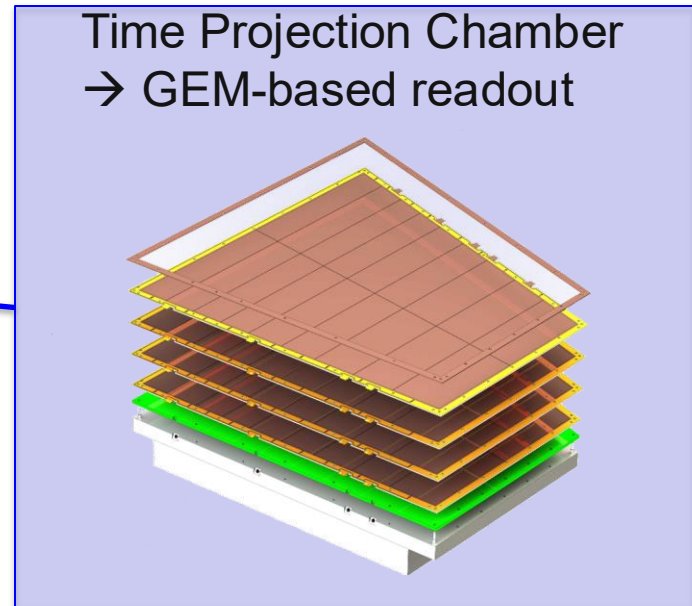
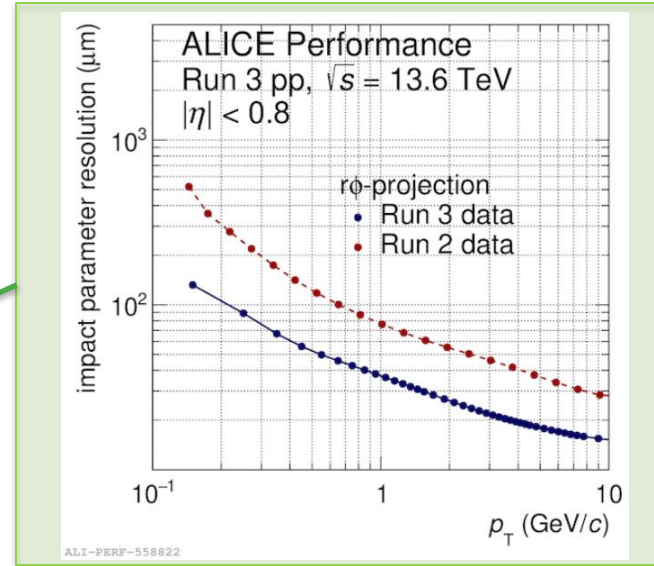
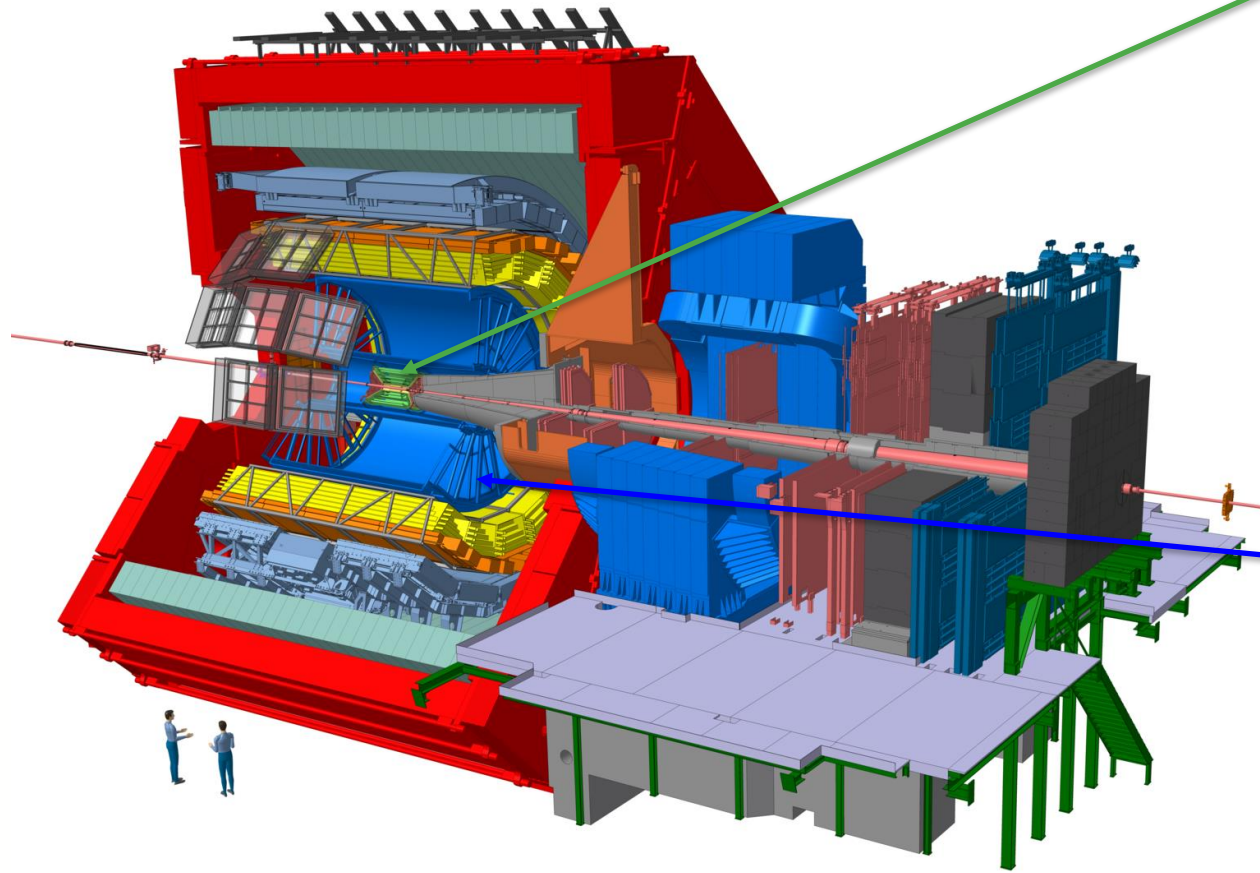


Time Projection Chamber
→ GEM-based readout



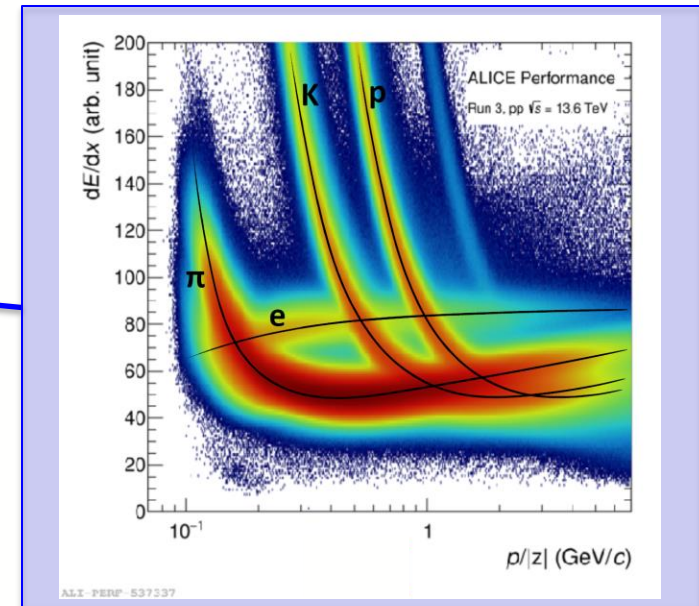
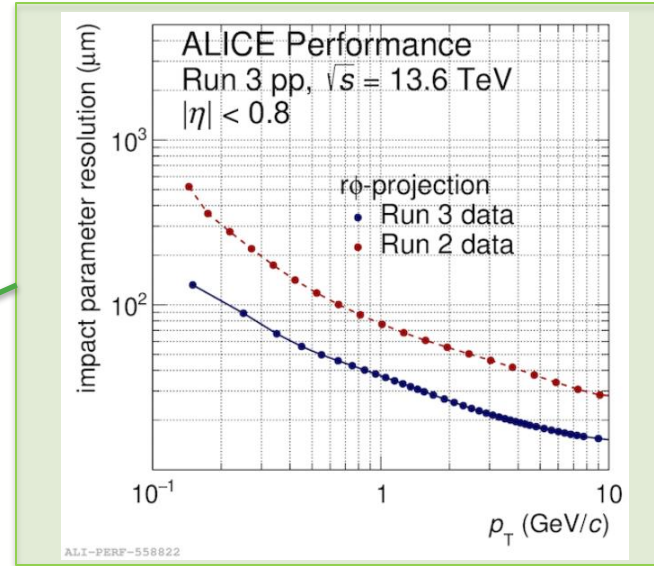
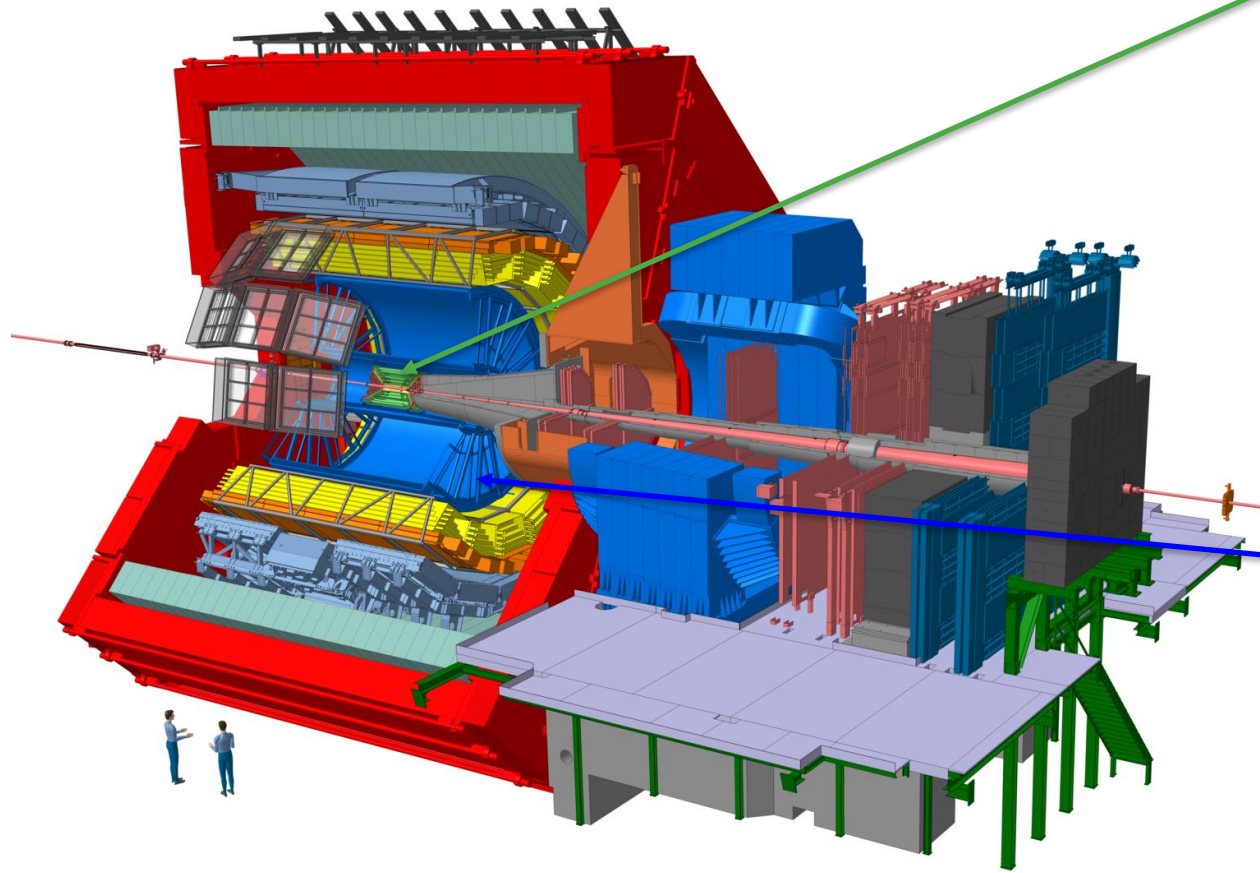
ALICE apparatus

Run 3 upgrades



ALICE apparatus

Run 3 upgrades



Dielectron production in Run 3

Raw yield in pp collisions at $\sqrt{s} = 13.6$ TeV

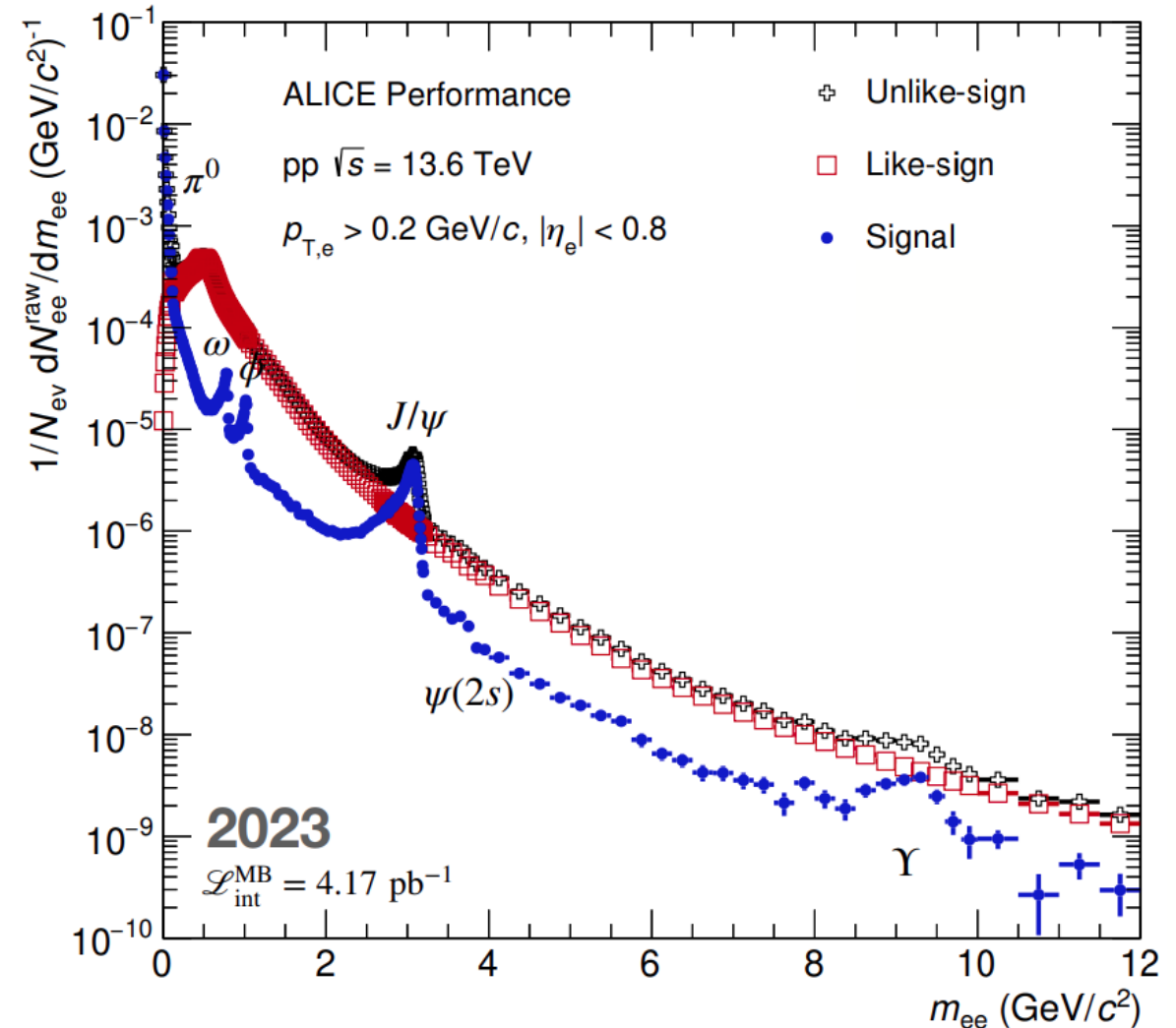
Run 3: $277 \cdot 10^9$ analysed MB events (2023)

→ Factor ~600 more compared to Run 2

Spectrum shows all key features of resonances with high precision

Large statistics allows to extract dielectron signal up to inv. mass of the Υ -meson

Entering a new era of precision measurements for dielectrons



ALI-PERF-603584



Dielectron production in Run 3

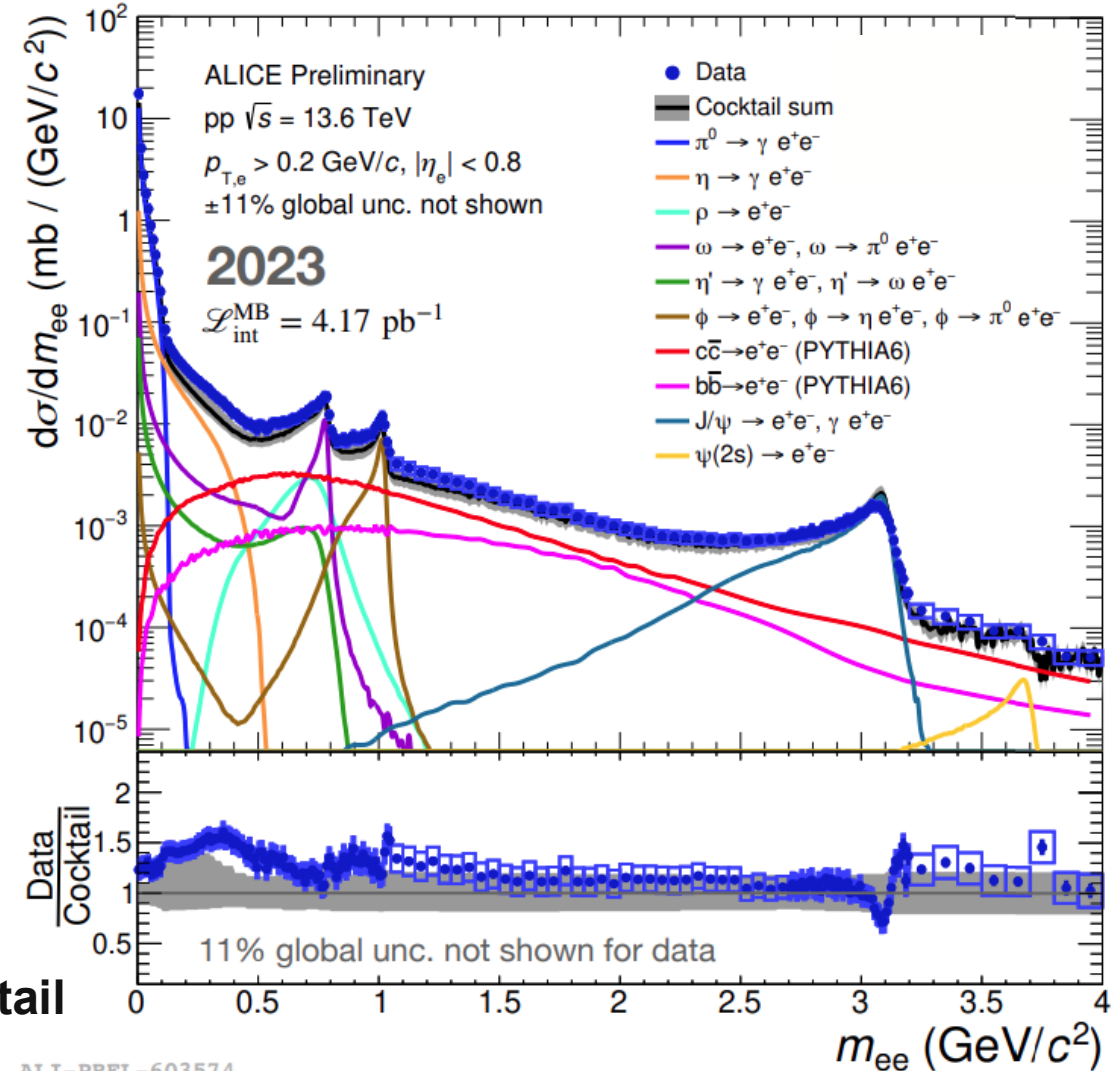
Corrected spectrum

First dielectron cross section from pp collisions at $\sqrt{s} = 13.6$ TeV in Run 3

Cocktail of expected dielectron sources based on Run 2 measurements:

- **Light**-flavour: Measured hadron spectra from pp 13 TeV
- **Heavy**-flavour: PYTHIA calculations fitted to dielectron results in pp 13 TeV
 - Energy dependence estimated with FONLL calculations
- Detector resolution from Run 3 applied
 - Different material budget due to new Run 3 detectors

Ratio shows overall agreement between **data** & **cocktail**



ALI-PREL-603574



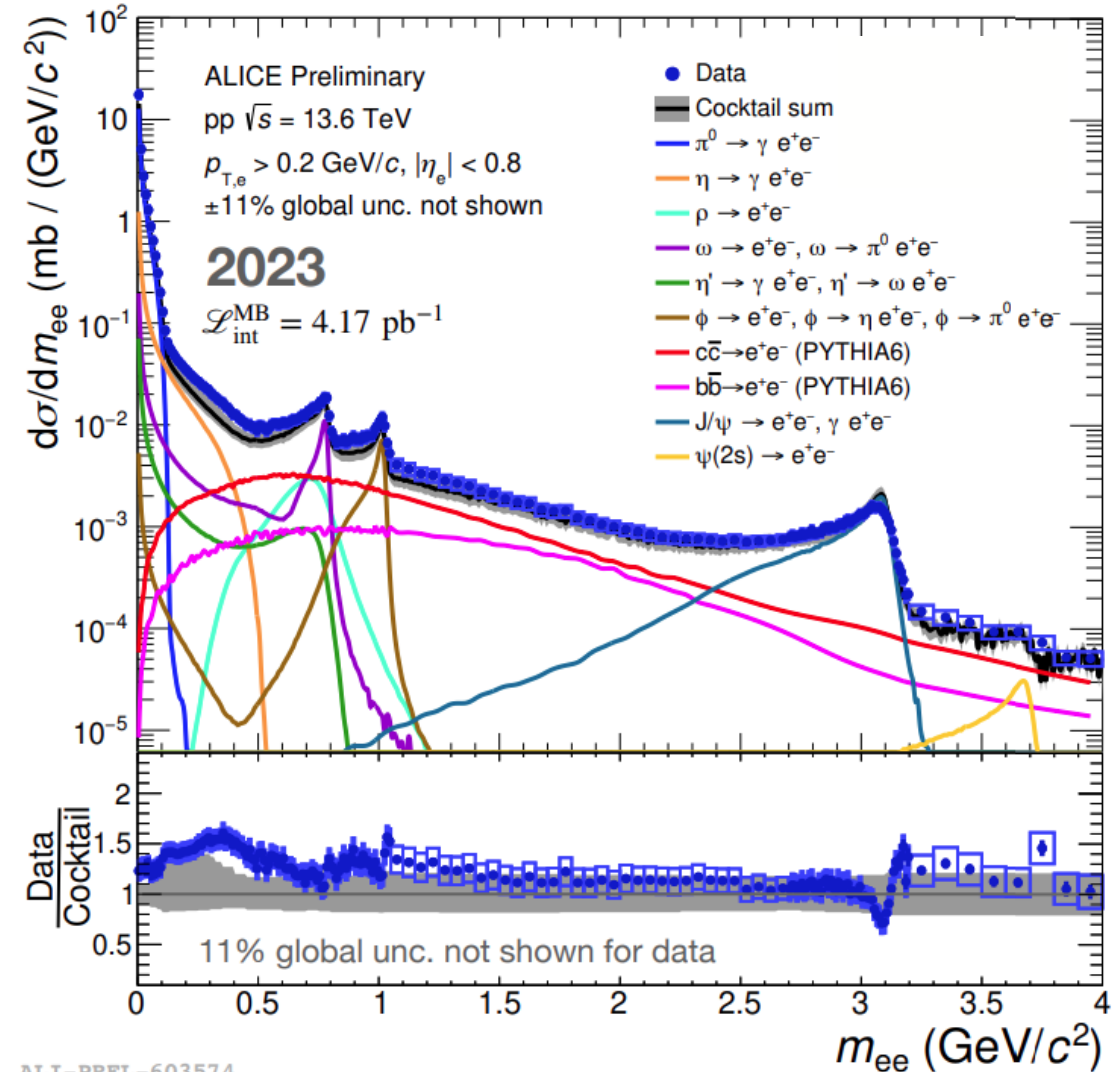
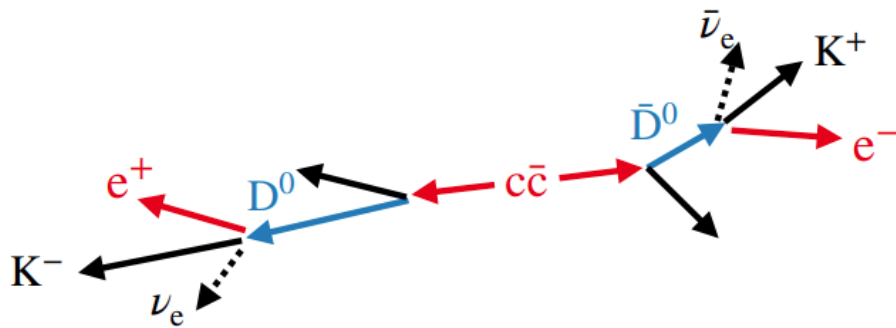
Dielectron production in Run 3

Corrected spectrum

Measurement of prompt sources in IMR:
- Drell–Yan, Thermal radiation

Intermediate mass range dominated by open heavy-flavour decays
→ Requires high precision of heavy-flavour sources
Very challenging with cocktail method

Exploit long lifetime of D- and B-mesons
- $(c\tau)_D$: $\sim 150 \mu m$, $(c\tau)_B$: $\sim 450 \mu m$



ALI-PREL-603574

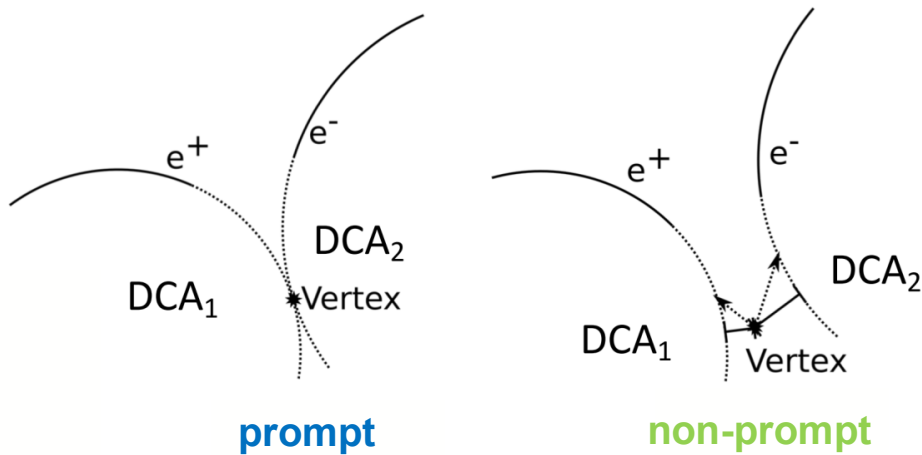
Goal: Unfold spectra through characteristic decay topologies



Dielectron production in Run 3

Separation of prompt and non-prompt sources

Distance-of-closest approach (DCA):



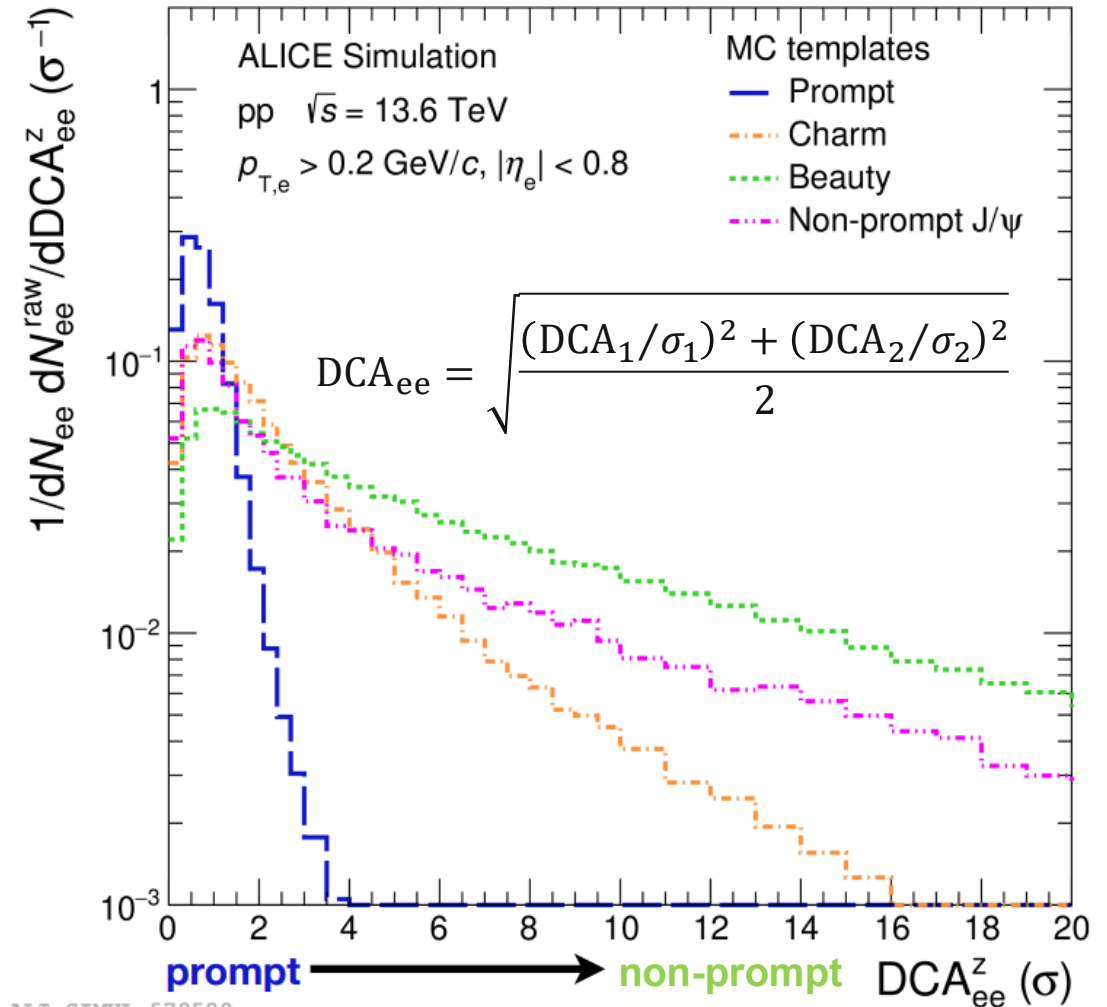
Decay length of charm and beauty hadrons much larger than that of prompt sources

→ Electrons do not point back the vertex

Method only relies on the well-known decay kinematic

→ Established during Run 2

→ Independent of cocktail and theory input

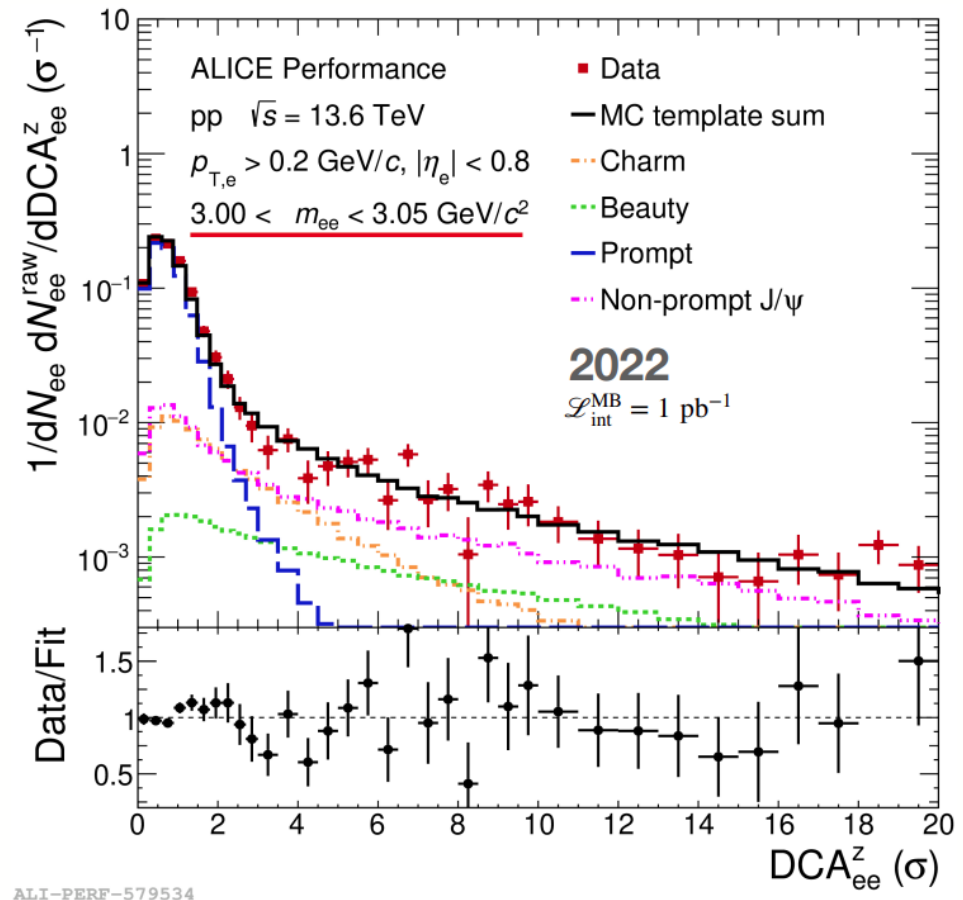
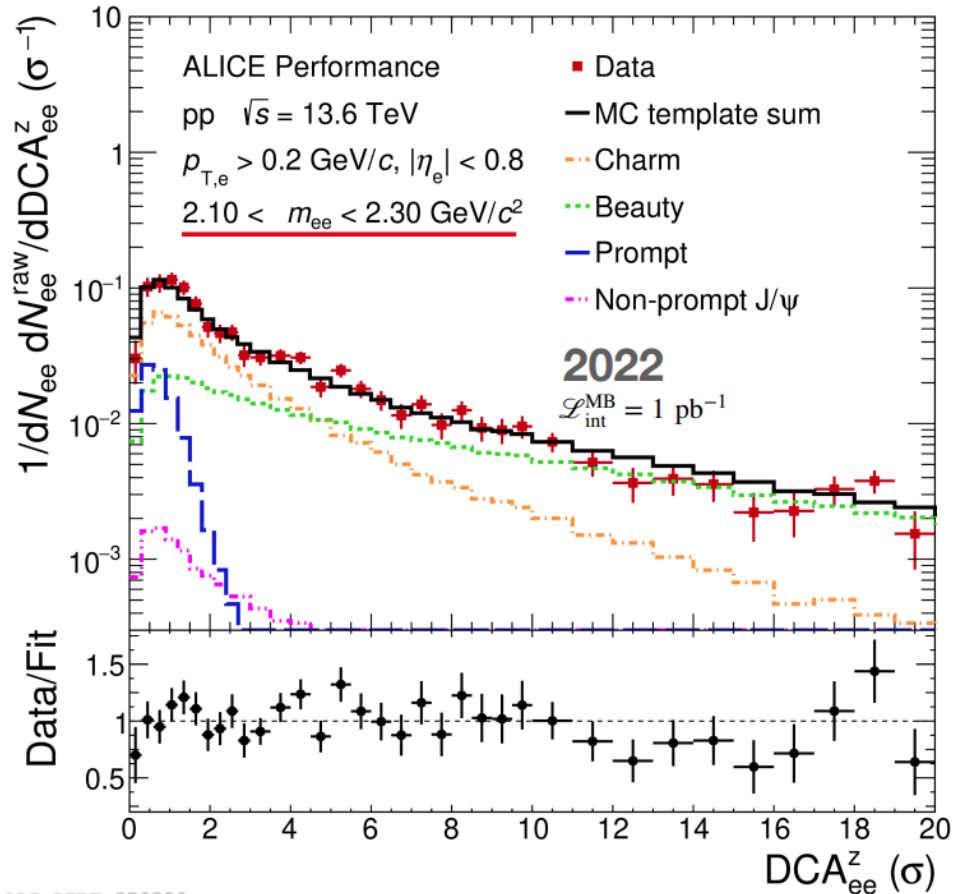


ALI-SIMUL-579529



Dielectron production in Run 3

Separation of prompt and non-prompt sources



Perform template fit differential in small mass intervals to unfold contributions in raw spectra
 → Good description of the data over a wide DCA range

Dielectron production in Run 3

Separation of prompt and non-prompt sources

First raw inv. mass spectra unfolded by source topology

Well separated prompt and non-prompt sources

Prompt:

- Clear resonance structures of pseudoscalar and vector mesons

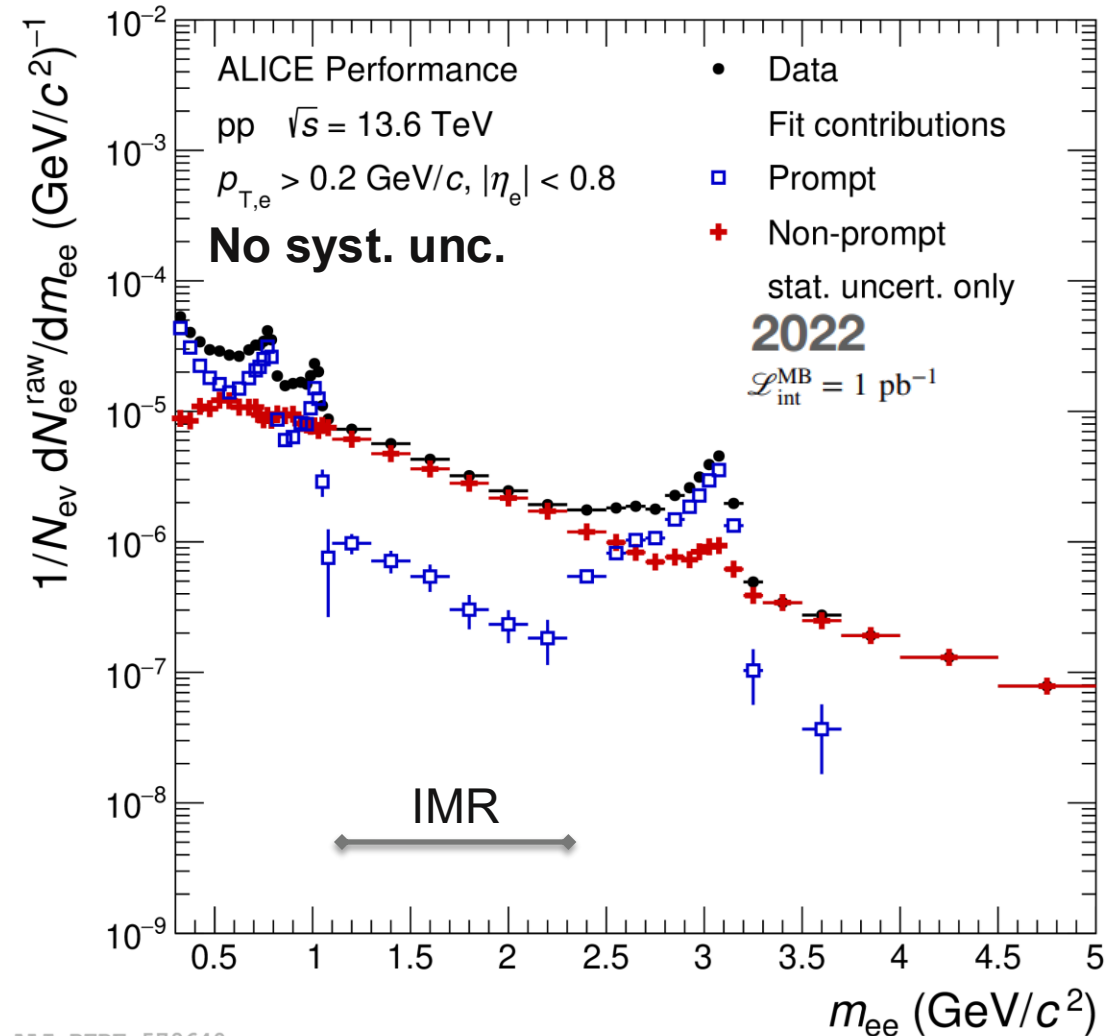
Non-prompt:

- Heavy-flavour continuum + non-prompt J/ψ

Fit prefers a prompt contribution in the Intermediate mass range (IMR: $1.1 < m_{ee} < 2.3 \text{ GeV}/c^2$)

→ Showcase of capabilities of new detector and analysis technique

→ Important baseline for Pb–Pb measurements

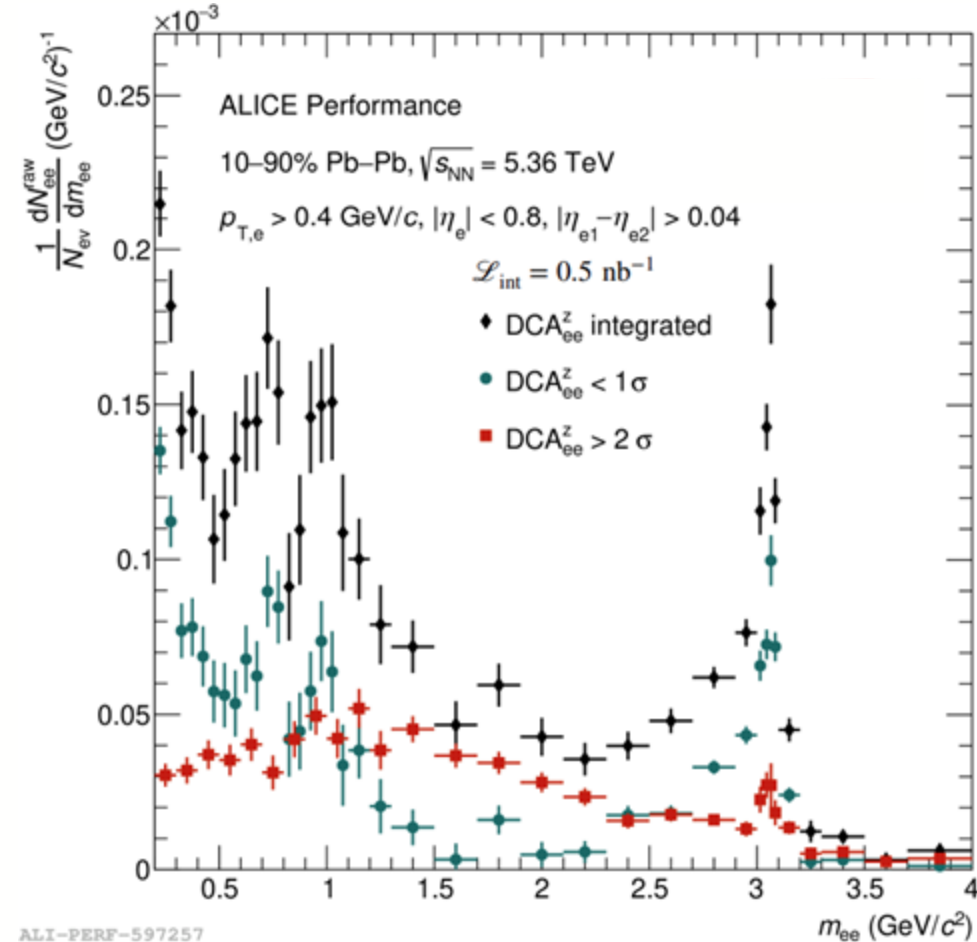
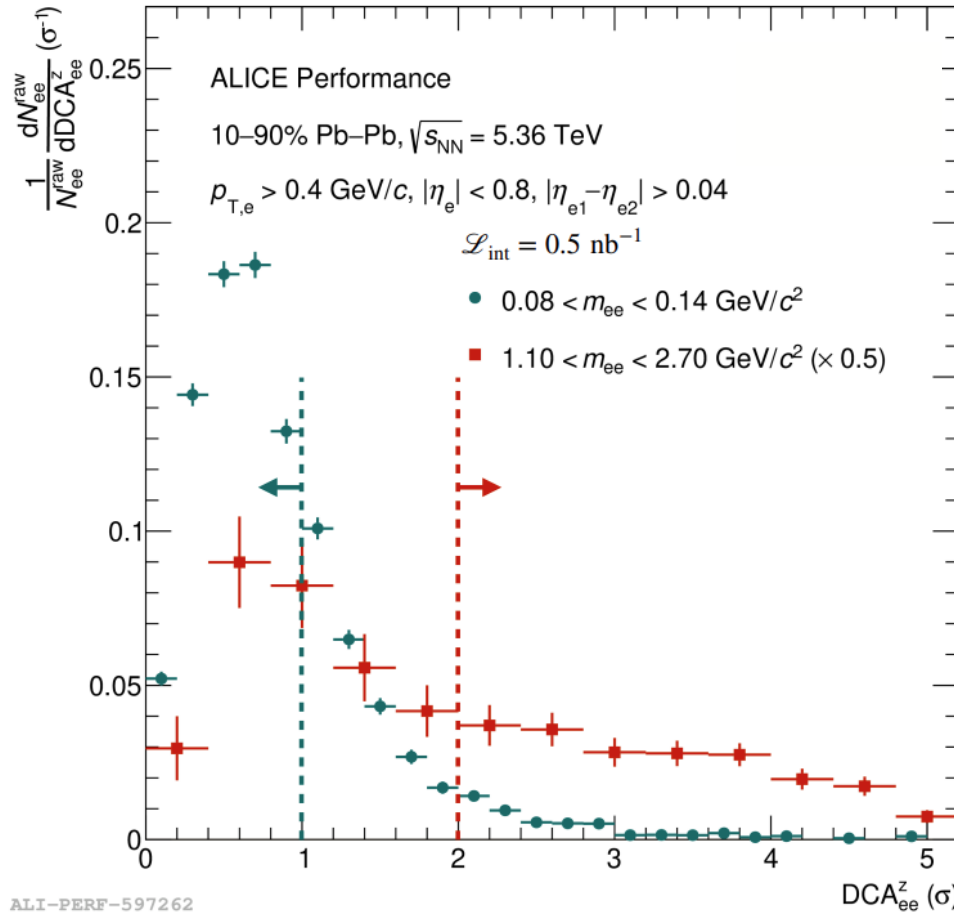


ALI-PERF-579640



Dielectron production in Run 3

Raw yield in Pb–Pb collisions at $\sqrt{s_{NN}} = 5.36$ TeV



First dielectron spectra of the new 2023 and 2024 Pb–Pb data

→ $3.8 \cdot 10^9$ analysed events in 10–90% centrality (Factor ~60 compared to Run 2)

→ Selection shows good separation of prompt & non-prompt sources



Summary

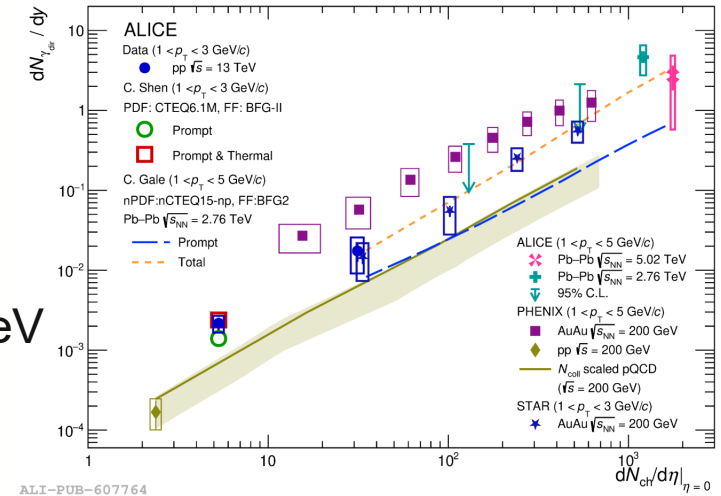
Analyses from Run 2 are finalized

Analysis of full Run 2 dataset of pp at $\sqrt{s} = 13$ TeV

→ Extraction of direct-photon fraction in MB & HM events

Measurement of dielectron production in central Pb–Pb at $\sqrt{s_{NN}} = 5.02$ TeV

→ First measurement of direct-photon yield

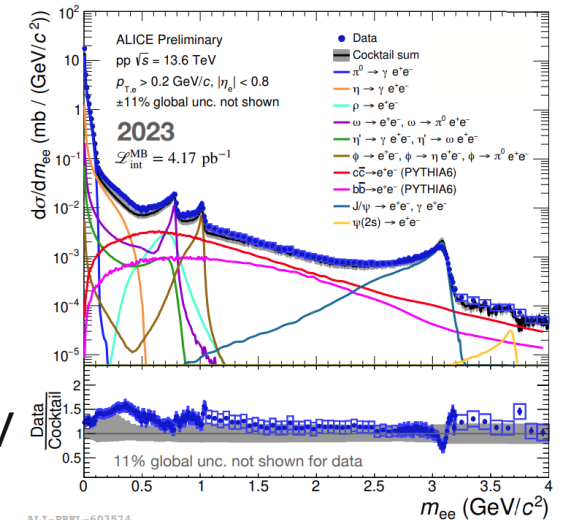


Data taken in Run 3/4 will significantly increase the precision of these results

- First corrected dielectron spectrum in pp at $\sqrt{s} = 13.6$ TeV

- First unfolded inv. mass spectra by source topology

- First raw inv. mass spectrum with DCA_{ee} selections in Pb–Pb at $\sqrt{s_{NN}} = 5.36$ TeV



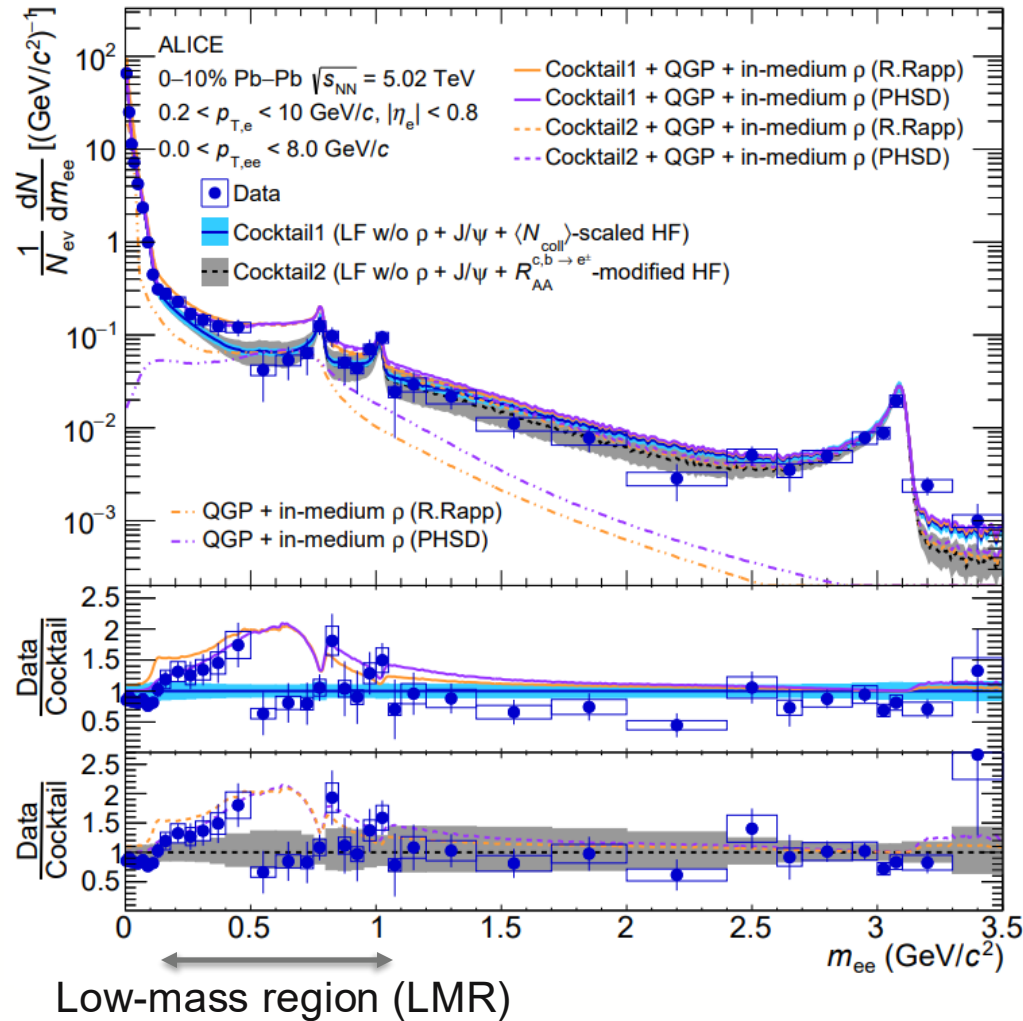


Backup

Dielectron production in central Pb–Pb at $\sqrt{s_{NN}} = 5.02$ TeV

Invariant-mass spectrum

ALICE, arXiv:2308.16704



Comparison to hadronic cocktail, including:

- N_{coll} -scaled HF measured in pp at $\sqrt{s} = 5.02$ TeV
→ Vacuum baseline
- Include measured R_{AA} of $c/b \rightarrow e^\pm$
→ Modified-HF cocktail

Comparison to theoretical models: **R. Rapp** & **PHSD**

Rapp, Adv. HEP. 2013 (2013) 148253

PHSD, PRC 97 (2018) 064907

→ Excess in LMR: Expected from ρ mesons produced thermally in the medium

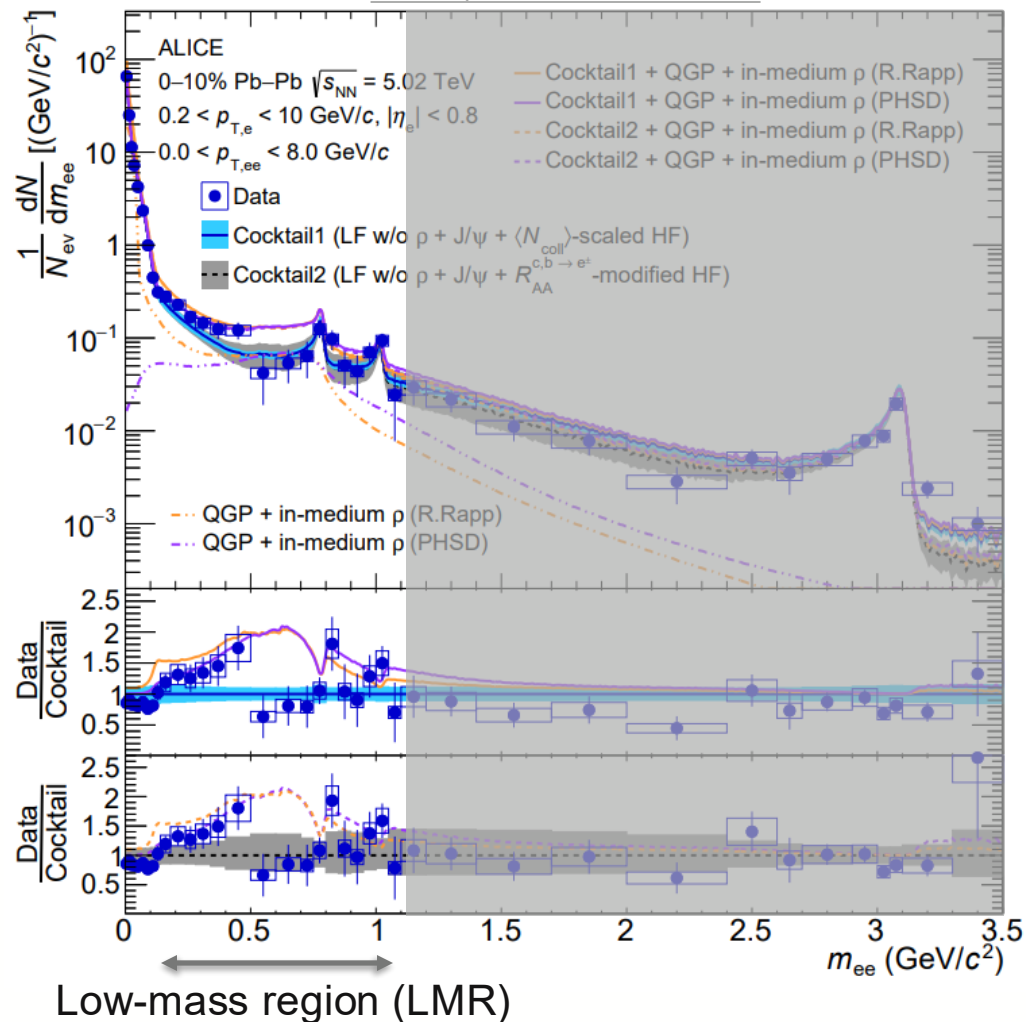
→ Short lifetime and strong coupling to $\pi^+\pi^-$ channel

→ Regeneration in the hot hadronic phase & broadening of its spectral function

Dielectron production in central Pb–Pb at $\sqrt{s_{NN}} = 5.02$ TeV

Invariant-mass spectrum

ALICE, arXiv:2308.16704



Comparison to hadronic cocktail, including:

- N_{coll} -scaled HF measured in pp at $\sqrt{s} = 5.02$ TeV
→ Vacuum baseline
- Include measured R_{AA} of $c/b \rightarrow e^\pm$
→ Modified-HF cocktail

Comparison to theoretical models: **R. Rapp** & **PHSD**

Rapp, Adv. HEP. 2013 (2013) 148253

PHSD, PRC 97 (2018) 064907

→ Excess in LMR: Expected from ρ mesons produced thermally in the medium

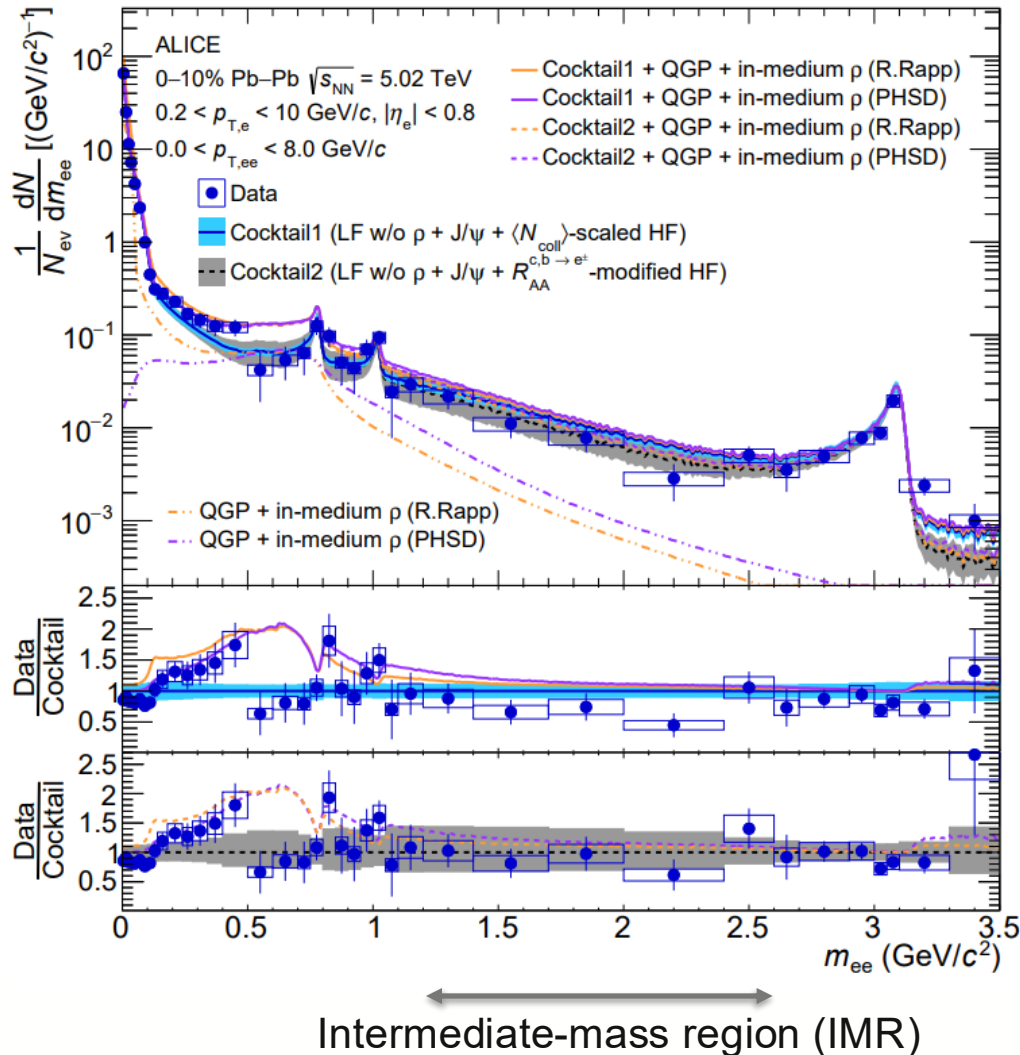
→ Short lifetime and strong coupling to $\pi^+\pi^-$ channel

→ Regeneration in the hot hadronic phase & broadening of its spectral function

Dielectron production in central Pb–Pb at $\sqrt{s_{NN}} = 5.02$ TeV

Invariant-mass spectrum

ALICE, arXiv:2308.16704



Comparison to hadronic cocktail, including:

- N_{coll} -scaled HF measured in pp at $\sqrt{s} = 5.02$ TeV
→ Vacuum baseline
- Include measured R_{AA} of $c/b \rightarrow e^\pm$
→ Modified-HF cocktail

Focus on IMR:

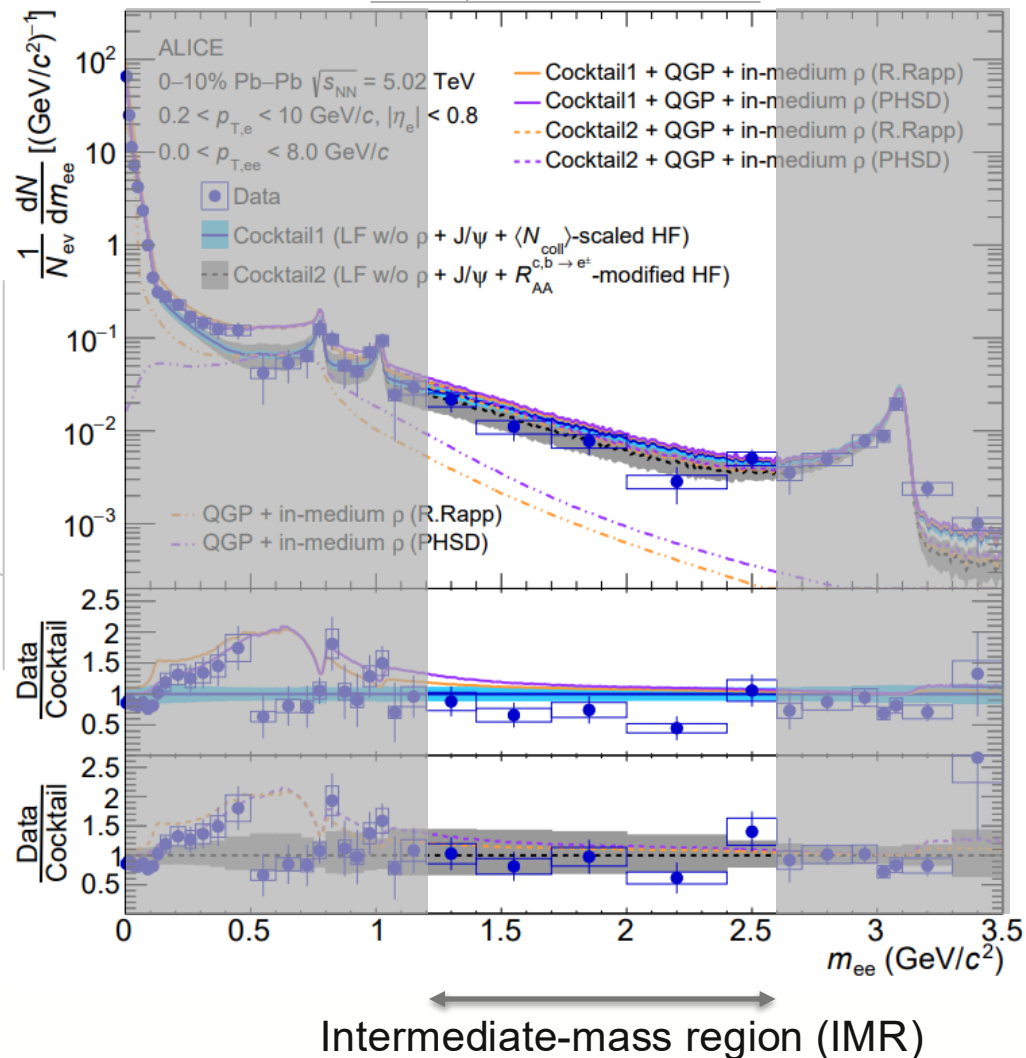
→ Dominated by HF contributions

→ Most sensitive for radiation of the QGP

Dielectron production in central Pb–Pb at $\sqrt{s_{NN}} = 5.02$ TeV

Invariant-mass spectrum

ALICE, arXiv:2308.16704



Comparison to hadronic cocktail, including:

- N_{coll} -scaled HF measured in pp at $\sqrt{s} = 5.02$ TeV
→ Vacuum baseline
- Include measured R_{AA} of $c/b \rightarrow e^\pm$
→ Modified-HF cocktail

Focus on IMR:

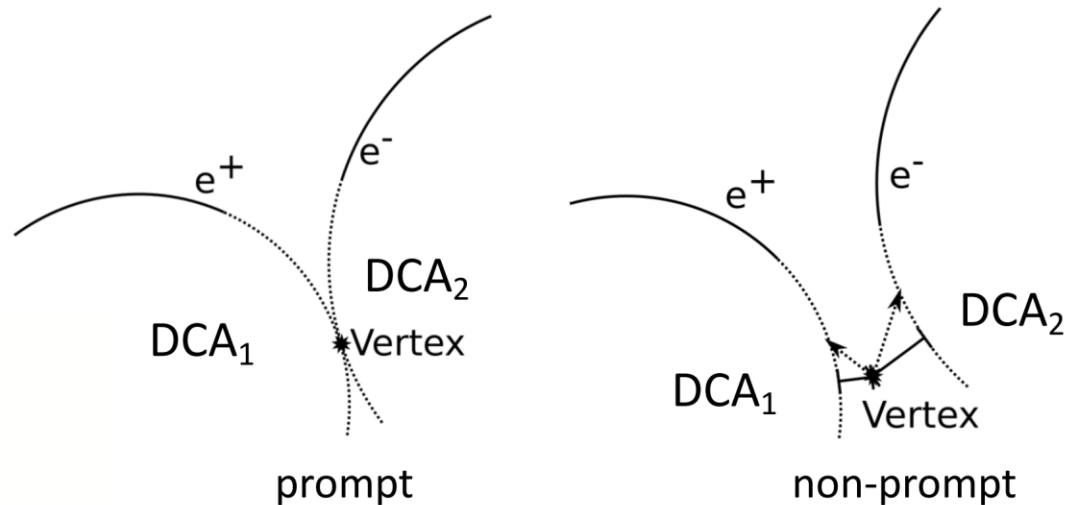
→ Dominated by HF contributions

→ Most sensitive for radiation of the QGP

Topological separation

Approach

Distance-of-closest approach (DCA):



→ $DCA_{ee}(\text{thermal}) < DCA_{ee}(\text{HF})$

Separation of prompt and non-prompt sources based on their decay topology:

- Decay length of charm and beauty hadrons much larger than that of prompt sources
- Electrons do not point back the vertex

DCA for pairs taking into account the DCA resolution:

$$DCA_{ee} = \sqrt{\frac{(DCA_1/\sigma_1)^2 + (DCA_2/\sigma_2)^2}{2}}$$

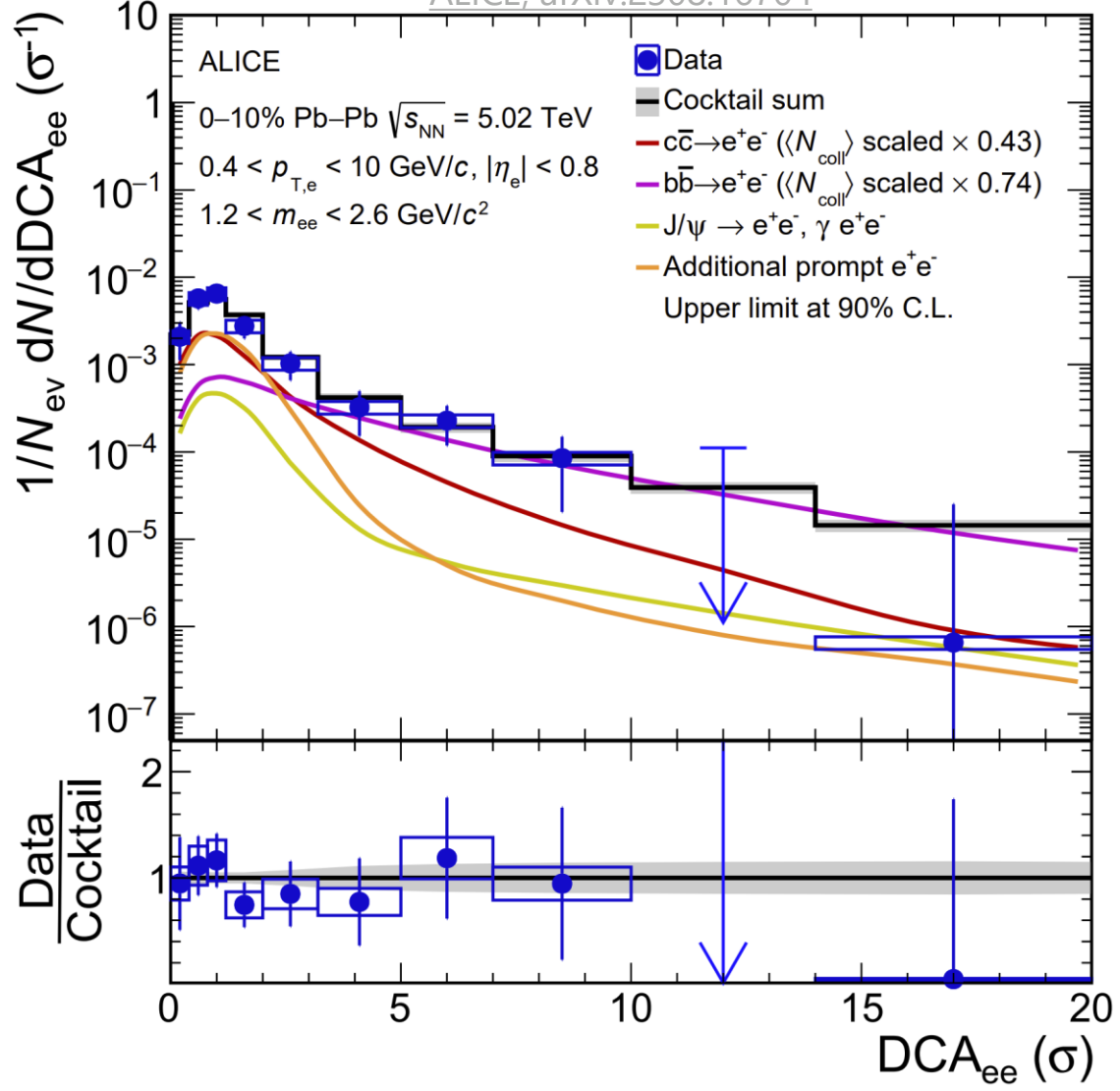
- Method only relies on the well-known decay kinematic
- Independent of cocktail and theory input



Dielectron production in central Pb–Pb at $\sqrt{s_{NN}} = 5.02$ TeV

Topological separation - DCA_{ee} in IMR fitted

ALICE, arXiv:2308.16704



Extraction of prompt thermal signal via template fits:

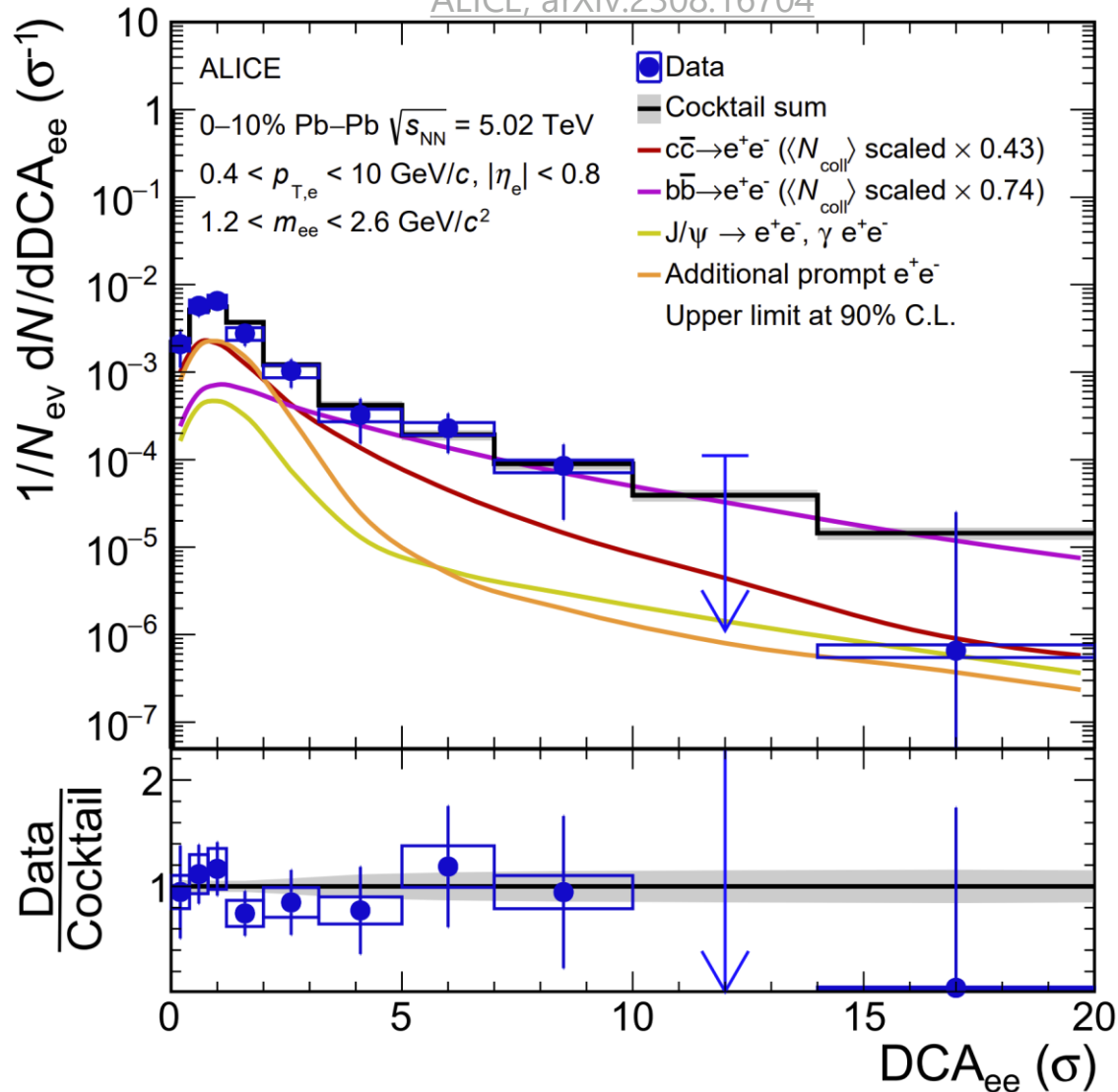
- Beauty contribution fixed via separate fit at high $p_{T,ee}$
 $b\bar{b}$: $0.74 \pm 0.24(\text{stat.}) \pm 0.12(\text{syst.})$ (w.r.t. N_{coll} scaling)
- Simultaneous fit of charm and prompt contribution
 $c\bar{c}$: $0.43 \pm 0.40(\text{stat.}) \pm 0.22(\text{syst.})$ (w.r.t. N_{coll} scaling)
 prompt: $2.64 \pm 3.18(\text{stat.}) \pm 0.29(\text{syst.})$ (w.r.t. R. Rapp)



Dielectron production in central Pb–Pb at $\sqrt{s_{NN}} = 5.02$ TeV

Topological separation - DCA_{ee} in IMR fitted

ALICE, arXiv:2308.16704



Extraction of prompt thermal signal via template fits:

- Beauty contribution fixed via separate fit at high $p_{T,ee}$
 $b\bar{b}$: $0.74 \pm 0.24(\text{stat.}) \pm 0.12(\text{syst.})$ (w.r.t. N_{coll} scaling)
- Simultaneous fit of charm and prompt contribution
 $c\bar{c}$: $0.43 \pm 0.40(\text{stat.}) \pm 0.22(\text{syst.})$ (w.r.t. N_{coll} scaling)
 prompt: $2.64 \pm 3.18(\text{stat.}) \pm 0.29(\text{syst.})$ (w.r.t. R. Rapp)

Results in agreement with:

- Charm suppression
- Thermal contribution in the order of expectations by Rapp/PHSD

Method independent of hadronic cocktail:

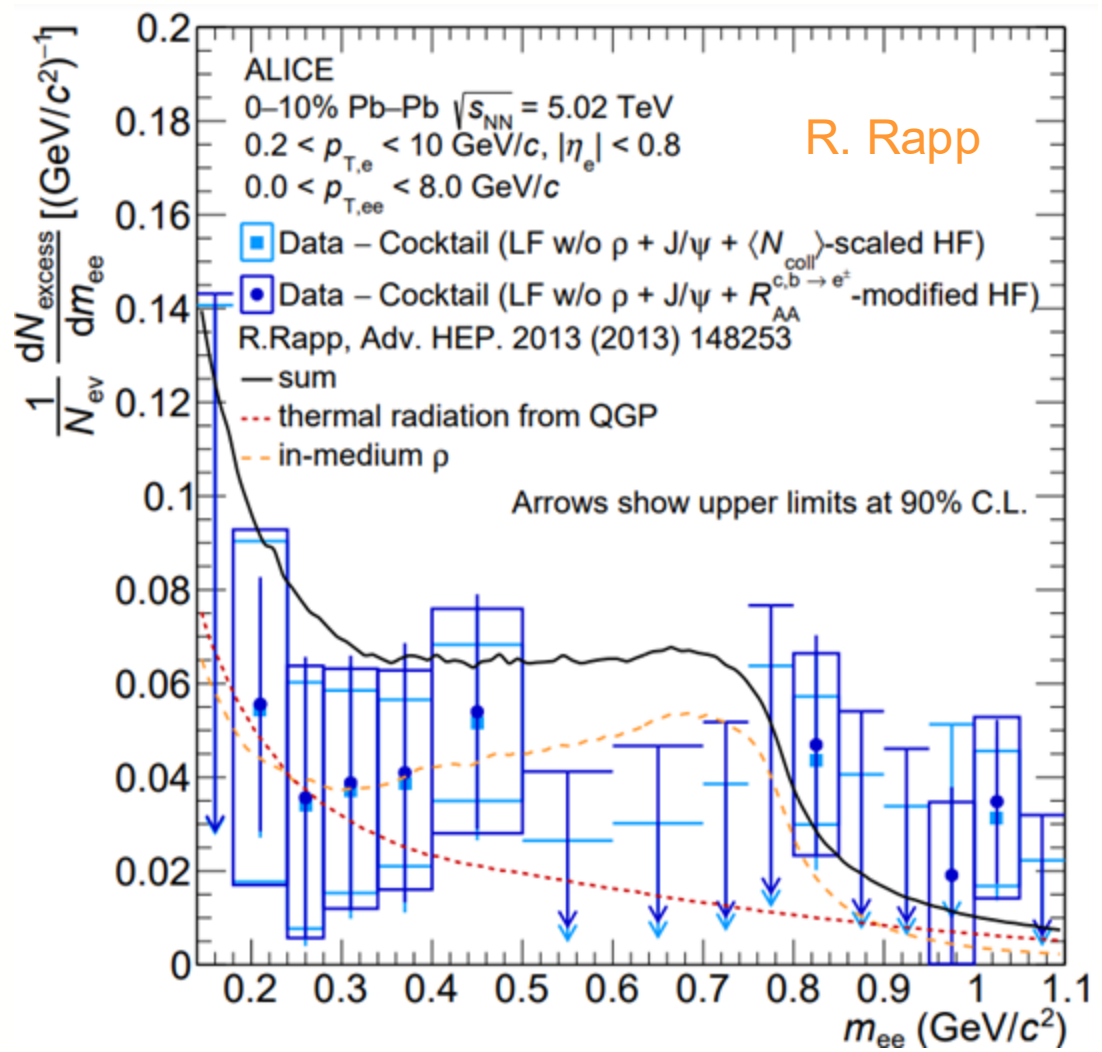
- Smaller syst. uncertainties
- More statistics enables the extraction of a thermal dielectron yield in the IMR



Dielectron production in central Pb–Pb at $\sqrt{s_{NN}} = 5.02$ TeV

Excess spectrum

ALICE, arXiv:2308.16704



Subtraction of known hadronic sources without ρ

Compared with sum of 2 contributions:

- In-medium ρ produced thermally in hot hadronic matter
- Thermal radiation from QGP

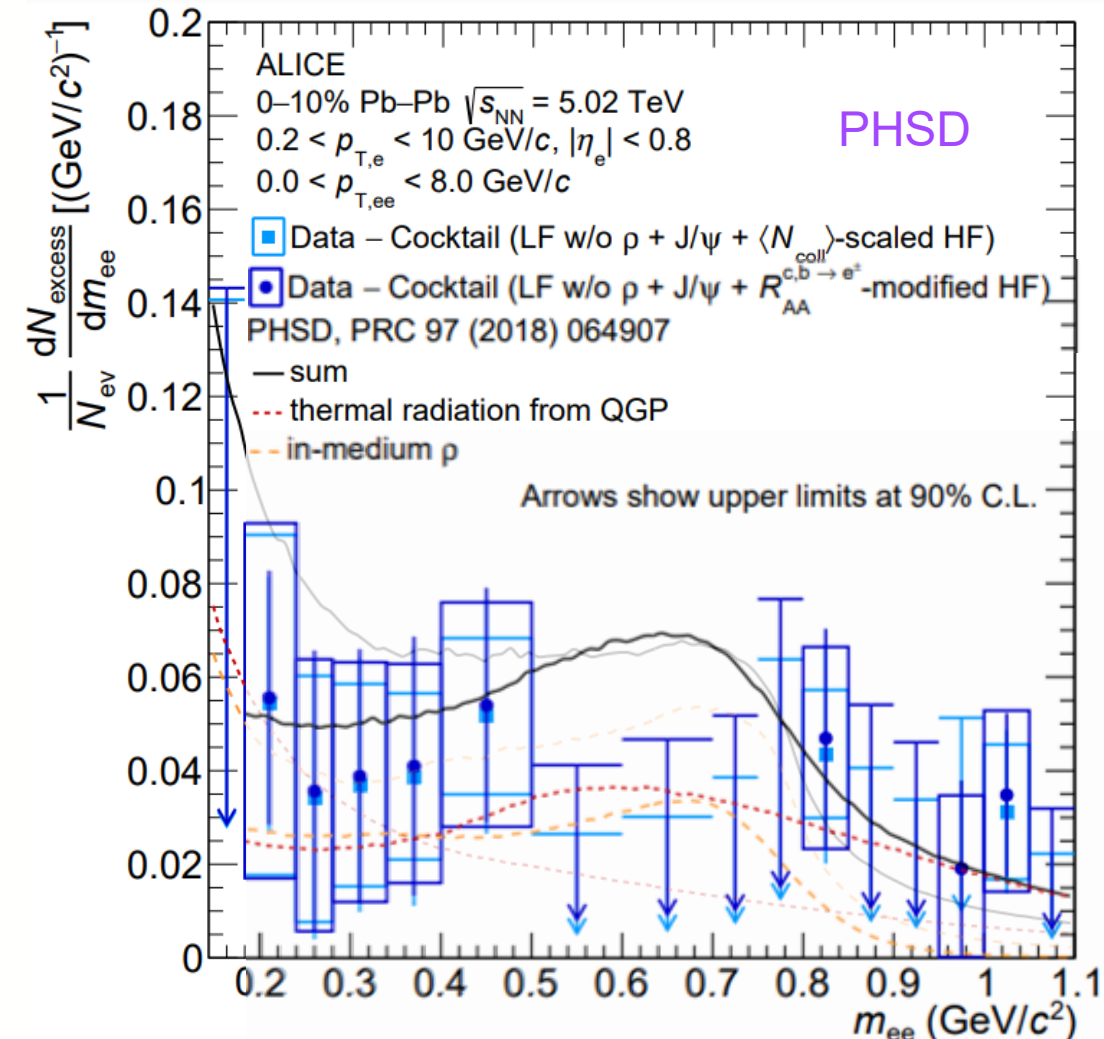
Implemented in 2 different ways:

- R. Rapp's expanding fireball model

Dielectron production in central Pb–Pb at $\sqrt{s_{NN}} = 5.02$ TeV

Excess spectrum

ALICE, arXiv:2308.16704



Subtraction of known hadronic sources without ρ

Compared with sum of 2 contributions:

- In-medium ρ produced thermally in hot hadronic matter
- Thermal radiation from QGP

Implemented in 2 different ways:

- R. Rapp's expanding fireball model
- Parton-Hadron-String Dynamics (PHSD): transport model

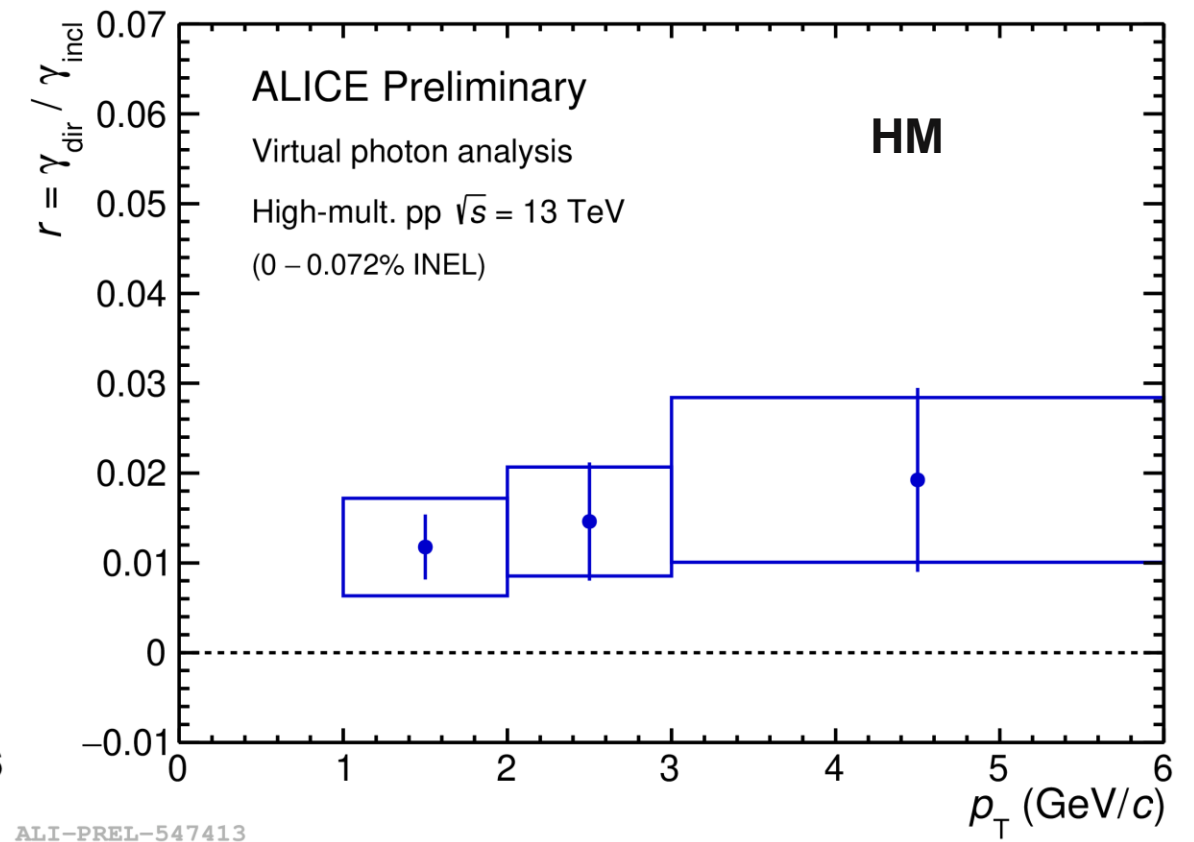
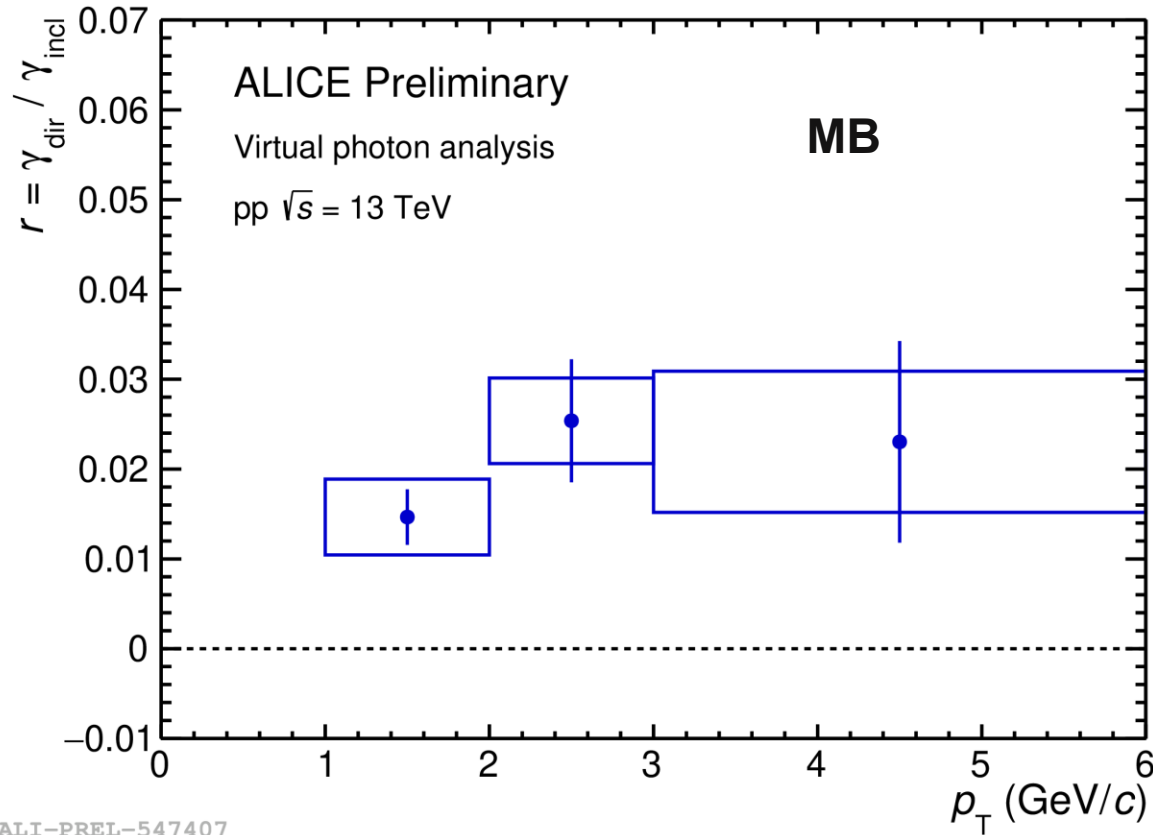
Both models compatible with data:

- Less yield predicted by PHSD
- Some tension in $0.5 < m_{ee} < 0.7$ GeV/c² by 2.7σ (4.0σ)
→ More data needed to confirm



Direct-photon fraction in pp at $\sqrt{s} = 13$ TeV

Comparison to published results



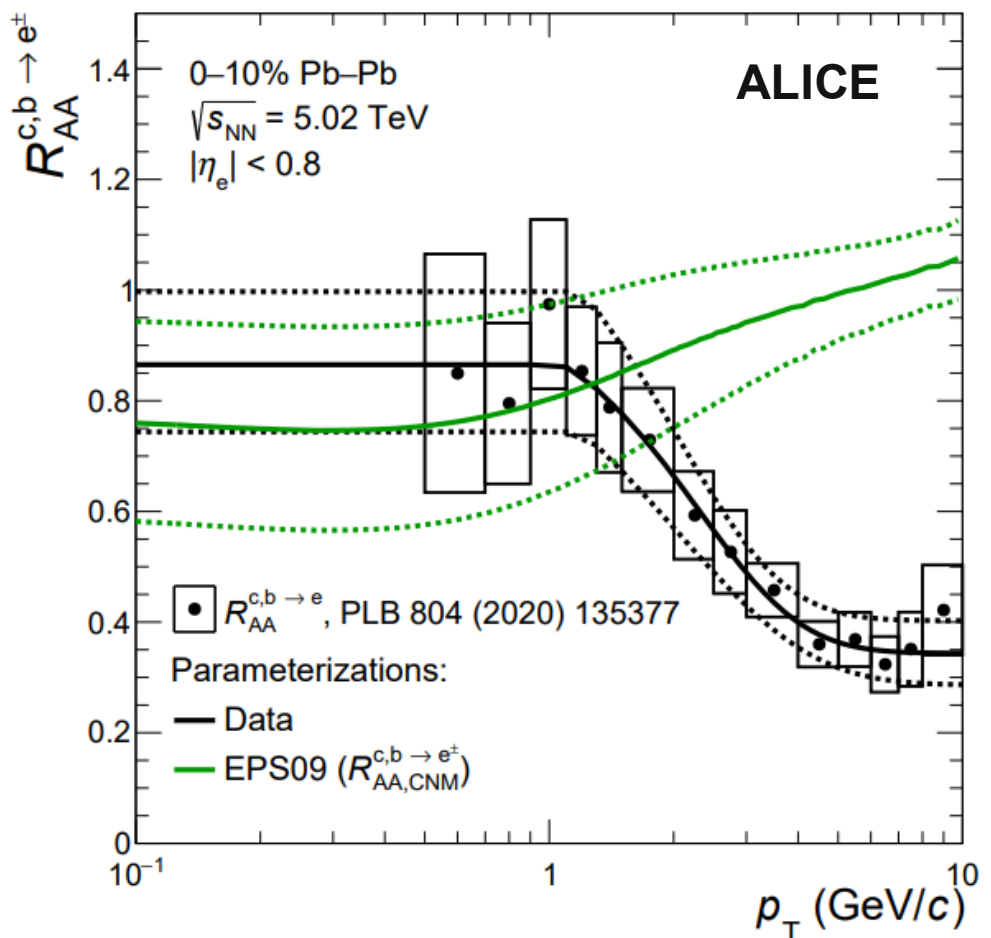
Significant reduction of statistical and systematic uncertainties in new analysis

- Notable contribution of direct-photons in MB & HM collisions
- Measurement in HM compatible with MB results

Hadronic-cocktail improvements

Modeling of HF suppression

Ratio of HF electrons in Pb–Pb/pp



Dielectron spectrum dominated by 1-2 GeV/c region

Modify cocktail: Measured $R_{AA}^{c,b \rightarrow e^\pm}$ as p_T -dependent weights

Contains both CNM & HNM effects

→ However: Affects dielectrons differently

CNM: whole pair

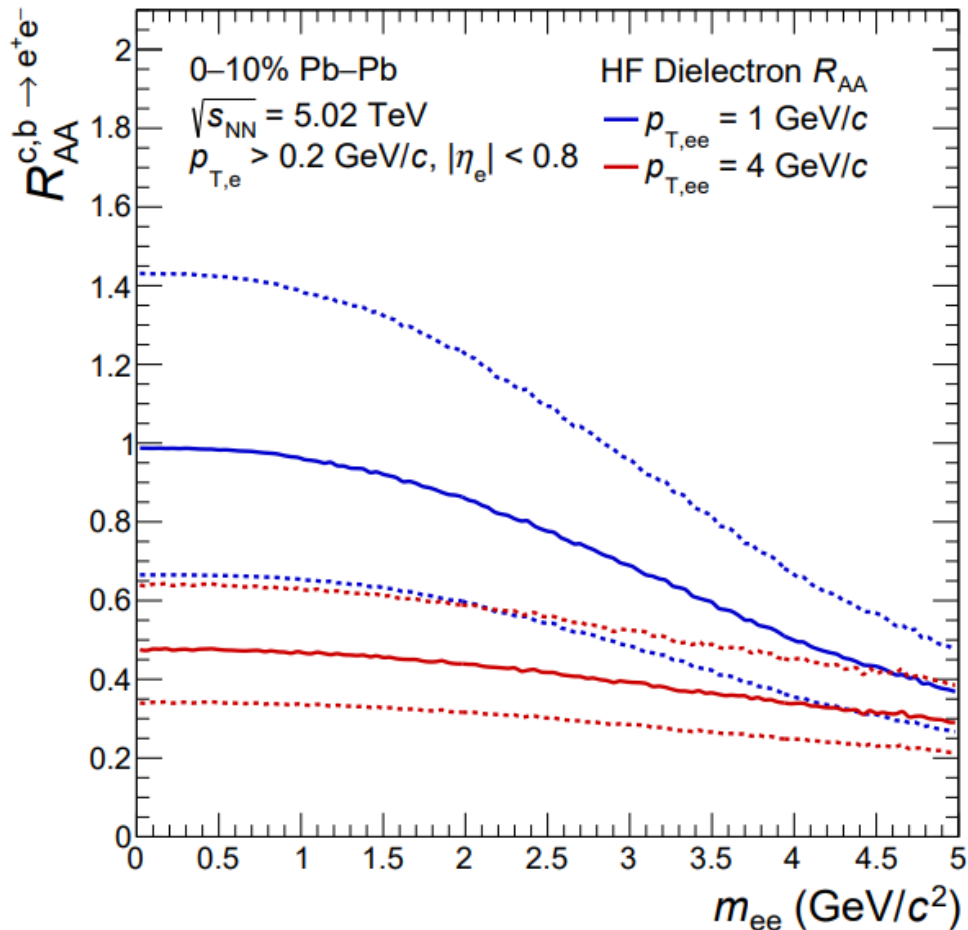
HNM: each electron independently

Disentangle CNM effects using EPS09

Hadronic-cocktail improvements

Modeling of HF suppression

Effective cocktail modification



Modify cocktail: Measured $R_{AA}^{c,b \rightarrow e^\pm}$ as p_T -dependent weights

Contains both CNM & HNM effects

→ However: Affects dielectrons differently

CNM: whole pair

HNM: each electron independently

Disentangle CNM effects using EPS09

Final modification factor $R_{AA}^{c,b \rightarrow ee}$ combining CNM & HNM weights

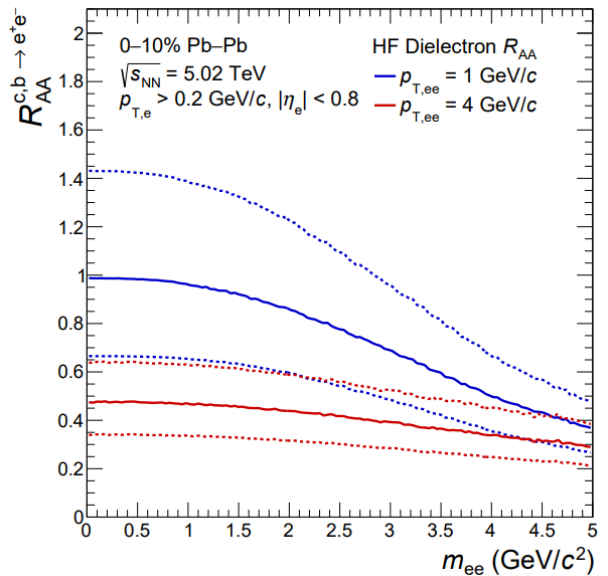
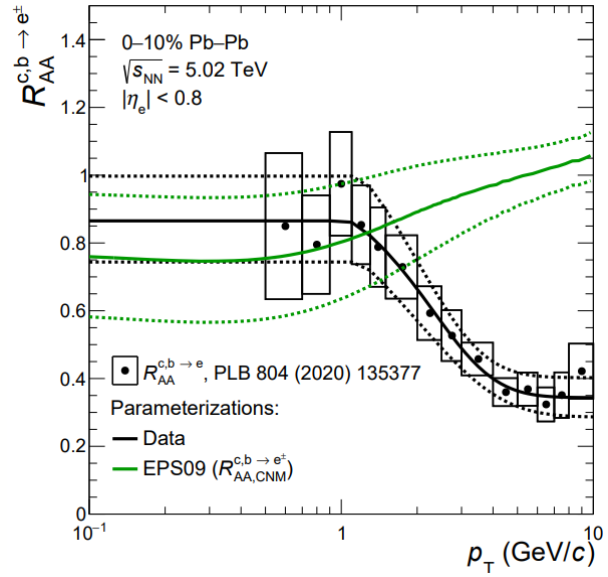
→ More suppression of pairs at higher m_{ee} & $p_{T,ee}$

However: Large uncertainties from HFe R_{AA} & EPS09 inputs

Same suppression for charm & beauty hadrons

Hadronic-cocktail improvements

Modeling of HF suppression



Parametrisation of measured of HF electron R_{AA}
 → Contains CNM effects & energy loss in the medium

Disentangle CNM effects using EPS09: $R_{AA}^{c,b \rightarrow e^\pm} = R_{AA,CNM}^{c,b \rightarrow e^\pm} \times R_{AA,HNM}^{c,b \rightarrow e^\pm}$

CNM effects & energy-loss affect pair production differently

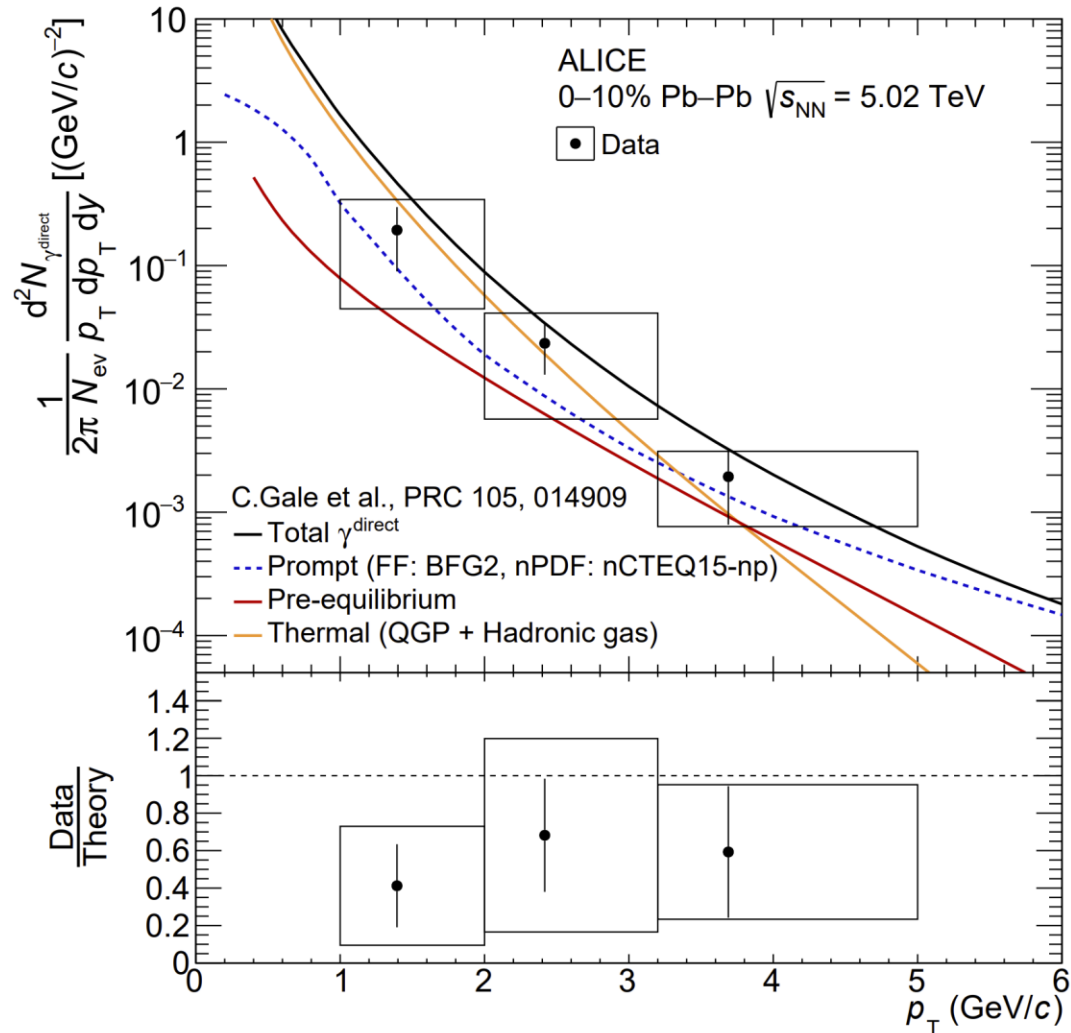
CNM: $R_{AA,CNM}^{c,b \rightarrow ee}$	Energy loss/HNM: $R_{AA,HNM}^{c,b \rightarrow ee}$
Affects whole pair	Affects each electron independently
$\frac{R_{AA,CNM}^{c,b \rightarrow e^\pm}(p_T^{e^+}) + R_{AA,CNM}^{c,b \rightarrow e^\pm}(p_T^{e^-})}{2}$	$R_{AA,HNM}^{c,b \rightarrow e^\pm}(p_T^{e^+}) \times R_{AA,HNM}^{c,b \rightarrow e^\pm}(p_T^{e^-})$

→ Total weight $R_{AA}^{c,b \rightarrow ee}(m_{ee}, p_{T,ee}) = R_{AA,CNM}^{c,b \rightarrow ee} \times R_{AA,HNM}^{c,b \rightarrow ee}$



Direct-photon yield in central Pb–Pb at $\sqrt{s_{NN}} = 5.02$ TeV

p_T -differential spectrum



First direct-photon p_T -differential spectrum at $\sqrt{s_{NN}} = 5.02$ TeV

Hybrid model: Contributions from all stages of the collision

- Prompt photons from NLO pQCD calculations
- Pre-equilibrium contributions
- Thermal (QGP & hadronic gas)

$N_{\gamma^{dir}}$ consistent with only prompt photons

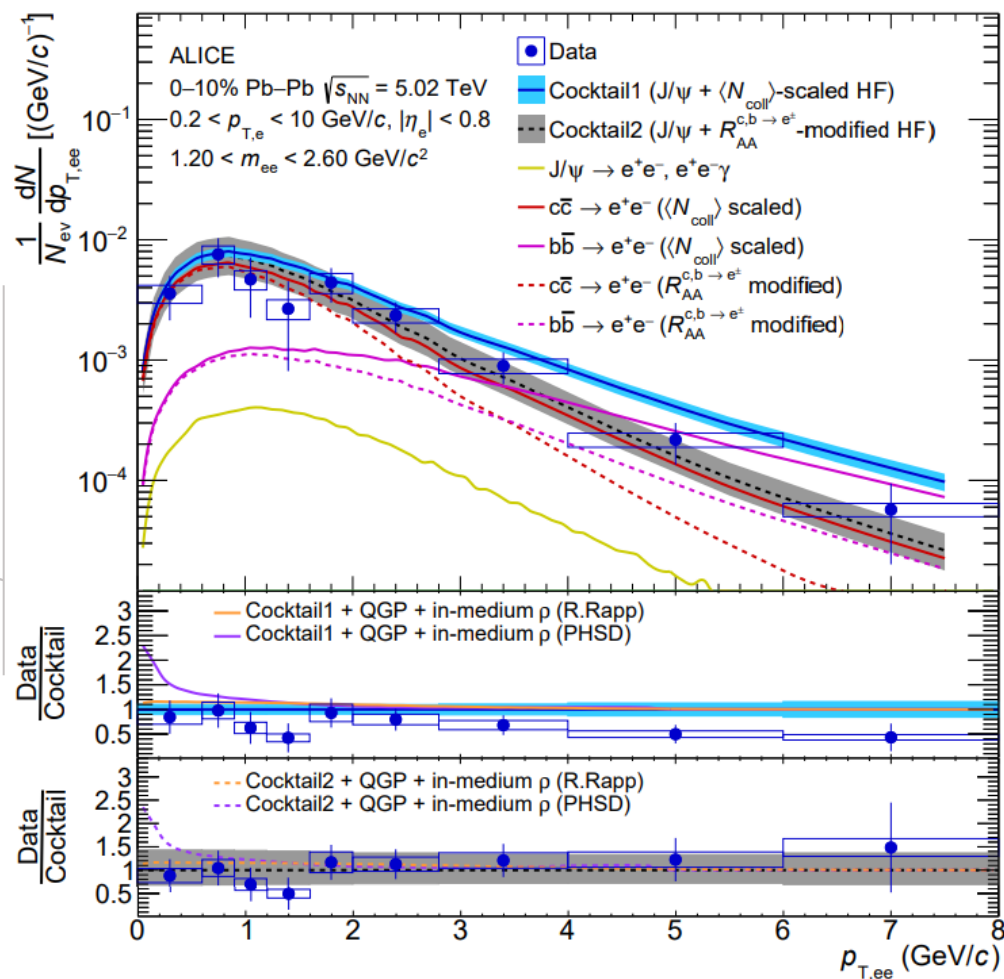
However: All central values above pQCD baseline

Measurement also described by full model prediction

But: Data overestimated by $\sim 1\sigma$

Dielectron production in central Pb–Pb at $\sqrt{s_{NN}} = 5.02$ TeV

Pair-momentum spectrum



Comparison to hadronic cocktail, including:

- N_{coll} -scaled HF measured in pp at $\sqrt{s} = 5.02$ TeV
→ Vacuum baseline
- Include measured R_{AA} of $c/b \rightarrow e^\pm$
→ Modified-HF cocktail

Studying the HF as a function of pair momentum:

- Increasing suppression at high $p_{T,ee}$ compared to pp
- Modified-HF cocktail improves the data description

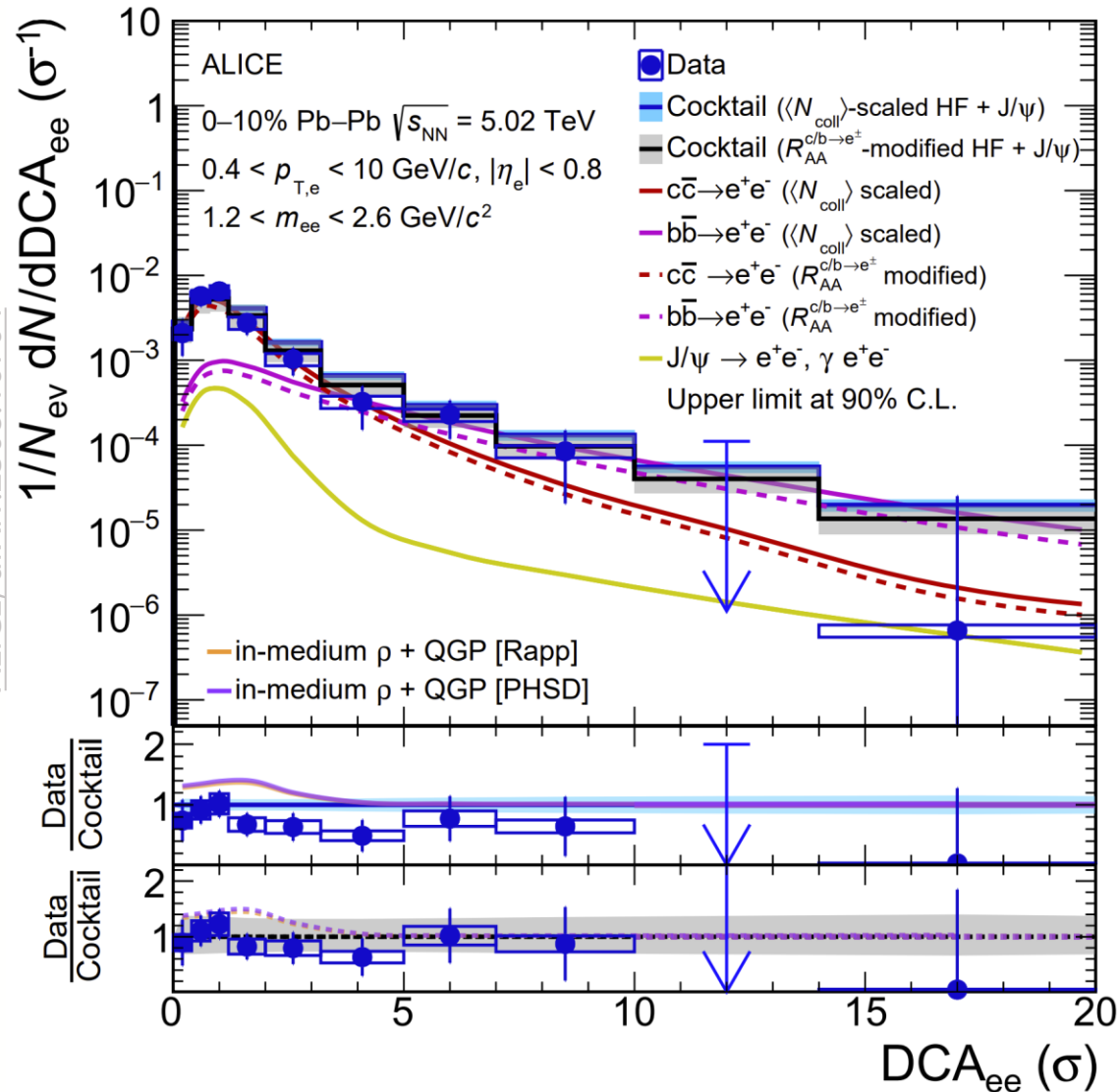
Caveats: Cocktail modification introduces additional uncertainties

- Large uncertainties limit the interpretation of the data
- Applies same modification to **charm** and **beauty**

→ Cocktail independent method needed to access QGP

Dielectron production in central Pb–Pb at $\sqrt{s_{NN}} = 5.02$ TeV

Topological separation – DCA_{ee} in IMR scaled



Comparison to cocktail-scaled templates in the IMR:

- N_{coll} -scaled HF measured in pp at $\sqrt{s} = 5.02$ TeV
 → Vacuum baseline
- Include measured R_{AA} of $c/b \rightarrow e^\pm$
 → Modified-HF cocktail

Again, the data favors a reduced contribution of HF
 → Hint for a larger suppression of charm

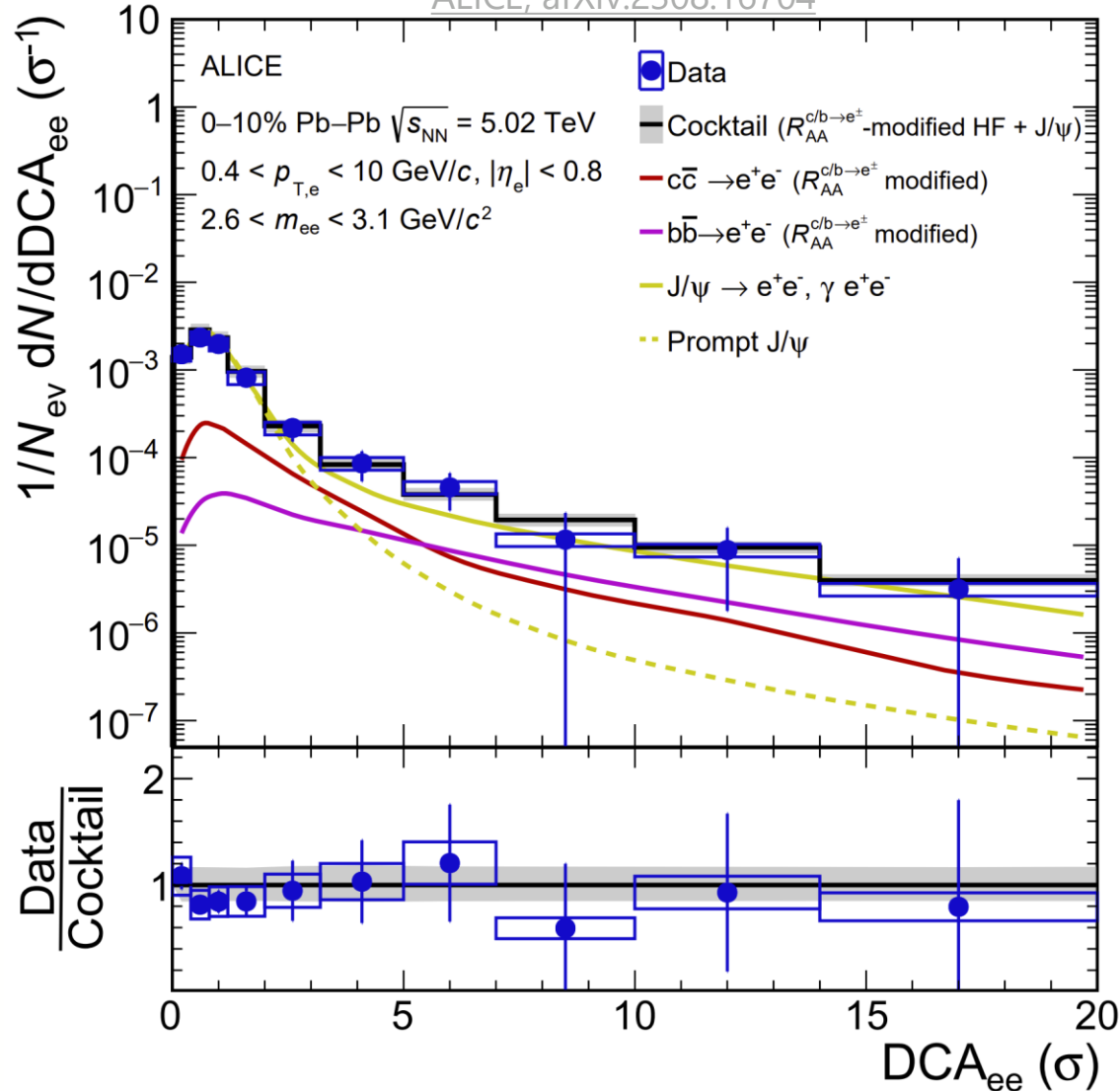
Comparison to expectation from theory by normalizing the prompt template to their respective integral

- Expected thermal signal in the order of 10-40%
- Consistent within current uncertainties

Dielectron production in central Pb–Pb at $\sqrt{s_{NN}} = 5.02$ TeV

Topological separation - DCA_{ee} in J/ψ region

ALICE, arXiv:2308.16704



Test separation of prompt and non-prompt sources in J/ψ mass region:

- J/ψ contribution dominates and is well constrained by independent ALICE measurements
- Only 2 other components: **charm** & **beauty** scaled by the modified-HF cocktail
 - Relative contributions of different hadrons: Combined based on measured fragmentation functions and branching ratios

Data well described by the sum of all templates
 → Validating the DCA resolution in the MC simulation

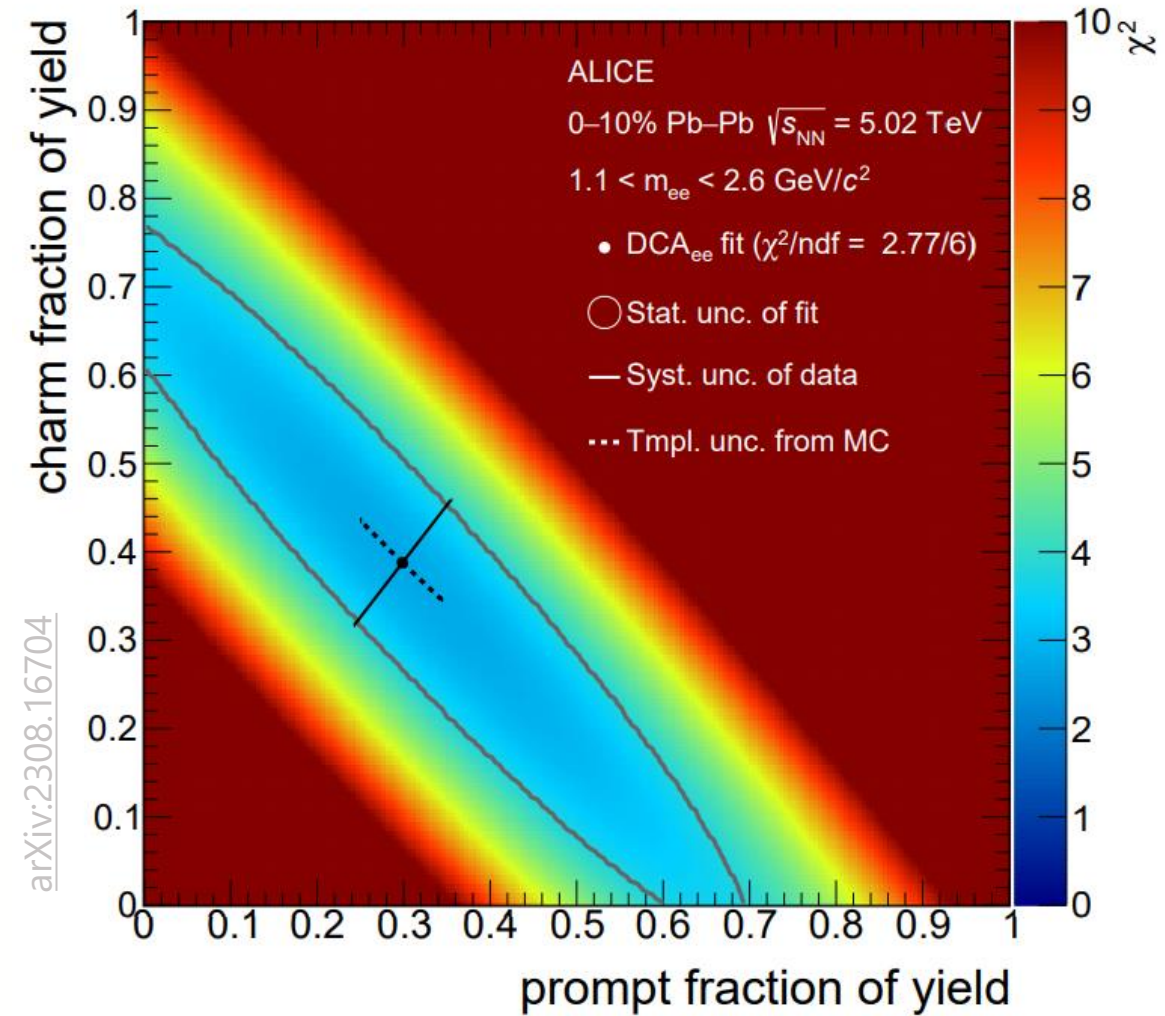


Dielectron production in central Pb–Pb at $\sqrt{s_{NN}} = 5.02$ TeV

Topological separation – DCA_{ee} in IMR fitted

Extraction of prompt thermal signal via template fits:

- Beauty contribution fixed via separate fit at high $p_{T,ee}$
 $b\bar{b}$: $0.74 \pm 0.24(\text{stat.}) \pm 0.12(\text{syst.})$ (w.r.t. N_{coll} scaling)
- Simultaneous fit of charm and prompt contribution
 $c\bar{c}$: $0.43 \pm 0.40(\text{stat.}) \pm 0.22(\text{syst.})$ (w.r.t. N_{coll} scaling)
 prompt: $2.64 \pm 3.18(\text{stat.}) \pm 0.29(\text{syst.})$ (w.r.t. R. Rapp)



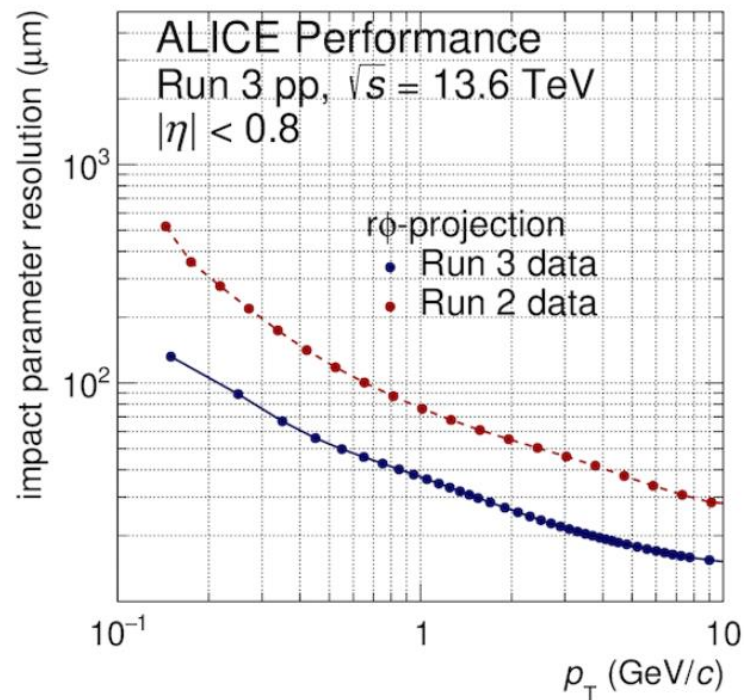
arXiv:2308.16704

Outlook

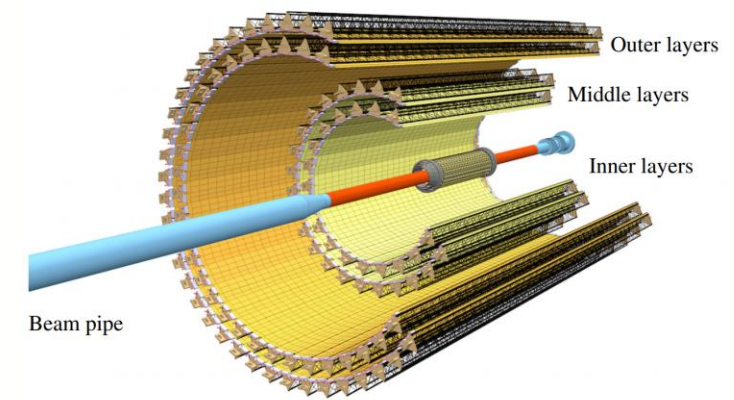
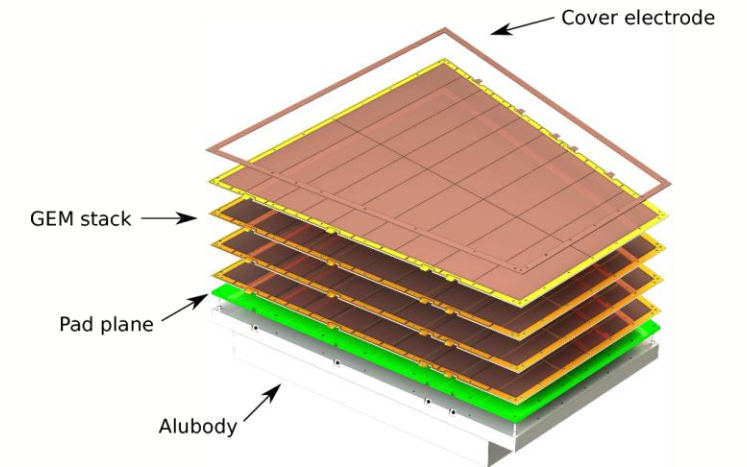
Dielectron production in Run 3 and 4

New ITS and upgrade of the TPC to a GEM based readout system:

- Increase the readout rate in Pb–Pb by a factor 100
- Improve the vertex pointing resolution by a factor 3-6
→ Improves topological separation (DCA_{ee})



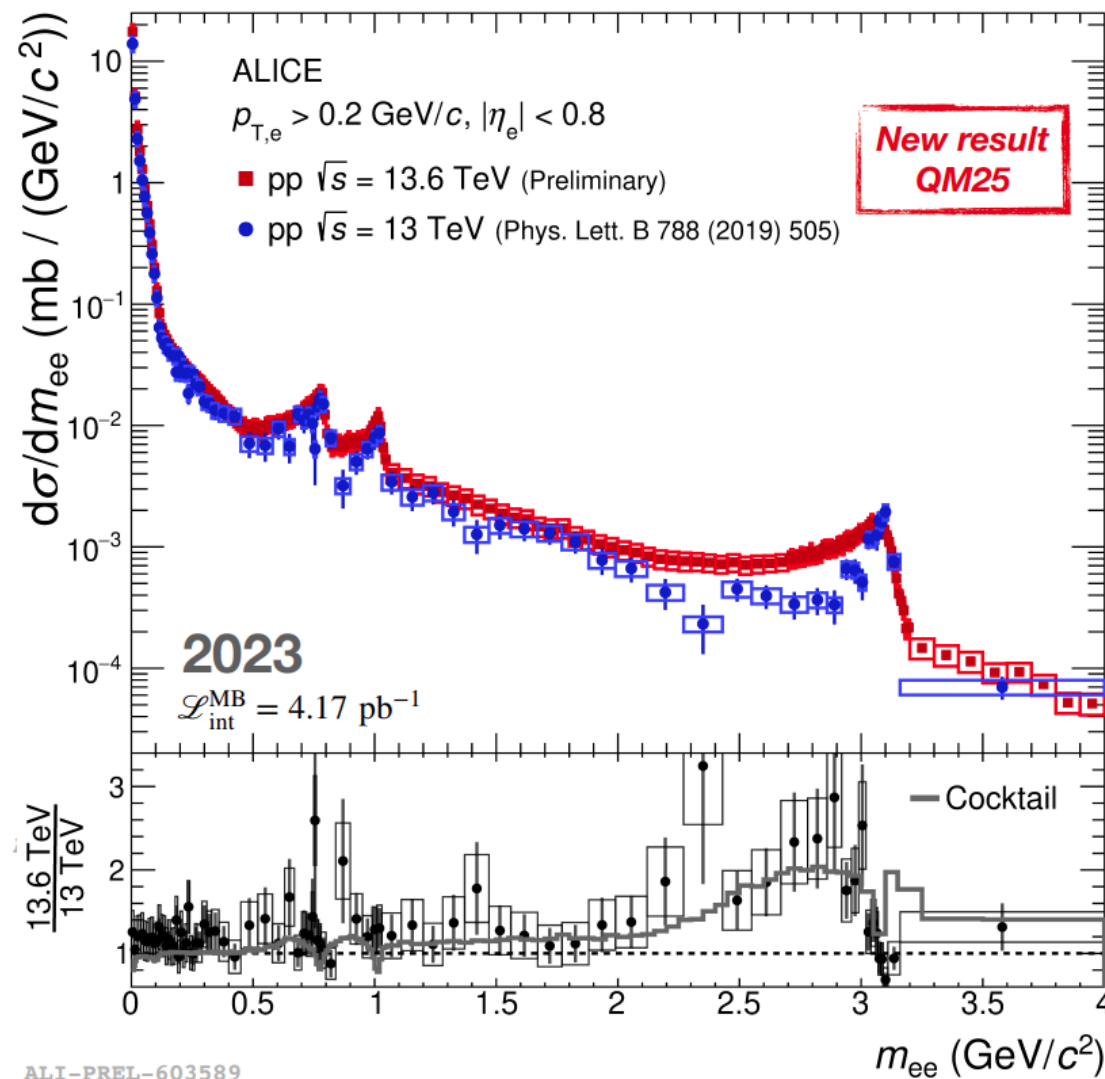
ALI-PERF-558822



arXiv:2111.08301v3

Dielectron production in Run 3

Raw yield



ALI-PREL-603589